

**UCSF**

**UC San Francisco Electronic Theses and Dissertations**

**Title**

Mechanisms of drug resistance in Leishmania major and the characterization of the drug-target, the bifunctional protein, thymidylate synthase-dihydrofolate reductase

**Permalink**

<https://escholarship.org/uc/item/00d8f8g5>

**Author**

Garvey, Edward P.

**Publication Date**

1986

Peer reviewed|Thesis/dissertation

Mechanisms of Drug Resistance in Leishmania major  
and the Characterization of the Drug-Target,  
the Bifunctional Protein, Thymidylate Synthase-  
Dihydrofolate Reductase.

Edward P. Garvey

DISSERTATION

Submitted in partial satisfaction of the requirements for the degree of

DOCTOR OF PHILOSOPHY

in

Pharmaceutical Chemistry

in the

GRADUATE DIVISION

of the

UNIVERSITY OF CALIFORNIA

San Francisco

Date

University Librarian

Degree Conferred:

MAR 30 1966

**I dedicate this thesis  
the years and the energy it represents  
to my wife, Susan.**

## Acknowledgements

There are three groups of people I would like to acknowledge: those who specifically performed experiments that are described in this thesis, those who supported me with their expertise, knowledge, encouragement, and friendship, and those who played a special role in the development of this work.

William Hensell, Ric Harkins, and David Hardman performed the amino acid analysis described in Chapter 4. Henry Rodriguez and Ric Harkins sequenced the first 28 amino acids of the isolated peptide that is described in Chapter 5. Jeff Coderre selected for the drug-resistant *L. major* organisms which are described in Chapters 1 and 2.

There are many people that fit into the second group. First, I want to acknowledge how important the members of the laboratory in which I have worked have been to my development as a scientist. I do not mean to lessen the importance of others by specifically mentioning Alfonso Pogolotti and Larry Hardy, who have always answered my questions as the friends they are, and who have given their expert advice in the field of enzymology; I only mention these two because they have helped me the most. I would like to acknowledge also everyone in the Pharmaceutical Chemistry and Biochemistry & Biophysics Departments who have likewise been supportive and given their expertise so freely; again, I specifically mention Barry Selick who guided me through the field of molecular biology. Two people, Frank Bayliss and Ric Nelson, had very important roles in the development of my use of orthogonal-field-alternation gel electrophoresis, which was the basis for the project described in Chapter 3. I would also like to acknowledge and thank my wife Susan, who, aside from deserving the dedication of this thesis, helped in its preparation. Finally, I would like to acknowledge my research advisor, Dan Santi. I have been fortunate to be presented the many opportunities in the field of research that he has provided, even before I began this graduate program. In addition, the breadth and depth of his knowledge of science have aided me greatly in finishing the projects.

Two individuals fit into the last group that I must acknowledge. Thomas Meek



and Jeff Coderre were postdoctoral fellows in the laboratory at the beginning of my studies, and I had the great luck to be able to work closely with both. Tom and I accomplished an amazing amount of work together in a short period of time; it was truly an example of the whole being greater than the sum of the parts. Specifically, Tom and I achieved the purification and characterization of the bifunctional protein from *L. major*, and I readily acknowledge that without him, this thesis would be sadly shorter. Likewise, Jeff and I worked together on the description of the *L. major* resistant to 10-propargyl-5,8-dideazafolate. Although our collaboration was more defined than was Tom's and mine (Jeff's work centered on the characterization of the amplified DNA), we worked hand in hand, sharing the planning, experiments, and writing of this project.

Lastly, I note that Chapters 1,4, and 5 have been published as follows:

Garvey, E.P., Coderre, J.A., Santi, D.V. (1985) Mol.Biochem.Parasitol. **17**, 19-91.

Meek, T.D., Garvey, E.P., and Santi, D.V. (1985) Biochem. **24**, 678-686.

Garvey, E.P., and Santi, D.V. (1985) Proc.Natl.Acad.Sci.USA **82**, 7188-7192.

## Abstract

*Leishmania major* promastigotes have been selected which are highly resistant to the thymidylate synthase (TS) inhibitor, 10-propargyl-5,8-dideazafolate (CB3717). As reported for *L. major* resistant to methotrexate (MTX), an inhibitor of dihydrofolate reductase (DHFR), CB3717-resistant organisms have high levels of the bifunctional protein TS-DHFR and amplified DNA sequences. The amplified unit of DNA has a uniform restriction-site map throughout the selection and is nearly identical to the 30-kb amplified unit of R-region DNA found in MTX-resistant cells. These and other findings support the proposal that the R-region DNA possesses the sequences that encode TS-DHFR.

We previously reported that the relative stability of amplified DNA in drug-resistant *L. major* was dependent upon location: unstable amplified DNA was extrachromosomal and stable amplified DNA was chromosomal. We have now examined leishmanial chromosomes directly through the technique of orthogonal-field-alternation gel electrophoresis (OFAGE). The amplified DNAs in three resistant cell lines displayed unusual migration and were clearly extrachromosomal, regardless of whether the amplified DNAs were stable or unstable. To our knowledge, this is the first demonstration in eukaryotic cultured cells of stable, amplified DNA that is extrachromosomal.

In an independent study, *L. major* promastigotes have been again selected for resistance against MTX. These MTX-resistant cells display amplified R-region DNA, which contains the gene for TS-DHFR. Of greater interest, these resistant organisms also possess a structurally-altered TS-DHFR. This alteration has weakened the affinity of DHFR toward MTX some 30-fold, lessened the catalytic efficiency of DHFR by 4-fold, and shifted the pI of TS-DHFR to a more negatively-charged molecule.

TS and DHFR in *L. major* exist as a bifunctional protein. By use of a resistant strain, which overproduces the bifunctional enzyme, the protein was purified 80-fold to

apparent homogeneity in two steps. Kinetic parameters and structural properties were extensively examined, and kinetic evidence indicates that most, if not all, of the 7,8-dihydrofolate produced by TS is channeled to DHFR faster than it is released into the medium.

The structure and activity of the bifunctional TS-DHFR were examined by limited proteolysis with five different endopeptidases. Data suggested that the proteolyzed protein remains a dimer with the gross structure of the subunits more or less undisturbed. In contrast, kinetic data indicate that some aspects of higher-order structure in the native protein are affected by proteolysis. Results also indicate that the TS-DHFR polypeptide consists of a DHFR sequence at the blocked NH<sub>2</sub>-terminal and a TS sequence at the COOH-terminal end of the protein.

Finally, an unique substrate-enzyme binary complex between deoxyuridylate and the TS activity of the bifunctional protein is described.

Title Page

Dedication

Acknowledgments

Abstract

List of Tables

List of Figures

Introduction

**Chapter 1.**

to 10-propanol

**Chapter 2.**

*Leishmania m*

**Chapter 3. S**

*Leishmania ex*

**Chapter 4. P**

thymidylate syn

**Chapter 5. Lim**

dihydrofolate red.

**Chapter 6. A Ur**

Deoxyuridylate-T

Appendix 1. Em

Orthogonal-Field-

Appendix 2. Cro

Thymidylate Syn

## Table of Contents

Title Page	i
Dedication	ii
Acknowledgements	iii
Abstract	v
List of Tables	viii
List of Figures	x
Introduction	1
<b>Chapter 1. Selection and properties of <i>Leishmania major</i> resistant to 10-propargyl-5,8-dideazafolate, an inhibitor of thymidylate synthase.</b>	3
<b>Chapter 2. An altered dihydrofolate reductase in methotrexate-resistant <i>Leishmania major</i>.</b>	26
<b>Chapter 3. Stable amplified DNA in drug-resistant <i>Leishmania</i> exists as extrachromosomal circles.</b>	55
<b>Chapter 4. Purification and characterization of the bifunctional thymidylate synthase-dihydrofolate reductase from resistant <i>Leishmania major</i>.</b>	79
<b>Chapter 5. Limited proteolysis of the bifunctional thymidylate synthase-dihydrofolate reductase from <i>Leishmania major</i>.</b>	111
<b>Chapter 6. A Unique Substrate-Enzyme Binary Complex: Deoxyuridylate-Thymidylate Synthase from <i>Leishmania major</i>.</b>	134
<b>Appendix 1. Empirically-determined parameters for Orthogonal-Field-Alternation Gel Electrophoresis.</b>	162
<b>Appendix 2. Cross-Reactivity of the antibody for Thymidylate Synthase-Dihydrofolate Reductase to Other TSs and DHFRs.</b>	168

**Chapter 1.**

Table I: Qu

levels in *L.*

**Chapter 2.**

Table I: DH

from D7B ce

Table II: Kin

Table III: Su

from wildtyp

**Chapter 4.**

Table I: Purif

Table II: Ami

Table III: Cou

from *L. casei*

**Chapter 5.**

Table I: Summ

**Chapter 6.**

Table I: Comp

dUMP bound f

Table II: Comp

FdUMP/CH<sub>2</sub>H

Table III: Disso

binary complex.

## List of Tables

### Chapter 1.

Table I: Quantitation of R-region DNA copy number and TS and DHFR levels in <i>L. major</i> promastigotes resistant to increasing amounts of CB3717.	12
--	----

### Chapter 2.

Table I: DHFR and TS levels in crude extracts from wildtype cells and from D7B cells resistant to MTX.	34
Table II: Kinetic constants of wildtype and D7BR1000 TS-DHFR.	40
Table III: Summary of interaction between MTX and DHFR from wildtype cells and from D7BR1000 cells.	47

### Chapter 4.

Table I: Purification of TS-DHFR from <i>L. major</i> .	92
Table II: Amino acid composition of TS-DHFR.	95
Table III: Coupled TS-DHFR assays using mixtures of TS and DHFR from <i>L. casei</i> and the bifunctional TS-DHFR from <i>L. major</i> .	102

### Chapter 5.

Table I: Summary of limited proteolysis of <i>L. major</i> TS-DHFR.	117
---	-----

### Chapter 6.

Table I: Competition between dUMP and FdUMP/CH <sub>2</sub> H <sub>4</sub> folate: dUMP bound first.	150
Table II: Competition between dUMP and FdUMP/CH <sub>2</sub> H <sub>4</sub> folate: FdUMP/CH <sub>2</sub> H <sub>2</sub> folate bound first.	151
Table III: Dissociation of [6- <sup>3</sup> H]dUMP from the isolated binary complex.	153

**Table IV: Limited proteolysis of TS-DHFR,  
in the presence and absence of the binary complex.** 155

**Appendix 2.**

**Table I: Cross-reactivity of Ab for TS-DHFR.** 172



## Chapter 1.

Figure 1: Com

resistant to M

Figure 2: Com

in the CB50 a

Figure 3: Elec

from cell lines

Figure 4: Stabi

elevated TS-D

## Chapter 2.

Figure 1: Deme

Figure 2: Two-

wildtype and D

Figure 3: Rates

MTX-NADPH-

Figure 4: Chara

## Chapter 3.

Figure 1: Chrom

Figure 2: Demon

in R1000-11 cell

Figure 3: Compa

(unstable) and R

Figure 4: Compa

drug-resistant *L.*

Figure 5: Demor

## List of Figures

### Chapter 1.

- Figure 1: Comparison of DNA amplification in *L. major* resistant to MTX or CB3717. 14
- Figure 2: Comparison of the regions of DNA amplified in the CB50 and R1000 cell lines. 15
- Figure 3: Electrophoresis of DNA (unrestricted) from cell lines resistant to increasing concentrations of CB3717. 17
- Figure 4: Stability of the amplified DNA and the elevated TS-DHFR levels in *L. major* CB50. 19

### Chapter 2.

- Figure 1: Demonstration of a structurally-altered TS-DHFR. 35
- Figure 2: Two-dimensional gel electrophoresis of wildtype and D7BR1000 crude extracts. 37
- Figure 3: Rates of MTX dissociation from the MTX-NADPH-enzyme complex. 42
- Figure 4: Character and extent of DHFR inhibition by MTX. 44

### Chapter 3.

- Figure 1: Chromosomal gel of wildtype *L. major*. 60
- Figure 2: Demonstration that stable amplified DNA in R1000-11 cells is extrachromosomal. 61
- Figure 3: Comparison of R1000-3 amplified DNA (unstable) and R1000-11 amplified DNA (stable). 63
- Figure 4: Comparison of amplified DNAs from two drug-resistant *L. major*: R1000-11 and CB50-10 DNAs. 65
- Figure 5: Demonstration that R1000-11 amplified DNAs are circular. 69

Figure 6: L

Figure 7: L

#### Chapter 4

Figure 1: A

Figure 2: N

following ea

Figure 3: Exp

in the TS-DH

#### Chapter 5.

Figure 1: NaD

*L. major* TS-D

Figure 2: Time

*L. major* TS-D

Figure 3. Comp

fragment from *L*

and homologous

#### Chapter 6.

Figure 1: Dissoci

Figure 2: Rates of

as a function of d

Figure 3: Sephad

Appendix 1. Ch

Figure 6: Determination of the size of the amplified DNA in R1000-11 cells.	70
Figure 7: Determination of the size of the amplified DNA in CB50-10 cells.	73
<b>Chapter 4.</b>	
Figure 1: Affinity chromatography of TS-DHFR.	89
Figure 2: NaDodSO <sub>4</sub> -PAGE (12.5% polyacrylamide) of <i>L. major</i> TS-DHFR following each step of protein purification.	93
Figure 3: Experimental and simulated time courses for NADP formation in the TS-DHFR coupled assay using the enzymes from <i>L. casei</i> and <i>L. major</i> .	101
<b>Chapter 5.</b>	
Figure 1: NaDodSO <sub>4</sub> -PAGE analysis of limited proteolysis of <i>L. major</i> TS-DHFR, and subsequent Western blot analysis.	119
Figure 2: Time course of limited proteolysis of <i>L. major</i> TS-DHFR by the V-8 protease.	121
Figure 3. Comparison of the NH <sub>2</sub> -terminal sequence of the M <sub>r</sub> 20,000 fragment from <i>L. major</i> TS-DHFR, generated by the V-8 protease, and homologous sequences found within other TSs.	124
<b>Chapter 6.</b>	
Figure 1: Dissociation of dUMP from the dUMP-enzyme binary complex.	141
Figure 2: Rates of association of dUMP binding to TS-DHFR as a function of dUMP concentration.	143
Figure 3: Sephadex-25 chromatography of the dUMP-enzyme binary complex.	145
<b>Appendix 1. Chromosome size versus OFAGE migration.</b>	165

nature of

Although

persistence

young (ch

parasitic di

curtail the d

Am

malaria in te

caused by *Le*

*donovani*; cu

mucocutaneou

(promastigotes

(amastigote) in

sandfly. Ironi

macrophage, w

(vector control,

effective chemot

is no successful d

(diamidines, triv

stibogluconate, a

This dis

leishmaniasis by

in *Leishmania*, a

organism. These

## Introduction

The prevalent parasitic diseases of the third world play a large role in the cyclical nature of ill health, poverty, and lack of education found in those countries (1-4).

Although most of these diseases are not life-threatening, their wide-spread chronic persistence greatly lessens the quality of life and continually restricts the development of the young (children are more frequently infected by these diseases than are adults). Thus, parasitic diseases both help to create the human condition found in the third world and also curtail the development of awareness and skill that is necessary to change this condition.

Among the protozoan disease, leishmaniasis is regarded as second only to malaria in terms of human suffering and economic impact (1). Three principal diseases are caused by *Leishmania*: visceral leishmaniasis (kala-azar), the result of infection by *L. donovani*; cutaneous leishmaniasis (oriental sore), *L. major*; and American mucocutaneous leishmaniasis, *L. braziliensis*. These protozoans assume a flagellated form (promastigotes) in the insect vector and in culture, and an ovoid unflagellated form (amastigote) in man. They are transmitted from insect to man through the bite of the sandfly. Ironically, once inside man, the parasite resides and divides within the macrophage, whose role is to combat against such invasion. Although prevention methods (vector control, immunization) are the ideal response to this and all parasitic diseases, effective chemotherapy is essential until prevention is achieved. At the current time, there is no successful chemotherapy; drugs used against leishmaniasis are either extremely toxic (diamidines, trivalent antimonials) or impractical (pentavalent antimonials such as sodium stibogluconate, amphotericin B) (4,5).

This dissertation addresses the need for effective drug treatment against leishmaniasis by developing two areas of chemotherapy: 1) mechanisms of drug resistance in *Leishmania*, and 2) the characterization of a potential chemotherapeutic target against the organism. These two areas will be bridged by common denominator, the bifunctional

protein thymidylate synthase-dihydrofolate reductase (TS-DHFR). This unique enzyme is both the biological target chosen to study drug resistance in this parasite, and also a potential drug target for a new, more effective chemotherapy.

### References

1. Walsh, J.A., and Warren, K.S. (1979) N.Engl.J.Med. 301, 967-973.
2. Zuckerman, A. and Lainson, R. (1977) In Parasitic Protozoa, Vol. 1, Ed. J.P. Kreier, Academic Press.
3. Gutteridge, W.E. and Coombs, G.H. (1977) In Biochemistry of Parasitic Protozoa, University Park Press.
4. Pratt, W.B. (1977) In Chemotherapy of Infection, pp 305-408 Oxford University Press.
5. Rollo, I.M. (1980) in The Pharmacological Basis of Therapeutics (A.G. Gilman, L.S. Goodman, and A. Gilman, Eds) pp 1038-1060, MacMillan Publishing Co., Inc.

## Chapter 1

### **Selection and Properties of Leishmania Resistant to 10-Propargyl-5,8-dideazafolate, an Inhibitor of Thymidylate Synthase**



Leishma

resistant t

5,8-dideaza

methotrexat

CB3717-resi

TS-DHFR and

the protein.

alteration t

DNA has a ur

nearly ident

MTX-resistan

fragment tha

rearrangemen

do not posse

cells. The a

appears as a

DNA of MTX-re

of drug, the

When resistan

DNA and level

resistant le

R-region DNA

protein.

1 743/200

of 1987. Leishmania is a unicellular, flagellated protozoan.

It is the causative agent of leishmaniasis, a group of diseases that affect humans and animals.

### Abstract

Leishmania major promastigotes have been selected which are highly resistant to the thymidylate synthetase (TS) inhibitor, 10-propargyl-5,8-dideazafolate (CB3717). As reported for L. major resistant to methotrexate (MTX), an inhibitor of dihydrofolate reductase (DHFR), CB3717-resistant organisms have high levels of the bifunctional TS-DHFR and amplified DNA sequences. TS-DHFR represents up to 2% of the protein in cell extracts and does not appear to have a structural alteration that contributes to drug resistance. The amplified unit of DNA has a uniform restriction-site map throughout the selection and is nearly identical to the 30-kb amplified unit of R-region DNA found in MTX-resistant cells, except for a small increase in size of the fragment that contains a junction believed to be the site of DNA rearrangements generated during amplification. CB3717-resistant cells do not possess the amplified H-region DNA found in MTX-resistant cells. The amplified DNA in cells resistant to low levels of CB3717 appears as a 30-kb extrachromosomal circle, similar to the amplified DNA of MTX-resistant organisms. In cells resistant to higher levels of drug, the amplified DNA appeared as higher molecular weight forms. When resistant cells were grown in the absence of drug, the amplified DNA and levels of TS-DHFR gradually fell to approximately 10% of the resistant levels. These findings support the proposal that the R-region DNA possesses the sequences that encode the bifunctional protein.

document

1. The first part of the document discusses the importance of maintaining accurate records of all transactions and activities. It emphasizes that this is essential for the proper management of the organization and for ensuring that all stakeholders are kept informed of the current status of affairs.

2. The second part of the document outlines the various methods and techniques used to collect and analyze data. It describes how these methods are applied in different contexts and how they can be used to identify trends and patterns in the data.

3. The third part of the document discusses the importance of data security and privacy. It outlines the various measures that can be taken to protect data from unauthorized access and to ensure that it is used in a responsible and ethical manner.

4. The fourth part of the document discusses the importance of data quality and accuracy. It outlines the various methods that can be used to ensure that data is accurate and reliable and that it is used in a way that is consistent with the organization's goals and objectives.

5. The fifth part of the document discusses the importance of data integration and interoperability. It outlines the various methods that can be used to ensure that data from different systems and sources can be integrated and used together in a seamless and efficient manner.

6. The sixth part of the document discusses the importance of data governance and compliance. It outlines the various methods that can be used to ensure that data is managed in a way that is consistent with applicable laws and regulations and that it is used in a way that is consistent with the organization's policies and procedures.

7. The seventh part of the document discusses the importance of data analytics and reporting. It outlines the various methods that can be used to analyze data and to generate reports that provide insights into the organization's performance and help to inform decision-making.

8. The eighth part of the document discusses the importance of data visualization and communication. It outlines the various methods that can be used to present data in a clear and concise manner and to ensure that it is understood and used in a way that is consistent with the organization's goals and objectives.

9. The ninth part of the document discusses the importance of data archiving and backup. It outlines the various methods that can be used to ensure that data is preserved and that it can be recovered in the event of a disaster or other emergency.

10. The tenth part of the document discusses the importance of data retention and disposal. It outlines the various methods that can be used to ensure that data is retained for the appropriate amount of time and that it is disposed of in a secure and responsible manner.

exi

numb

prom

metho

shows

organi

(appro

extrach

they wer

fragment

generate

kb in wil

the ampli

H-regions

of MTX, and

continued e

DNA; levels

H-region dec

absence of M

the degree of

the amount of

the gene cod

The propo

determined by

resistant to

Thymidylate synthase (TS)<sup>1</sup> and dihydrofolate reductase (DHFR) exist as a bifunctional protein in Leishmania major, as well as in a number of other protozoa (1,2). We have reported a strain of L. major promastigotes, selected for resistance to the DHFR inhibitor methotrexate (MTX), which overproduces the bifunctional TS-DHFR and shows two distinct and uniform amplified regions of DNA (3). When the organisms were propagated in 1 mM MTX for short periods of time (approx. 3 months), much of the amplified DNA existed as two distinct extrachromosomal circles, designated as the R- and H-regions because they were initially identified by use of recombinant EcoRI or HindIII fragments of the amplified DNA (4). The R-region was apparently generated by the joining of two regions of DNA separated by about 30 kb in wildtype organisms, yielding a rearranged "junctional" region in the amplified DNA. When present as extrachromosomal DNA, both R- and H-regions were unstable when the organisms were grown in the absence of MTX, and decreased coordinately with levels of TS-DHFR. Upon continued exposure to MTX, both regions became integrated into genomic DNA; levels of the R-region DNA and TS-DHFR remained high, but the H-region declined. Further, when these organisms were grown in the absence of MTX, the R-region and TS-DHFR levels were stable. Since the degree of amplification and stability of the R-region paralleled the amount of TS-DHFR, it was proposed that the R-region DNA possesses the gene coding for the bifunctional protein.

The properties described for MTX-resistant L. major were determined by use of organisms with a common lineage that were resistant to high concentrations of the drug. We have initiated



independent selections of drug-resistant L. major for the following reasons. First, we wished to ascertain whether the properties observed for the MTX-resistant cell line would be preserved in an independent selection of L. major towards another inhibitor of TS-DHFR, and whether new properties would emerge. Second, cells resistant to low concentrations of MTX were unavailable and we wanted to characterize cells during the selection process. Third, we required a new abundant source of TS-DHFR for enzymatic studies because, for unknown reasons, continued propagation of the MTX-resistant line has resulted in a gradual loss of the enzyme. In this paper, we describe L. major promastigotes that are highly resistant to 10-propargyl-5,8-dideazafolate (CB3717), a potent inhibitor of TS (5,6). This represents the second independent selection of L. major resistant to an inhibitor of TS-DHFR that has responded by overproduction of TS-DHFR and amplification of nearly identical units of R-region DNA. The properties of these organisms are compared and contrasted with those of the original MTX-resistant line of L. major.

#### Materials and Methods

**Growth of Organisms.** L. major promastigotes used here were derived from the POJ-1 clone (B. Ullman, University of Kentucky, Lexington, KY) isolated from strain 252, Iran (S. Meshnik, Cornell University, New York). Organisms were grown at 26°C in M199 medium (GIBCO) supplemented with 20% fetal calf serum, 25 mM HEPES, pH 7.4, 50 µg ml<sup>-1</sup> gentamycin, and, when specified, CB3717 (a gift from A.H. Calvert, Institute of Cancer Research, Sutton, Surrey, U.K.). The doubling time ( $t_2$ ) for wildtype organisms was 10-12 h and maximal



cell density was about  $4 \times 10^7$  cells  $\text{ml}^{-1}$ . One passage refers to 5 generations of growth or a 32-fold expansion in cell number. Cells were counted with a Coulter Counter ZBI.

**Selection of CB3717-resistant L. major.** CB3717-resistant strains of L. major promastigotes were obtained by stepwise selection of resistant organisms at drug concentrations of 0.01, 0.05, 0.25, 0.80, 2.0, 5.0, 25, 50, and 250  $\mu\text{M}$ . Cells were seeded at  $10^6$  cells  $\text{ml}^{-1}$  in 10 ml of medium containing the specified amount of CB3717. When cells density exceeded  $10^7$  cells  $\text{ml}^{-1}$ , or if growth rate began to plateau, cells were diluted into fresh medium containing the same concentration of drug. When growth had reached a constant rate for a few passages, cells were seeded in the next higher concentration of CB3717. The resistant cell lines are designated as CB followed by the  $\mu\text{M}$  concentration of drug to which they are resistant, e.g., CB50 refers to cells that are resistant to 50  $\mu\text{M}$  CB3717.

**Enzyme Assays and Purification.** Cells in CB3717 were grown to a density of about  $3 \times 10^7$  cells  $\text{ml}^{-1}$ , pelleted by centrifugation, washed with drug-free medium, and resuspended in drug-free medium. For determination of enzyme levels, cultures were harvested by centrifugation when the cell density was  $2-10 \times 10^6$  cells  $\text{ml}^{-1}$ , a range in which the specific activity was constant. For enzyme purification, cells were harvested when they reached a density of  $3-4 \times 10^7$  cells  $\text{ml}^{-1}$ . Cell extracts were prepared as previously described (7).



... ..  
... ..  
... ..

... ..  
... ..  
... ..

... ..  
... ..  
... ..  
... ..  
... ..

... ..  
... ..  
... ..  
... ..

... ..  
... ..  
... ..  
... ..

... ..  
... ..  
... ..  
... ..

... ..

TS was quantitated by nitrocellulose filter binding of the covalent [ $^3\text{H}$ ]FdUMP- $\text{CH}_2\text{H}_4$ folate-enzyme complex or assayed spectrophotometrically (7); the  $K_i$  of CB3717 for TS is in the nanomolar range (see Results) and its removal or sufficient dilution is required to assess TS activity. DHFR activity was determined spectrophotometrically as previously described (7). One unit of activity is defined as the amount of enzyme that produces 1 nmol of product per min.

TS-DHFR from cells resistant to 250  $\mu\text{M}$  CB3717 was purified by slightly modifying the procedure used to purify TS-DHFR from MTX-resistant cells (7). All procedures were performed at 4°C. The crude extract (60-80 ml; about 200 mg protein) was applied at a rate of 0.5 ml min $^{-1}$  to a column of MTX-Sepharose CL-6B (0.8 X 4.0 cm) that was previously equilibrated with 10 mM  $\text{K}_2\text{HPO}_4$ , pH 7.0. The column was first washed with 10 mM  $\text{K}_2\text{HPO}_4$ , pH 7.0, containing 1 M KCl until protein was undetectable in the effluent, and then with 10 ml of equilibration buffer. The column was equilibrated for 20 min with one column volume of 1 mM  $\text{H}_2$ folate, 50 mM 2-[[tris(hydroxymethyl)methyl]amino]ethane sulfonate, pH 7.4, 5 mM dithiothreitol, and 1 mM EDTA, and then eluted with the same buffer. Fractions containing TS-DHFR were pooled and  $\text{H}_2$ -folate was removed as previously described (7). All other procedures for protein analysis were as previously described (7).

Faint, illegible text, possibly bleed-through from the reverse side of the page.

Nucleic A  
(8) excep  
0.1 M EDT  
sources an  
fragments  
boric acid  
with restr  
with the s  
were used  
translatio  
hybridizat  
The hyb  
plasmid pL  
R-region an  
(3); Charon  
R-region wh  
R-region. I  
unamplified  
The copy  
relative to  
previously r  
DNA from wild  
resistant org  
nitrocellulos  
After autora  
determined an  
Corrections f

**Nucleic Acid Techniques.** Total L. major DNA was prepared as described (8) except the cell lysis buffer contained 0.2 M Tris-HCl, pH 8.0, and 0.1 M EDTA. Restriction endonucleases were obtained from commercial sources and used as recommended by the supplier. Restriction fragments were electrophoresed in 0.7% agarose with 89 mM Tris, 89 mM boric acid, and 0.2 mM EDTA, pH 8.4 (9). DNA that was not treated with restriction endonucleases was electrophoresed in 0.4% agarose with the same buffer at 10 V for 72 h (4). The following procedures were used as described (9): labeling of DNA with [ $\alpha$ - $^{32}$ P]dCTP by nick translation, transfer of DNA from agarose gels to nitrocellulose, and hybridization of  $^{32}$ P-labeled probes to DNA bound to nitrocellulose.

The hybridization probes used were as previously described: plasmid pLR-R1 contained a 2.0 kilobase (kb) insert of the amplified R-region and plasmid pLR-HM3 contained a 1.9 kb insert of the H-region (3); Charon 4A  $\lambda$  LTS-14 and  $\lambda$  LTS-2 (4) contained inserts of the R-region which together span all but about 2 kb of the 30 kb R-region. Plasmid pLR-L54, which contained a 2-kb insert of unamplified L. major DNA, was a gift from S.M. Beverley.

The copy number of CB3717-resistant L. major R- and H-region DNA, relative to wildtype organisms, was determined by modifying a previously reported procedure (8). For the R-region, EcoRI digests of DNA from wildtype L. major and 1:2 serial dilutions of DNA from resistant organisms were electrophoresed, transferred to nitrocellulose, and hybridized to nick-translated [ $^{32}$ P]pLR-R1. After autoradiography the grain densities of the 2-kb fragments were determined and the intensities were compared to that of wildtype DNA. Corrections for the amount of DNA applied were performed by

Faint, illegible text, possibly bleed-through from the reverse side of the page. The text is too light to transcribe accurately.

H  
Sel  
were  
incr  
decre  
passa  
passag  
( $t_2 - 2$   
selecti  
during t  
 $t_2$  of ab  
medium, t  
comparabl  
cells with  
degenerati  
cross-resis  
medium cont  
cells, grow  
Overproduct  
extracts of  
protein)<sup>-1</sup>  
respectivel

standardization, with pLR-L54 used as a probe. A similar procedure was used to quantitate the H-region except the DNA was restricted with HindIII, and pLR-HM3 was used as the hybridization probe.

### Results

**Selection of CB3717-resistant L. major.** When L. major promastigotes were placed in medium containing 0.01  $\mu\text{M}$  CB3717, the doubling time increased from about 10 to 50 h; after 5-6 passages the doubling time decreased to about 20 h and remained constant through subsequent passages. This pattern of slow growth ( $t_2 \sim 50$  h) during initial passage in a higher drug concentration followed by more rapid growth ( $t_2 \sim 20$  h) was observed in the subsequent three steps of the selection procedure. At higher concentrations of drug, growth rate during the first passage was not affected, and organisms grew with a  $t_2$  of about 20 h. When resistant cells were seeded in drug-free medium, there was a short lag in growth followed by a growth rate comparable to wildtype organisms ( $t_2 \sim 12$  h). Treating wildtype cells with 1  $\mu\text{M}$  or higher concentrations of CB3717 resulted in their degeneration and death. Cells resistant to CB3717 showed cross-resistance to MTX; for example, when CB250 cells were seeded in medium containing 1.0 mM MTX, a lethal concentration for wildtype cells, growth rate did not change.

**Overproduction of TS-DHFR in CB3717-resistant L. major.** Soluble extracts of the wildtype organisms used here possessed 4 pmol (mg protein)<sup>-1</sup> and 6 units (mg protein)<sup>-1</sup> of TS and DHFR, respectively. Although enzyme levels were not determined at each step



of the selection procedure, it is clear that cells resistant to CB3717 overproduce TS-DHFR. Cells resistant to  $2.0 \mu\text{M}$  CB3717 showed a 15-fold increase in the bifunctional protein, whereas those resistant to 25, 50, and  $250 \mu\text{M}$  all showed similar increases of about 50-fold over wildtype organisms (Table I). The CB50 and CB250 cell lines have thus far been kept in continuous culture in the presence of CB3717 for 4 months without change in enzyme levels.

**Purification and Properties of TS-DHFR.** TS-DHFR from CB250 cells was initially purified by ion-exchange chromatography on DEAE-cellulose followed by affinity chromatography on MTX-Sepharose, as described for the protein from MTX-resistant cells (7). Subsequently, we found that affinity chromatography alone was sufficient to purify the enriched TS-DHFR to homogeneity. For example, starting with a crude extract from CB250 cells containing  $340 \text{ units mg}^{-1}$  of DHFR, affinity chromatography on MTX-Sepharose provided a 40-fold purification with 90% recovery of the purified protein.

The purified TS-DHFR showed a single band on denaturing gel electrophoresis ( $M_r = 56,200$ ) and on isoelectric focusing ( $\text{pI} = 6.4$ ); reverse phase high performance liquid chromatography showed a single peak with retention volume of 12.0 ml. For TS, the apparent  $K_m$  values of dUMP and (6R)-L- $\text{CH}_2\text{H}_4$ folate were 2.8 and  $32 \mu\text{M}$ , respectively;  $V_{\text{max}}$  was  $3.2 \mu\text{mol min}^{-1} \text{ mg}^{-1}$ . For DHFR, the  $K_m$  for  $\text{H}_2$ folate was  $1.3 \mu\text{M}$  and  $V_{\text{max}}$  was  $25 \mu\text{mol min}^{-1} \text{ mg}^{-1}$ . These structural and kinetic properties are well within experimental error of those previously reported for TS-DHFR from MTX-resistant L. major (7).





**Table 1.** Quantitation of R-region DNA copy number and TS and DHFR levels in *L. tropica* promastigotes resistant to increasing amounts of CB3717.

Cell line	R-region DNA copy number <sup>a</sup>	TS (pmol·mg <sup>-1</sup> ) <sup>b</sup>	DHFR (units·mg <sup>-1</sup> ) <sup>b</sup>
CB.01	1	4	6
CB.05	1	- <sup>c</sup>	- <sup>c</sup>
CB.8	8	- <sup>c</sup>	- <sup>c</sup>
CB2	20	60	110
CB25	120	170	320
CB50	110	130	290
CB250	110	240	430

<sup>a</sup>Average of two to three determinations; range of values was  $\pm 20\%$  of the mean.

<sup>b</sup>Average of values from at least four different crude extract preparations, Values varied  $\pm 15\%$  from the mean.

<sup>c</sup>Not determined.

When the standard TS assay was initiated with enzyme from either CB3717- or MTX-resistant L. major, double reciprocal plots indicated that CB3717 was a competitive inhibitor with respect to  $\text{CH}_2\text{H}_4$ folate with  $K_i = 4.0$  nM. In addition to its effect on TS, CB3717 also inhibited DHFR from both CB3717- and MTX-resistant cell lines; the inhibition was competitive with respect to  $\text{H}_2$ folate and the  $K_i$  was  $0.2 \mu\text{M}$ .

**Amplified DNA in CB3717-resistant L. major.** When DNA from wildtype and CB3717-resistant cells was digested with various restriction enzymes, electrophoresed in agarose gels, and stained with ethidium bromide, specific fragments could be visualized in the DNA of resistant cells that were not apparent in DNA from wildtype cells, and that corresponded to the amplified R-region of stable MTX-resistant cells (Fig. 1). These amplified regions were visible in DNA from cells resistant to  $0.8 \mu\text{M}$  CB3717 and persisted in DNA from cells resistant to higher concentrations of the drug. When  $\lambda$  LTS-14 and  $\lambda$  LTS-2 were used as hybridization probes for the 30-kb amplified R-region, Southern blot analysis of five restriction digests of the DNA from CB3717-resistant cells and MTX-resistant L. major possessing the amplified R-region showed that the amplified fragments were almost identical (Fig. 2); the only detectable difference was that the 4.1-kb BglII fragment was about 200 bp larger in the cells resistant to CB3717. There was no apparent change in the restriction maps during the selection or after resistant organisms were propagated in  $50 \mu\text{M}$  CB3717 for up to 6 months. The restriction-site maps of the amplified DNA from CB2, CB25, CB50, and CB250 cells were all the same.



## Figure 1

Comparison of DNA amplification in L. major resistant to MTX or CB3717. DNA was isolated from wildtype (WT) CB3717-resistant (CB50), and MTX-resistant (R1000) cell lines and digested with the indicated restriction endonucleases. Approximately 1  $\mu$ g of DNA was applied to each lane. The R1000 DNA was prepared from a cell line that had been adapted to 1 mM MTX and propagated in 1 mM MTX for an additional 12 months. The CB50 DNA was prepared from the cell line undergoing the stepwise CB3717 selection after growing in 50  $\mu$ M CB3717 for 35 generations (approx. 1 month). Electrophoresis was in 0.8% agarose; size standards were from a HindIII digest of  $\lambda$  DNA. Gel was stained with ethidium bromide.

1  
2  
3  
4  
5  
6  
7  
8  
9  
10  
11  
12  
13  
14  
15  
16  
17  
18  
19  
20  
21  
22  
23  
24  
25  
26  
27  
28  
29  
30  
31  
32  
33  
34  
35  
36  
37  
38  
39  
40  
41  
42  
43  
44  
45  
46  
47  
48  
49  
50  
51  
52  
53  
54  
55  
56  
57  
58  
59  
60  
61  
62  
63  
64  
65  
66  
67  
68  
69  
70  
71  
72  
73  
74  
75  
76  
77  
78  
79  
80  
81  
82  
83  
84  
85  
86  
87  
88  
89  
90  
91  
92  
93  
94  
95  
96  
97  
98  
99  
100

1  
2  
3  
4  
5  
6  
7  
8  
9  
10  
11  
12  
13  
14  
15  
16  
17  
18  
19  
20  
21  
22  
23  
24  
25  
26  
27  
28  
29  
30  
31  
32  
33  
34  
35  
36  
37  
38  
39  
40  
41  
42  
43  
44  
45  
46  
47  
48  
49  
50  
51  
52  
53  
54  
55  
56  
57  
58  
59  
60  
61  
62  
63  
64  
65  
66  
67  
68  
69  
70  
71  
72  
73  
74  
75  
76  
77  
78  
79  
80  
81  
82  
83  
84  
85  
86  
87  
88  
89  
90  
91  
92  
93  
94  
95  
96  
97  
98  
99  
100

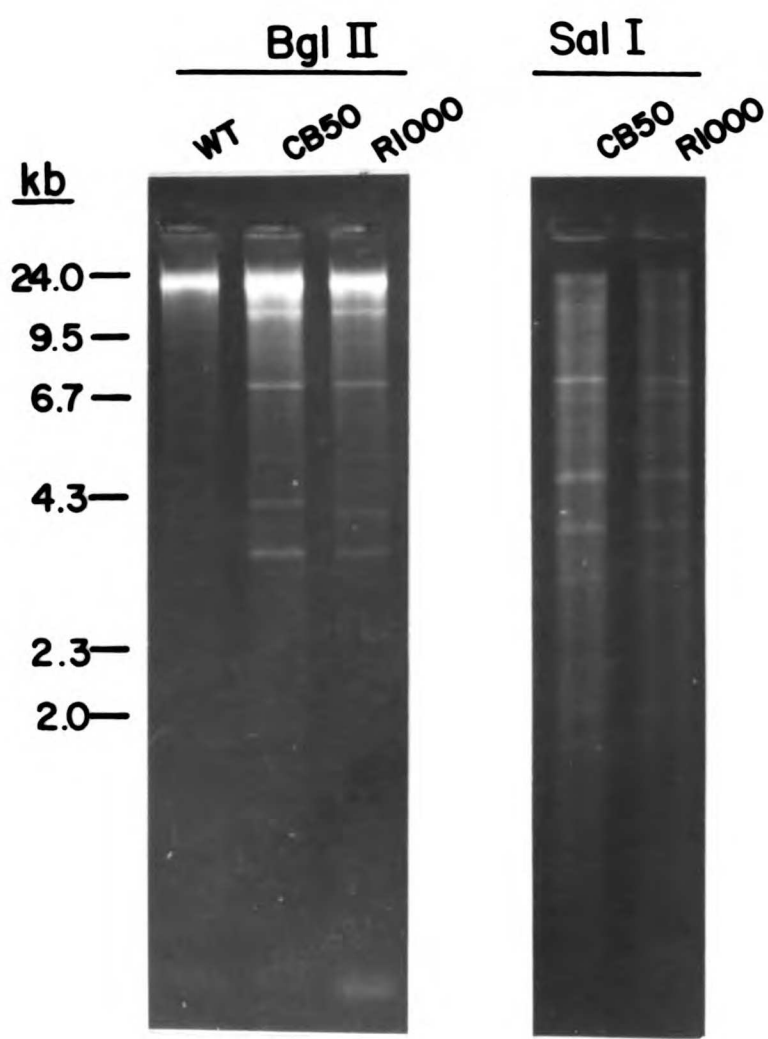
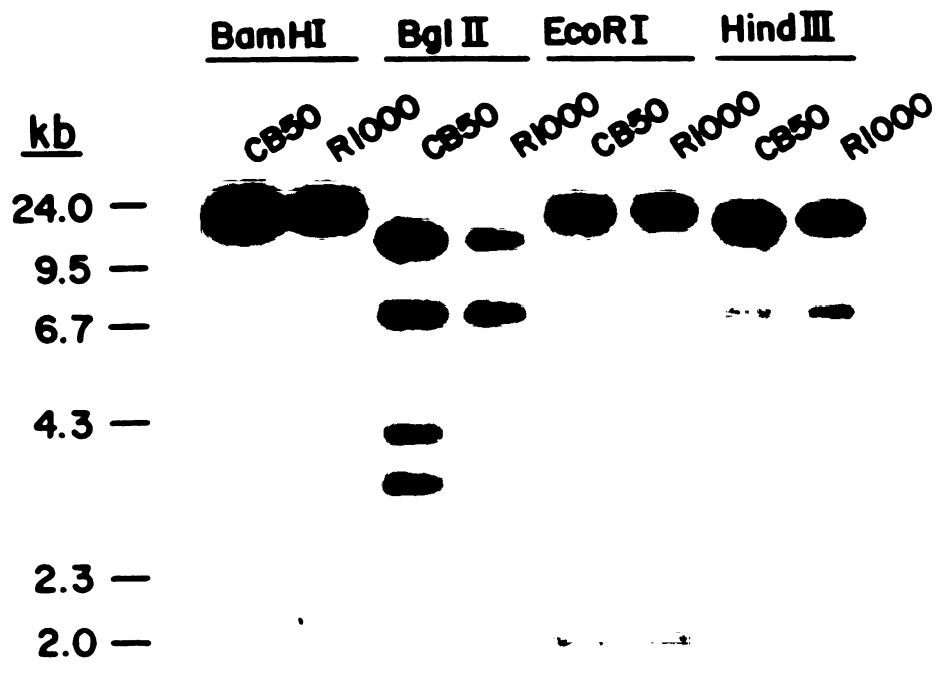


## Figure 2

Comparison of the regions of DNA amplified in the CB50 and R1000 cell lines. CB50 DNA and R1000 DNA were digested with the indicated restriction endonucleases, electrophoresed in 0.8% agarose, and transferred to nitrocellulose. The probe used was a mixture of the 2 recombinant phage from the wildtype genomic library ( $\lambda$  LTS-14,  $\lambda$  LTS-2), which together contain all but 2 kb of the 30-kb R-region of DNA. The probe specific activity was approximately  $7 \times 10^7$  cpm ( $\mu\text{g DNA}$ )<sup>-1</sup>; hybridization was carried out as described in Materials and Methods.







To determine the copy number of the amplified DNA, EcoRI digests of DNA from wildtype L. major and 1:2 serial dilutions of DNA from resistant organisms were electrophoresed, transferred to nitrocellulose, and hybridized to nick-translated [<sup>32</sup>P]pLR-R1; after autoradiography, the grain densities of the 2-kb fragments were determined and the intensities were compared to that of wildtype DNA. As shown in Table I, cells resistant to 0.8 and 2.0  $\mu$ M CB3717 have an 8- and 20-fold increase, respectively, of the R-region DNA; cells lines resistant to higher concentrations all have about a 100-fold increase in copy number compared to wildtype organisms. In a similar experiment, HindIII digests of DNA from wildtype and CB3717-resistant organisms were probed with the H-region specific probe, pLR-HM3; in resistant organisms, the copy number of the H-region was identical to that of wildtype organisms.

As previously described (4), during the initial phase of development of MTX-resistant L. major, the amplified R-region exists as a 30-kb supercoiled circle of extrachromosomal DNA which migrates on 0.4% agarose gels with an apparent size of 17 kb. Cells resistant to 0.8 and 2  $\mu$ M CB3717 also had native DNA which migrated on electrophoresis with an apparent size of 17 kb and hybridized with the R-region pLR-R1 probe (Fig. 3). After the DNA was transferred to nitrocellulose and autoradiography was performed, scanning densitometry indicated that about 40% of the amplified DNA in CB0.8 cells and 20% of the amplified DNA in CB2 cells migrated with an apparent size of 17 kb; the remainder was associated with higher molecular weight forms of DNA. With cells resistant to higher

Vertical text on the left margin, possibly bleed-through from the reverse side of the page. The text is mostly illegible but appears to contain a list or index of items.

Main body of text, consisting of several paragraphs of dense, mostly illegible printed matter. The text is arranged in a standard left-to-right, top-to-bottom format. There are some faint markings and what appears to be a small rectangular box or stamp near the top center of the page.

Figure 3

Electrophoresis of DNA (unrestricted) from cell lines resistant to increasing concentrations of CB3717. Approximately 1  $\mu\text{g}$  of DNA was applied per lane; the agarose concentration was 0.4%. Electrophoresis was carried out at 10 V (constant voltage) for 72 h. The gel was soaked in 0.25 M HCl (2 X 7 min), 0.5 M NaOH, 1.5 M NaCl (2 X 15 min), and 1.0 M Tris, pH 8.0, 1.5 M NaCl (2 X 15 min), and the DNA was transferred to nitrocellulose. The probe used was the R-region specific pLR-R1; the specific activity was approx.  $8 \times 10^7$  cpm ( $\mu\text{g}$  DNA)<sup>-1</sup>.



WT    CB .01    CB .05    CB .8    CB2    CB25    CB50    CB250    R1000

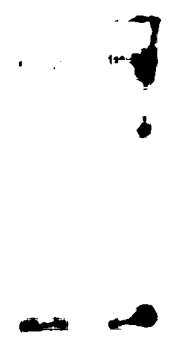
kb

30.0—  
24.0—

15.0—

9.5—

6.7—



concentrations of CB3717, we could detect no DNA with an apparent size of 17 kb; all amplified DNA migrated as higher molecular weight forms (Fig. 3).

**Reversion of CB3717-resistance.** When CB50 cells that had been propagated in 50  $\mu$ M CB3717 for about 2 months were grown in the absence of drug, growth rate increased ( $t_2 \sim 12$  h) and TS-DHFR as well as amplified DNA levels gradually declined (Fig. 4). By 125 generations, the TS-DHFR level had decreased to about 5 times the amount in wildtype organisms and appeared to remain at this level through subsequent passages up to at least 200 generations. Similarly, the amplified DNA decreased to levels about 10-fold higher than the wildtype organisms. Amplified DNA from CB50 organisms grown for 80, 185, and 250 generations in the absence of CB3717 showed higher molecular weight forms identical to amplified DNA from CB50 cells. Also, upon digestion with various restriction enzymes, DNA from cells 200 generations removed from CB3717 was the same as the digested DNA from CB50. When organisms grown in the absence of drug for 105, 170, and 180 generations were seeded in media containing 50  $\mu$ M CB3717, the cells resumed growth with  $t_2 \sim 20$  hr within one day; after 5 generations the organisms contained levels of TS-DHFR comparable to the original CB50 cell line. As mentioned above, when wildtype organisms were exposed to 1  $\mu$ M CB3717, cell death ensued.



120  
R-region  
DNA copy number (●)

Stability  
major CB  
propagated  
into drug  
as described  
determined

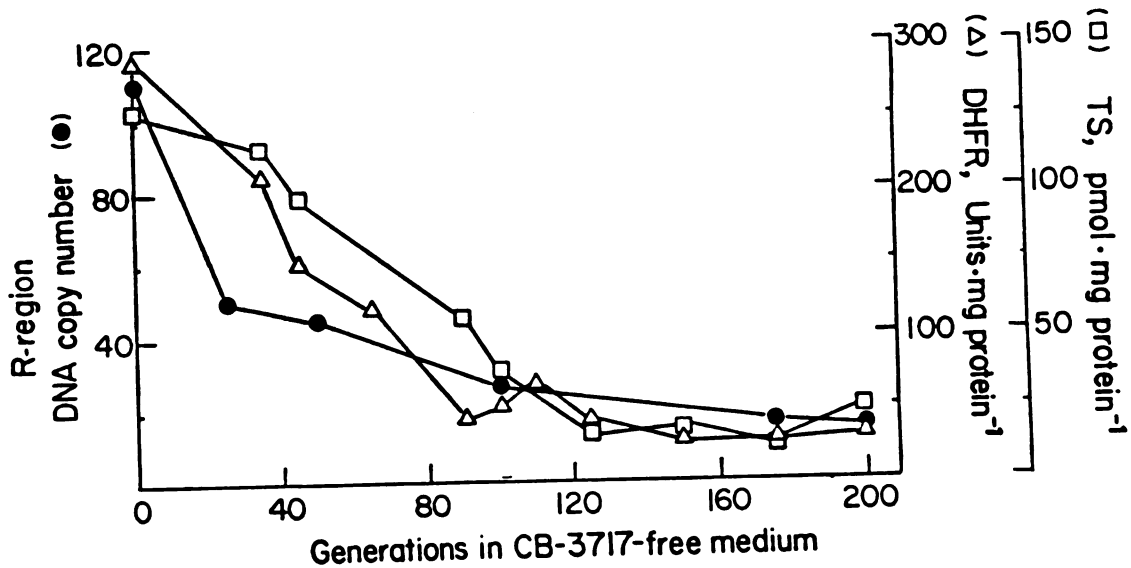


Figure 4

Stability of the amplified DNA and the elevated TS-DHFR levels in L. major CB50. L. major promastigotes adapted to 50  $\mu\text{M}$  CB3717, and propagated for 75 generations in this drug concentration, were seeded into drug-free medium. TS content and DHFR activity were determined as described in Materials and Methods; the gene copy number was determined by quantitative blot hybridization and densitometry.

### Discussion

As previously reported for mammalian TS (5,6), CB3717 is a potent inhibitor of the enzyme from L. major; the  $K_i$  is 4 nM and inhibition is competitive with respect to the folate cofactor  $\text{CH}_2\text{H}_4$ folate.

In response to stepwise selection with CB3717, L. major promastigotes were obtained that are resistant to high concentrations of the drug.

Organisms have been established that grow well in medium containing CB3717 at a concentration about 25,000-fold higher than is necessary to inhibit the growth of wildtype cells. Cells that are resistant to higher concentrations of CB3717 show a 50- to 60-fold increase in the level of TS-DHFR. The bifunctional enzyme represents about 2% of the total protein in crude extracts and can be purified to homogeneity in a single step by use of MTX-Sepharose affinity chromatography.

Kinetic properties ( $K_m$ ,  $K_{cat}$ ,  $K_i$  for CB3717) and structural parameters ( $M_r$ , pI) of TS-DHFR from resistant cells are essentially identical to those of the bifunctional enzyme from wildtype or MTX-resistant organisms (7). We conclude that a major factor in the resistance of L. major to CB3717 is overproduction of an apparently normal TS-DHFR.

When DNA from CB3717-resistant L. major was digested with several restriction endonucleases and electrophoresed, amplified DNA sequences were readily apparent upon visualization of gels stained with ethidium bromide. By restriction site map analysis and use of specific hybridization probes, the amplified DNA was shown to closely correspond to the R-region sequence of DNA found in the MTX-resistant cell line. As previously described (4), the restriction site map is consistent with a uniform amplified unit of DNA existing in a circular

The first part of the report deals with the general situation of the country and the progress of the war. It is followed by a detailed account of the operations of the army and the navy. The report also contains a list of the names of the officers and men who have been killed in action.

The second part of the report deals with the financial situation of the country. It contains a statement of the accounts of the Treasury and a list of the names of the officers and men who have been killed in action.

The third part of the report deals with the military situation of the country. It contains a statement of the accounts of the War Office and a list of the names of the officers and men who have been killed in action.

The fourth part of the report deals with the naval situation of the country. It contains a statement of the accounts of the Admiralty and a list of the names of the officers and men who have been killed in action.

The fifth part of the report deals with the general situation of the country. It contains a statement of the accounts of the Home Office and a list of the names of the officers and men who have been killed in action.

The sixth part of the report deals with the general situation of the country. It contains a statement of the accounts of the War Office and a list of the names of the officers and men who have been killed in action.

The seventh part of the report deals with the general situation of the country. It contains a statement of the accounts of the Admiralty and a list of the names of the officers and men who have been killed in action.

The eighth part of the report deals with the general situation of the country. It contains a statement of the accounts of the Home Office and a list of the names of the officers and men who have been killed in action.

The ninth part of the report deals with the general situation of the country. It contains a statement of the accounts of the War Office and a list of the names of the officers and men who have been killed in action.

The tenth part of the report deals with the general situation of the country. It contains a statement of the accounts of the Admiralty and a list of the names of the officers and men who have been killed in action.

form or repetitive arrays, or both. The only difference is a 200-bp increase in size of the amplified unit in the CB3717-resistant organisms. Interestingly, this difference occurs in the fragment that contains the junctional region believed to be the site of DNA rearrangements generated during amplification (4). As cells were selected for resistance to increasing concentrations of CB3717, the level of amplified R-region DNA, together with TS-DHFR, increased until the drug concentration was about 25  $\mu$ M. At this and higher levels of CB3717, resistant organisms showed about a 100-fold amplification of R-region DNA, which corresponds to over 5% of their nuclear DNA.

Throughout the selection and during continued propagation of L. major cells in CB3717, the restriction-site map of the amplified R-region DNA did not change. These results support the proposal that, after DNA rearrangements occur at an early step of amplification in these organisms, the amplified units of R-region DNA increase in number but do not change in structure. These features may be contrasted with gene amplification in drug-resistant mammalian cells (for review, see Ref. 10), which usually involves multiple DNA rearrangements and yields amplified DNA sequences with complex, heterogenous structures. Also, the structure of amplified DNA in mammalian cells is variable in independent selections, and often changes after the initial amplification or during continued propagation of cells in the drug.

Throughout the selection of CB3717-resistant L. major and upon continued propagation of organisms in the drug, there was no indication of amplified H-region DNA previously observed in

Faint, illegible text, possibly bleed-through from the reverse side of the page.

Faint, illegible text, possibly bleed-through from the reverse side of the page.

Faint, illegible text, possibly bleed-through from the reverse side of the page.

MTX-resistant cells (4). The function of H-region DNA remains unknown, but it is clearly not necessary for resistance to the drug. The absence of H-region DNA in the CB3717-resistant cells, together with the correlation of the levels of TS-DHFR and R-region DNA through the selection and reversion (see below), supports the proposal that R-region DNA contains the sequence that encodes the bifunctional protein. Further, we have recently identified four mRNAs that are abundant in both MTX- and CB3717-resistant cells and that specifically hybridize to probes derived from the R-region DNA; one of these has been shown to hybridize to a cDNA probe for mammalian TS and to direct the synthesis of TS-DHFR in an in vitro translation system (11).

At low concentrations of CB3717 (e.g., 0.8  $\mu\text{M}$ , 2.0  $\mu\text{M}$ ), resistant cells first acquire the amplified R-region DNA in a form which, upon gel electrophoresis, migrates as does the 30-kb extrachromosomal circle found in MTX-resistant cells (4). As cells were selected for resistance to higher concentrations of CB3717, the 30-kb circles were no longer observed, and the amplified DNA sequences migrated as high molecular weight forms. These probably represent extrachromosomal multimers of the R-region DNA or repetitive arrays of this sequence that have relocated into chromosomal DNA, or both.

When L. major promastigotes resistant to 50  $\mu\text{M}$  CB3717 were grown in drug-free medium, TS-DHFR and amplified DNA gradually declined. This is similar to what has been observed for the "unstable" MTX-resistant cell line, which undergoes an apparent reversion to wildtype levels of TS-DHFR and R-region DNA when propagated in drug-free media (3,4). However, these organisms did not completely revert to a wildtype phenotype. After about 125 generations in





drug-free media, the levels of TS-DHFR and amplified DNA were still about 5-fold and 10-fold, respectively, higher than in wildtype organisms; during continued propagation, further losses, if any, were minimal and even after 200 generations the levels of TS-DHFR and amplified DNA were significantly higher than in wildtype organisms. As with the MTX-resistant revertants, when these cells were re-challenged with drug, they rapidly reacquired the resistant phenotype. The revertant organisms may be a homogeneous population of cells that have a uniformly low copy number of stable R-region DNA; if so, the DNA must undergo rapid amplification since the concentration of drug used in the re-challenge would otherwise have been lethal. Alternatively, a subpopulation of revertants may exist that possesses high levels of R-region DNA and rapidly emerges when treated with CB3717. We are currently attempting to determine the distribution of amplified R-region DNA among cloned populations of the revertants.

In MTX-resistant L. major the loss of amplified DNA upon growth of organisms in drug-free medium has been attributed to independent segregation of the 30-kb extrachromosomal circles (4); the stable amplified sequences have been found to be associated with chromosomal DNA. This is analogous to mammalian cells that have undergone gene amplification where unstable amplified DNA is found in extrachromosomal elements and stable forms have become integrated into chromosomal DNA (10). The CB3717-resistant cells used to generate revertants were resistant to 50  $\mu$ M CB3717 and did not possess amplified DNA as the 30-kb extrachromosomal circle found in unstable MTX-resistant cells; rather, the amplified sequences were found in the aforementioned higher molecular weight forms of DNA. Most of the



amplified DNA in these organisms was lost upon growth in drug-free media but a fraction was stable under non-selective conditions. The stable amplified DNA of the revertants probably represents units of the R-region that have relocated as repetitive arrays into stable regions of chromosomal DNA. The amplified DNA that is lost during reversion may represent extrachromosomal elements that are multimers of R-region DNA; this would be in accord with previous observations on unstable amplified DNA in other systems (10). Although there is little precedent, we cannot rule out the possibility that amplified DNA was lost from chromosomal sequences that were unstable under non-selective conditions. Future studies of these revertants could reveal unusual DNA rearrangements or unusual structures of the amplified DNA.

#### References

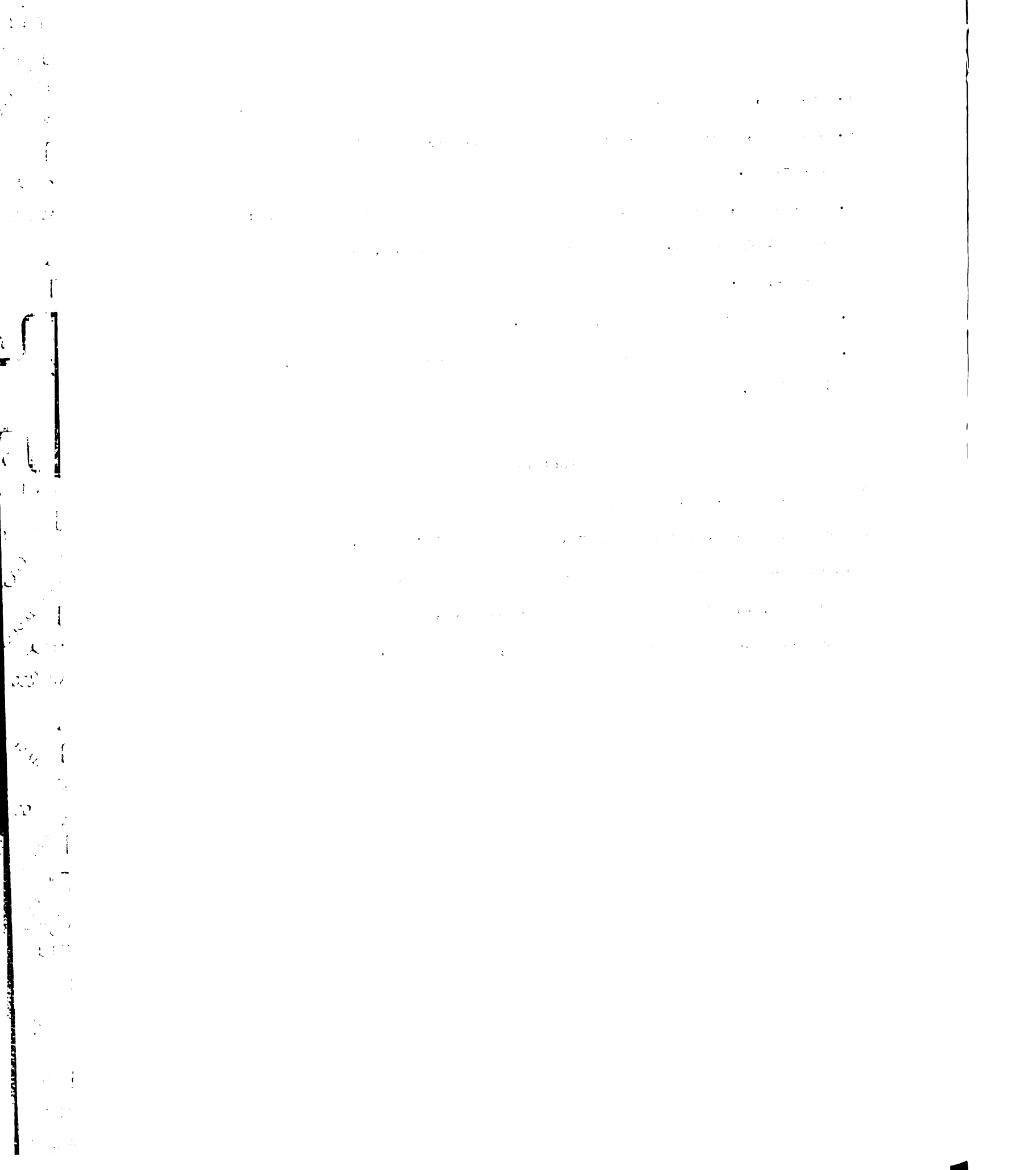
1. Garrett CE, Coderre JA, Meek TD, Garvey EP, Claman DM, Beverly SM, and Santi DV (1984) *Mol Biochem Parasitol* 11, 257-265.
2. Ferone R and Roland S (1980) *Proc Natl Acad Sci USA* 77, 5802-5806.
3. Coderre JA, Beverly SM, Schimke RT, and Santi D (1983) *Proc Natl Acad Sci USA* 80, 2132-2136.
4. Beverly SM, Coderre JA, Santi DV, and Schimke RT (1984) *Cell* 38, 431-439.
5. Jones TR, Calvert AH, Jackman AL, Brown SJ, Jones M, and Harrap KR (1981) *Eur J Cancer* 17, 11-19.
6. Jackson TR, Jackman AL, and Calvert AH (1983) *Biochem Pharmacol* 32, 3783-3790.



7. Meek TD, Garvey EP, and Santi DV (1985) *Biochemistry* 24, 678-686.
8. Brown PC, Beverley SM, and Schimke RT (1981) *Mol Cell Biol* 1, 1077-1083.
9. Maniatis T, Fritsch EF, and Sambrook J (1982) *Molecular cloning: a laboratory manual*. Cold Spring Harbor Laboratory, Cold Spring Harbor, NY.
10. Schimke RT (1984) *Cell* 37, 705-713.
11. Washtien WL, Grumont R, and Santi DV (1985) *J Biol Chem* 260, 7809-7812.

#### Footnote

<sup>1</sup> Abbreviations: TS, thymidylate synthase; DHFR, dihydrofolate reductase; CB3717, 10-propargyl-5,8-dideazafolate; FdUMP, 5-fluorodeoxyuridylate; MTX, methotrexate; H<sub>2</sub>folate, dihydrofolate; CH<sub>2</sub>H<sub>4</sub>folate, 5,10-methylenetetrahydrofolate; t<sub>2</sub>, time required for doubling the number of organisms; Kb, kilobase(s).



## **Chapter 2**

### **An Altered Dihydrofolate Reductase in Methotrexate-resistant**

#### ***Leishmania major***

### Abstract

*Leishmania major* promastigotes have been selected for resistance against the anti-folate methotrexate (MTX). This is the third such investigation in which the bifunctional protein thymidylate synthase- dihydrofolate reductase (TS-DHFR) has been used as the drug target to select for resistant organisms. These MTX-resistant cells display amplified R-region DNA, which contains the gene for TS-DHFR. Similar amplified DNA has been observed and characterized in the previous studies on resistance. Of greater interest, these MTX-resistant cells also possess a structurally-altered TS-DHFR. This alteration has weakened the affinity of DHFR toward MTX some 30-fold, lessened the catalytic efficiency of DHFR by 4-fold, and shifted the pI of TS-DHFR to a more negatively- charged molecule. These changes were observed both in crude extracts and in purified protein. It was also apparent both by structural and kinetic studies that cells resistant to high levels of MTX possessed both altered and wildtype enzymes in a 5-6 to 1 ratio. Finally, we examined the effect on MTX inhibition of DHFR. The initial inhibition complex appears to have been unaffected by the alteration. In contrast, the slow-binding step of inhibition, which has been attributed to a conformational change, seems to have been completely relieved.



Drug resistance in cultured animal cells has been well characterized. Three of the most common mechanisms by which these cells adjust to selection pressure have been defined: amplification of the gene for the drug target, reduction in the affinity of the drug target for the drug, and alteration in the transport of the drug into the cell (for review, see refs 1,2). Do these three mechanisms exist in the protozoan parasite, *Leishmania*? We have examined drug resistance in cultured *Leishmania major* promastigotes, and have previously described three resistant cell lines. In two studies, we used inhibitors of the bifunctional protein thymidylate synthase-dihydrofolate reductase (TS-DHFR) to select for resistance (3,4,5). In both of these studies, the major means by which these cells overcame selection pressure was the amplification of the gene for TS-DHFR. In the third study, *L. major* promastigotes were selected for resistance against Formycin B, a potent inhibitor of leishmanial growth (6); in these resistant cells the drug was blocked from entering the cell. Ullman and coworkers have also characterized *L. major* resistant to Formycin B (7).

The cells resistant to methotrexate (MTX) (3,4) or to 10-propargyl-5,8-dideazafolate (CB3717) (5) have both amplified a similar unit of DNA (labeled R-region DNA). This R-region DNA has been shown to be extrachromosomal and circular by electrophoresis on chromosomal gels (8). The size of both of the R-region circular units is about 30 kb, with the one generated in CB3717-resistant cells slightly larger. The gene for TS-DHFR is situated within the R-region sequence (9, 10), and it comprises approximately 1.5 kb of the 30-kb unit. In addition to the mRNA for TS-DHFR, we have shown that at least 3 mRNAs are overproduced and hybridize to the R-region DNA (9); we do not know, however, if these additional mRNAs translate into protein, or if these proteins, when expressed, play a functional role in resistance. In addition to the R-region DNA, another DNA has been amplified in the MTX-resistant (3) but not in the

CB3717-resistant cells (5). This DNA was labelled H-region DNA, and its function in these resistant organisms, if any, is unknown. In both of these studies, the kinetic and structural properties of TS-DHFR purified from cells resistant to either MTX (13) or CB3717 (5) were indistinguishable from those of the enzyme isolated from wildtype cells (13). We concluded that the major mechanism for resistance observed in these studies was gene amplification.

We have continued to explore the question of drug resistance in *Leishmania*, in order to more fully define the previous studies and also to develop independent resistant cell lines. We report here another *L. major* cell line which is again resistant to MTX. Like the two previous resistant cell lines, these *Leishmania* possess amplified R-region DNA. Unlike the previous resistant cells, they also contain an altered TS-DHFR in which the DHFR activity binds MTX less tightly. Interestingly, the initial MTX-enzyme complex appears to be unchanged, whereas the slow-binding step of MTX inhibition appears to have been relieved by this alteration in DHFR.

### Materials and Methods

**Selection of MTX-resistant *L. major*.** *L. major* promastigotes were derived from a clone (D7B) isolated from strain 252, Iran (S. Meshnik). Organisms were grown at 26 °C in M199 medium (Gibco) supplemented with 20% fetal calf serum, 25 mM Hepes, pH 7.4, and, when specified, MTX. MTX-resistant strains of *L. major* promastigotes were obtained by stepwise selection of resistant cells at drug concentrations of 5, 10, 25, 50, 100, 200, 500, and 1000 µM MTX. Detailed description of the development and properties of the resistant organisms was essentially the same as in the original MTX-resistant *L. major* (3). Resistant cell lines are designated as R followed by the µM concentration of drug to which they were resistant, e.g., R1000 refers to cells that

1  
2  
3  
4  
5  
6  
7  
8  
9  
10  
11  
12  
13  
14  
15  
16  
17  
18  
19  
20  
21  
22  
23  
24  
25  
26  
27  
28  
29  
30  
31  
32  
33  
34  
35  
36  
37  
38  
39  
40  
41  
42  
43  
44  
45  
46  
47  
48  
49  
50  
51  
52  
53  
54  
55  
56  
57  
58  
59  
60  
61  
62  
63  
64  
65  
66  
67  
68  
69  
70  
71  
72  
73  
74  
75  
76  
77  
78  
79  
80  
81  
82  
83  
84  
85  
86  
87  
88  
89  
90  
91  
92  
93  
94  
95  
96  
97  
98  
99  
100



1  
2  
3  
4  
5  
6  
7  
8  
9  
10  
11  
12  
13  
14  
15  
16  
17  
18  
19  
20  
21  
22  
23  
24  
25  
26  
27  
28  
29  
30  
31  
32  
33  
34  
35  
36  
37  
38  
39  
40  
41  
42  
43  
44  
45  
46  
47  
48  
49  
50  
51  
52  
53  
54  
55  
56  
57  
58  
59  
60  
61  
62  
63  
64  
65  
66  
67  
68  
69  
70  
71  
72  
73  
74  
75  
76  
77  
78  
79  
80  
81  
82  
83  
84  
85  
86  
87  
88  
89  
90  
91  
92  
93  
94  
95  
96  
97  
98  
99  
100

were resistant to 1000  $\mu\text{M}$  MTX. In addition, the clone name of D7B is used as a prefix to differentiate between the resistant cells described here and the original MTX-resistant cells (3).

**Nucleic acid techniques.** Total *L. major* DNA was prepared as described (11), except that the cell lysis buffer contained 0.2 M tris-HCl, pH 8.0, and 0.1 M EDTA. Restriction endonucleases were obtained from commercial sources and were used as recommended by the supplier. The following procedures were used as described (12): labeling of DNA by nick translation, transfer of DNA from agarose gels to nitrocellulose, and hybridization of [ $^{32}\text{P}$ ]-labelled probes to DNA bound to nitrocellulose. The R-region hybridization probes were previously described (4); the probe containing the cDNA for TS-DHFR was reported elsewhere (10). The copy number of MTX-resistant *L. major* R-region DNA was determined by the method described previously (5).

**Protein techniques.** Crude extracts, either for determination of TS-DHFR levels or for purification of the bifunctional protein, was the same as reported (13), as was the purification procedure. Electrophoretic procedures and Western blot analysis were performed as previously described (14). Two-dimensional electrophoresis was performed by Protein Database Inc, modifying the procedure of O'Farrell (15). All other protein techniques not mentioned were as previously described (13).

**Enzyme Assays.** The rate of [ $^3\text{H}$ ]MTX dissociation from the MTX-NADPH-enzyme complex was determined by: 1) incubating 2  $\mu\text{g}$  (18 pmol) of D7BR1000 TS-DHFR or 1.2  $\mu\text{g}$  (11 pmol) of TS-DHFR from CB250 cells (5) with 100  $\mu\text{M}$  NADPH and 0.1  $\mu\text{M}$  [ $^3\text{H}$ ]MTX (18 Ci/mmol; Moravek Biochemicals) in 1.2 mls of 50 mM TES (pH 7.4), 2 mM DTT, and 1 mM EDTA, at 25  $^{\circ}\text{C}$ , for 45 min; 2) initiating dissociation by addition of 50  $\mu\text{M}$  cold MTX; and 3) separating the macromolecular-bound

from free [ $^3\text{H}$ ]MTX by filtering 100  $\mu\text{l}$  aliquots of the reaction mix on small columns of Sephadex G-15 by a slight modification of a previously described method (16); the chromatographic separation was performed at 4  $^{\circ}\text{C}$ . In terms of calculating the pmol of complex formed, it should be noted that TS-DHFR binds one mol of MTX per mol of dimer (13).

DHFR activity was monitored at 25  $^{\circ}\text{C}$  on a CARY 118 spectrophotometer (17). The standard assay mixture (1.0 ml) contained 50 mM TES (pH 7.0), 75 mM 2-mercaptoethanol, 1 mM EDTA, 1 mg/ml BSA, 0.1 mM NADPH, 0.1 mM  $\text{H}_2\text{folate}$ , and limiting amounts of enzyme. One unit of enzyme activity is defined as that amount of enzyme that produces 1 nmol of product per min. To determine the character and extent of MTX inhibition, 5-100 nM MTX was added, prior to enzyme, and the mix was allowed to equilibrate at 25  $^{\circ}\text{C}$  for 5 min. Reaction was then initiated with either 1.2 nM CB250 enzyme (5), or 3.6 nM D7BR1000 enzyme.

TS was quantitated by nitrocellulose filter binding of the covalent [ $^3\text{H}$ ]FdUMP- $\text{CH}_2\text{H}_4\text{folate}$ -enzyme complex, as previously reported (13).

## Results

**Amplified R-region DNA.** This laboratory has previously reported (3) that DNA amplification of only 10-fold in *Leishmania* can be visualized in gels stained with ethidium bromide (EtBr). When DNA was isolated from D7BR10, R100, and R1000 cells, digested with various restriction enzymes, electrophoresed in agarose gels, and stained with EtBr, a number of distinct fragments were apparent that were absent in wildtype cells (data not shown). When DNA was transferred to nitrocellulose, most, but not all, of these amplified DNA fragments hybridized to specific probes of the R-region

DN

resi

add

CB

simi

were

How

R-re

unct

be de

signif

cells

30-fo

origin

(5) ha

copy n

increas

cells re

the R-r

the MT

was sig

concent

appear t

DNA, including the cDNA for TS-DHFR (10). Thus, it was shown that D7B *L. major* resistant to MTX possessed amplified DNA which contained the gene for TS-DHFR. In addition, when restriction-site maps of the amplified DNA from these MTX-resistant and CB3717-resistant cells were directly compared, the D7B amplified DNA was shown to be similar to the R-region DNA that has been previously described (4,5). No differences were detected in the restriction fragments that encompass the gene for TS-DHFR. However, the overall size of the D7B R-region DNA was significantly larger than the other R-region DNAs (37 kb vs. 30 kb); and this difference in size appeared to be located in the junctional region, as determined by the restriction-site map analysis. These findings will be developed more extensively in a future report.

Amplification of the R-region DNA in MTX-resistant D7B *L. major* occurred in a significantly different pattern from that observed in previous resistant cell lines. The D7B cells resistant to 10, 100, and 1000  $\mu$ M MTX possessed, respectively, 25-, 15-, and 30-fold increases of the R-region DNA when compared to the wildtype copy number. The original 1 mM MTX-resistant cells (3,4) and the cells resistant to high levels of CB3717 (5) had shown at least an 85-fold increase in copy number. In addition, when level of copy number was determined during the selection of CB3717-resistant cells, the level increased proportionately to the concentration of drug to which the cells were resistant; cells resistant to 0.8, 2, and 50  $\mu$ M CB3717 possessed 8-, 20-, and 110-fold increases in the R-region DNA copy number. Therefore, although DNA amplification had occurred in the MTX-resistant D7B cells, the amount of amplification in cells resistant to 1 mM MTX was significantly less than in resistant cells previously described; and the relation between concentration of drug and amount of amplification during the selection procedure did not appear to be simple.

**TS-DHFR in D7B crude extracts.** When compared with levels of TS-DHFR in wildtype cells, D7B cells resistant to 10, 50, 100, and 1000  $\mu\text{M}$  MTX possessed increased levels of the bifunctional protein (Table I). However, the levels of TS, and especially DHFR, did not directly correlate with the concentration of drug to which the cells were resistant and the amount of TS-DHFR overproduction (as the data for DNA amplification had also suggested). The ratio of DHFR activity to amount of TS (unit:pmol) is a fairly constant number in crude extracts of wildtype, the original MTX-resistant cells, and CB3717-resistant cells. The ratio is usually between 1.5 and 2.0, but it can be higher due to the lability of TS (this lability has been examined previously (11)). In D7B cells resistant to 50  $\mu\text{M}$  or higher MTX, the ratio of DHFR to TS (approx. 0.2) was significantly lower than the ratio in either D7BR10 or wildtype cells (approx. 1.5). Considering these and the DNA results previously mentioned, we were curious if TS-DHFR had been altered during the selection process.

We electrophoresed crude extracts from wildtype, D7BR50, R100, and R1000 cells in a non-denaturing polyacrylamide gel to determine if these cells contain a structurally-altered bifunctional protein existed in these cells. A band that migrated with the same mobility as pure TS-DHFR<sup>1</sup> was seen in wildtype crude extract (Fig 1A). A band with this same mobility was also present in each of the other resistant cells. In addition, a band with a slightly-faster migration was observed only in the resistant cells.

<sup>1</sup> We have previously demonstrated that there are no detectable differences in the kinetic or structural parameters when TS-DHFR from wildtype, the original MTX-resistant, and the CB3717-resistant organisms is examined. Thus, the TS-DHFR that was actually purified from CB3717-resistant cells is referred to as wildtype TS-DHFR in this study.



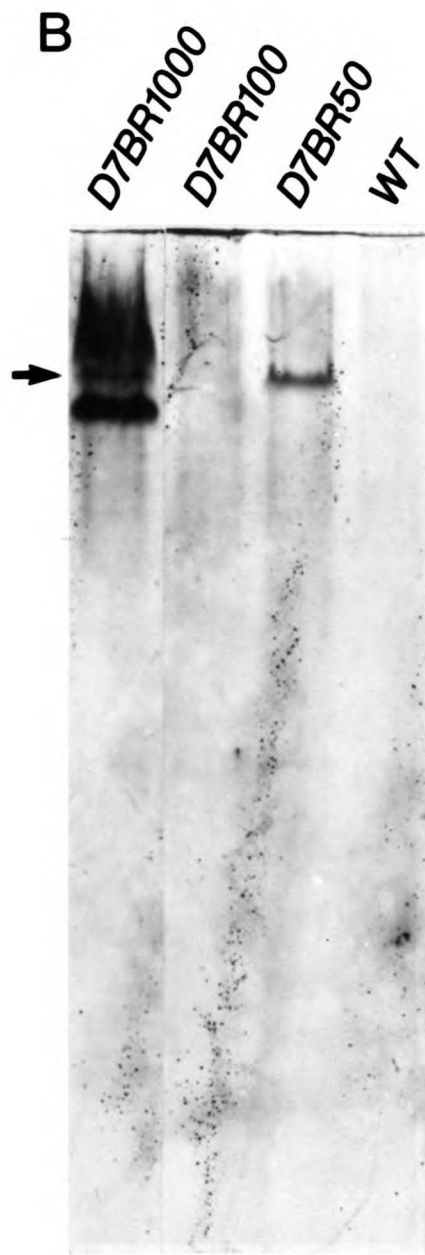
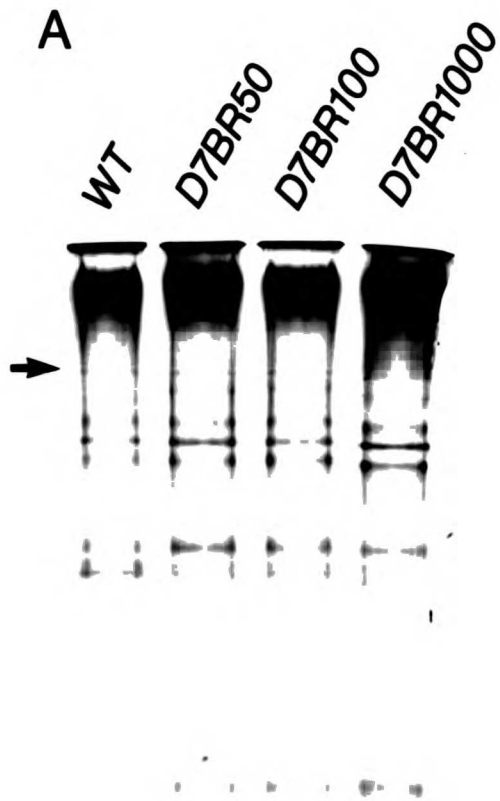
**Table I: DHFR and TS levels in crude extracts from D7B cells resistant to MTX and from wildtype cells**

<b>cell type</b>	<b>DHFR (u/mg)</b>	<b>TS (pmol/mg)</b>	<b>Ratio (DHFR u/TS pmol)</b>
wildtype	$6.0 \pm 1.5$	$4.0 \pm 2.0$	$1.5 \pm 0.8$
R10	$44 \pm 29$	$29 \pm 8$	$1.5 \pm 0.7$
R50	$35 \pm 9$	$92 \pm 16$	$0.38 \pm 0.08$
R100	$9.5 \pm 3.3$	$52 \pm 28$	$0.18 \pm 0.08$
R1000	$15 \pm 5$	$72 \pm 25$	$0.19 \pm 0.06$

Each value is an average from at least 4 different preparations of crude extract from the given cell line; each preparation taken from cells at least 10 generations apart. Each determination consists of assaying a crude extract for DHFR activity, TS binding, and protein; and each assay is done at least twice, with the average taken.

**Figure 1**

**Demonstration of a structurally-altered TS-DHFR. A.) Non-denaturing PAGE of crude extracts from wildtype, D7BR50, R100, and R1000 cells. The arrow points to the position to which pure wildtype TS-DHFR migrated in the lane directly adjacent to wildtype extract. B.) Western blot analysis of gel which was identical to Fig 1A. Again, arrow marks the wildtype TS-DHFR position.**



When the protein was transferred to nitrocellulose and probed with a polyclonal antibody to TS-DHFR, both of these bands displayed hybridization. The pure wildtype TS-DHFR, which hybridized to its antibody upon Western blot analysis, demonstrated that the slower-moving band was the wildtype bifunctional protein. We concluded that the faster-moving band represented TS-DHFR that had been structurally altered; in D7BR1000 cells, the faster-moving TS-DHFR clearly predominated over the wildtype enzyme.

We further analyzed the crude extracts from wildtype and D7BR1000 cells by two-dimensional (2-d) electrophoresis (Fig. 2). Initially, we located TS-DHFR on the 2-d map by immunoprecipitating TS-DHFR from crude extracts of 50  $\mu$ M CB3717-resistant cells (5), and then examined the wildtype extract with and without the immunoprecipitant.

When the extract from D7BR1000 cells was analyzed, a new spot was observed which had a slightly more basic pI relative to the wildtype TS-DHFR (Fig 2B). The relative intensity of the new spot was approximately 5 times greater than the spot that corresponded to wildtype TS-DHFR (as shown by densitometry). At least two other new spots also appeared in the D7BR1000 map, relative to the wildtype map: an acidic protein, with an approx. molecular weight of 60 kDa, and a protein with an approximate molecular weight of 40 kDa and with a pI of about 7. In conjunction with the data that showed amplified DNAs that do not hybridize to R-region probes, these proteins might represent additional responses to the MTX selection pressure.

To summarize, when extracts from MTX-resistant cells were analyzed either for amount of TS-DHFR or for possible structural changes in TS-DHFR, data indicated the existence of an altered bifunctional protein. The electrophoretic behavior of the altered protein was consistent when examined in two different systems; it migrated to a more basic pI in 2-d gels and migrated more quickly toward the anode in non-denaturing

## Figure 2

Two-dimensional gel electrophoresis of wildtype (A) and D7BR1000 (B) crude extract. Both figures show the upper righthand corner of the 2-d maps, so that the pH gradient runs from approximately 6 to 8, and the molecular weights decrease from the origin to approximately 25 kDa. The arrows point to the spot which represents the wildtype TS-DHFR, as determined by immunoprecipitating TS-DHFR from crude extracts of CB50 cells (5) and analyzing wildtype extract in the presence of the immunoprecipitate. The spot described in the text that is present in D7BR1000 extract (Fig 2B) and absent in wildtype extract (Fig 2A) is directly to the basic side of the wildtype TS-DHFR, at the same molecular weight.

A.

Acidic

Base



B.

Acidic

Base



polyacrylamide gels compared to wildtype TS-DHFR.

#### **Purification and structural characterization of D7BR1000 TS-DHFR.**

TS-DHFR from D7BR1000 cells was purified to apparent homogeneity in two steps, by a procedure previously described (13): ion-exchange chromatography on DEAE-Sepharose, followed by affinity chromatography on MTX-Sepharose. When we began with 12 DHFR u/mg, we were able to enrich the bifunctional protein about 400-fold and achieved a final specific activity of about 4000 DHFR u/mg. This is in contrast to the final specific activity of about 15,000 DHFR u/mg observed when TS-DHFR from wildtype, the original MTX-resistant cells (13), or the CB3717-resistant cells (5) is purified. When the purified TS-DHFR was analyzed by SDS-PAGE, a single band was observed with an apparent molecular weight of 56,300 (this TS-DHFR migrated with the same mobility as wildtype TS-DHFR). In order to ascertain the purity of the D7BR1000 TS-DHFR preparation, 10 ug of TS-DHFR was electrophoresed; no other band could be seen, demonstrating that the preparation was greater than 99% pure. In contrast, two bands were seen when the purified TS-DHFR was examined in urea-denaturing isoelectric-focusing (IEF) gels. One band comigrated with wildtype TS-DHFR; the other band was shifted toward a more basic pI. The ratio of the two bands was approximately 5, with the more basic protein being in excess. It is possible that the second band observed on the IEF gel represents a protein contamination of the TS-DHFR preparation. We felt that this is unlikely: the single, contaminating protein must have a subunit molecular weight that is virtually identical to TS-DHFR (different by less than a few hundred daltons), and the contaminating protein must have biospecifically bound to MTX-Sepharose and then have been eluted from the affinity column by dihydrofolate. Rather, data from the analysis of the purified TS-DHFR were consistent with data from examination of the crude extract, indicating that D7BR1000 cells contained both a wildtype and a structurally-altered

**TS-DHFR, with the altered enzyme in greater abundance.**

**Kinetic characterization of purified D7BR1000 TS-DHFR.** The kinetic parameters of the D7BR1000 TS-DHFR were measured (Table II). As detailed above, the D7BR1000 TS-DHFR preparation contained a mixed population of altered and wildtype enzymes, in an approximate ratio of 5 to 1. Hence, the following kinetic constants represent a mixture of values for the altered and wildtype enzymes. The  $K_m$ 's for both of the TS substrates were determined from double reciprocal plots in which the nonvaried substrate was kept at a fixed, saturating concentration. The  $K_m$  and the  $k_{cat}$  values were essentially the same as those previously reported for wildtype TS-DHFR (13). The slight decrease in  $k_{cat}$  is probably due to the lability of TS activity. The  $K_m$  values for both of the DHFR substrates were determined by analysis of progress curves (18); again, the second substrate was kept at a fixed, saturating concentration. The  $k_m$  values for NADPH and for dihydrofolate were similar to the values measured for the wildtype enzyme. However, the  $k_{cat}$  values obtained from both of these studies was significantly different from the values previously reported; the  $k_{cat}$  for DHFR from D7BR1000 cells was lower than the wildtype enzyme by a factor of 4. This lowering of the turnover number in DHFR catalysis partly explains the low ratios of DHFR to TS that had been observed in crude extracts (see Table I).

**MTX inhibition of D7BR1000 DHFR activity.** We analyzed the interaction of MTX with DHFR by two different approaches: measuring the rate of dissociation of [ $^3$ H]MTX from the MTX- NADPH-enzyme complex, and analyzing the progress curves resulting from DHFR activity in the presence and absence of MTX. Prior to measuring the rate of dissociation of MTX from the ternary complex, we attempted to



Table II: Kinetic constants for wildtype and D7BR1000 TS-DHFR

enzyme activity : substrate	$K_m$ (uM)	$k_{cat}$ (sec <sup>-1</sup> )
<b>TS: dUMP</b>		
wildtype <sup>a</sup>	$4.7 \pm 0.9$	$3.5 \pm 0.6$
D7BR1000 <sup>b</sup>	$5.8 \pm 0.9$	$2.5 \pm 0.4$
<b>(6R)-L-CH<sub>2</sub>-H<sub>4</sub>folate</b>		
wildtype <sup>a</sup>	$35 \pm 4$	$3.2 \pm 0.5$
D7BR1000 <sup>b</sup>	$29 \pm 3$	$1.8 \pm 0.4$
<b>DHFR: NADPH</b>		
wildtype <sup>c</sup>	$2.4 \pm 0.5$	$28 \pm 5$
D7BR1000 <sup>c</sup>	$1.0 \pm 0.1$	$6.0 \pm 0.5$
<b>H<sub>2</sub>folate</b>		
wildtype <sup>c</sup>	$0.4 \pm 0.1$	$26 \pm 6$
D7BR1000 <sup>c</sup>	$0.26 \pm 0.06$	$8.3 \pm 0.8$

a, values determined previously (13) by double reciprocal plots.

b, values determined by double reciprocal plots, taking initial vel. at various concentrations of the substrate. When  $K_{dUMP}$  was determined, CH<sub>2</sub>-H<sub>4</sub>folate was at 300 uM. When  $K_{CH-H folate}$  was determined, dUMP was at 100 uM.

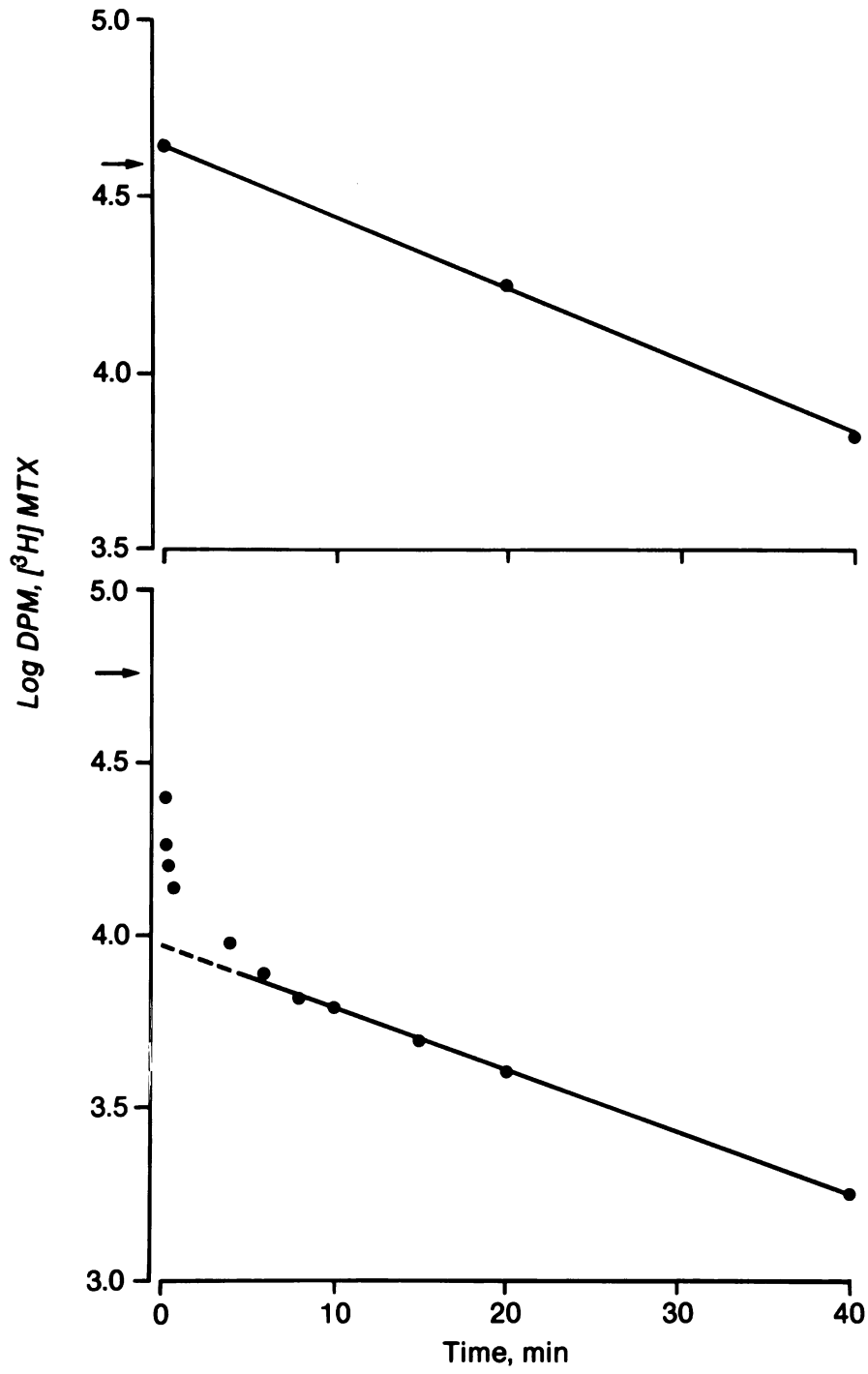
c, values determined by progress curve analysis (18); concentration of the fixed substrate was 100 uM.

measure the rate of dissociation from the [ $^3\text{H}$ ]MTX-enzyme binary complex. Wildtype TS-DHFR was incubated with [ $^3\text{H}$ ]MTX for 45 min, a 500-fold excess of cold MTX was added, and aliquots were assayed at different time points. Whereas some radioactivity was measured at the initial time point (immediately after cold MTX was added), it was only 50% of the amount expected, based on the amount of pure protein and the specific activity of [ $^3\text{H}$ ]MTX used. When the reaction was assayed either 5 min or later, no radioactivity was obtained. We took this as evidence that the rate of MTX dissociation from the binary complex was too fast to measure by the assay used. Therefore, the rate of MTX dissociation measured previously (13) and in this study was the rate from the ternary complex.

When we used pure wildtype TS-DHFR and measured the rate of MTX dissociation from the ternary complex, the results were similar to those previously measured (13); MTX dissociated with  $k=0.046 \text{ min}^{-1}$  (Fig 3A). Also, the amount of TS-DHFR measured at the initial time point was in agreement with the amount calculated from the protein concentration of TS-DHFR. When we used purified enzyme from D7BR1000 cells, we obtained quite different results (Fig 3B). The radioactivity detected at the initial time point was only 40% of what was expected; and during the first minute after the cold MTX was added, a very rapid drop in radioactivity was observed (the rate of dissociation was determined in three separate experiments). This quick drop in radioactivity was followed by a rate of dissociation that was indistinguishable from the rate when wildtype enzyme was employed. When the slower rate was extrapolated back to the zero, it intercepted the y-axis at a value that represented 17% of the total amount of enzyme used (based on the specific activity of the [ $^3\text{H}$ ]MTX). Thus, it was apparent that the dissociation of MTX from its ternary complex with NADPH and the enzyme from

### Figure 3

**Rates of MTX dissociation from the MTX-NADPH-enzyme complex. Top figure shows the rate observed when wildtype TS-DHFR was used. Bottom figure displays the results when D7BR1000 purified enzyme was used. Assay is described in Materials and Methods. The arrows indicate the amount of radioactivity expected to be present at the zero time point, based on the protein concentration of TS-DHFR and the specific activity of [<sup>3</sup>H]MTX. The data presented in the top figure represent the average of two separate determinations of the dissociation rate; the data presented in the bottom figure represents the average of three separate determinations of the rate.**



D7BR1000 cells displayed biphasic kinetics, in contrast with the monophasic kinetics of dissociation observed previously when wildtype TS-DHFR was used. These data were consistent with all the previous data and suggested a heterogeneous population of TS-DHFR within D7BR1000 cells, with the amount of structurally-altered enzyme approximately 83%/17%=5 times the amount of wildtype enzyme. We interpreted the rapid drop of radioactivity during the first minute as representing the rapid rate of MTX dissociation from the structurally-altered TS-DHFR, in the presence of NADPH; this rate was too fast to measure by this assay. Thus, the alteration in TS-DHFR appeared to have caused DHFR to bind less tightly to its potent inhibitor.

We had previously characterized the steady-state inhibition patterns observed when *L. major* DHFR was treated with MTX (13). MTX inhibition of DHFR displayed characteristics of a stoichiometric inhibitor, and had an apparent  $K_i=0.13\pm 0.04$  nM when analyzed by the method reported by Cha (19). In these experiments, we had preincubated enzyme with MTX and NADPH for 10 min, and then initiated the reaction with dihydrofolate. Subsequent to these studies, we have further examined the steady-state inhibition patterns. When the DHFR reaction was initiated with enzyme and the MTX concentration was varied from 0-30 nM, a time-dependent decrease in the enzyme-catalyzed rate was seen that varied as a function of inhibitor concentration (Fig 4A). This pattern was characteristic of the slow-binding step of DHFR inhibition by MTX that has been extensively studied with the enzyme from other sources (20, 21, 22). We obtained an approximate value for the rate constant of this slow-binding process by assuming it was analogous to the rate-limiting step of enzyme inactivation by a mechanism-based inhibitor (Scheme I). First, the progress curves were analyzed by assuming that the rates reflected a pseudo-first order process; we computer-fitted the data

**Figure 4**

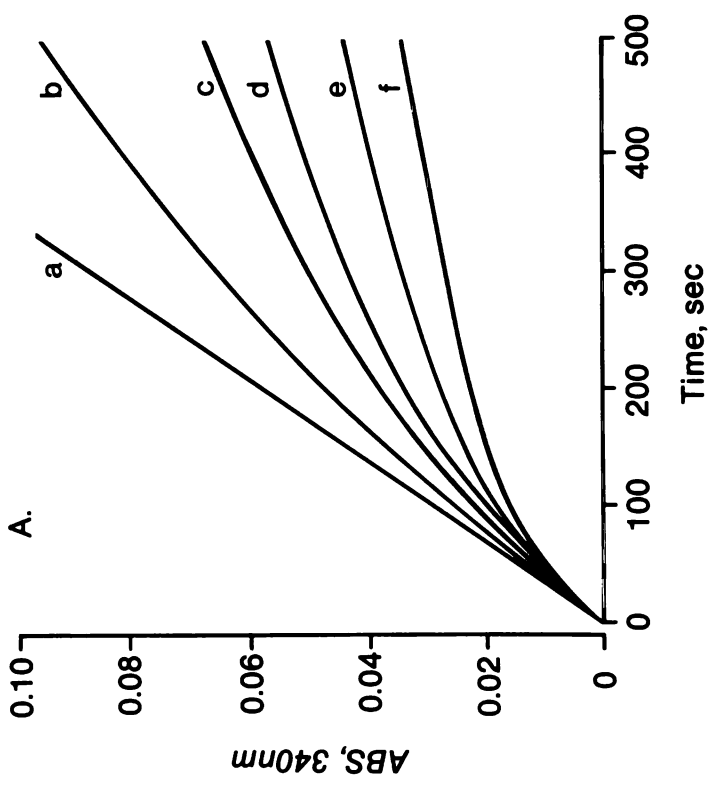
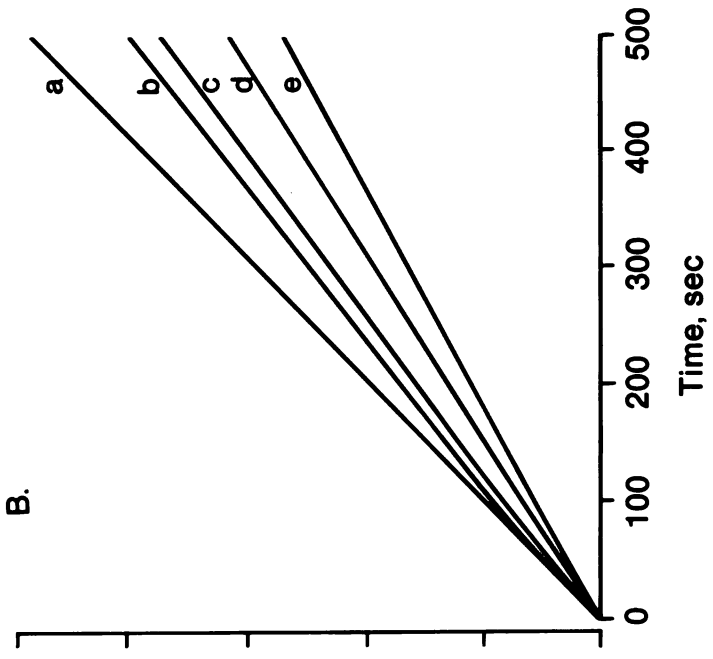
**Character and extent of DHFR inhibition by MTX. A.) Progress curves for the slow development of inhibition of wildtype DHFR by MTX. Reactions were started by addition of enzyme (1.2 nM). Composition of reaction is given in Materials and Methods.**

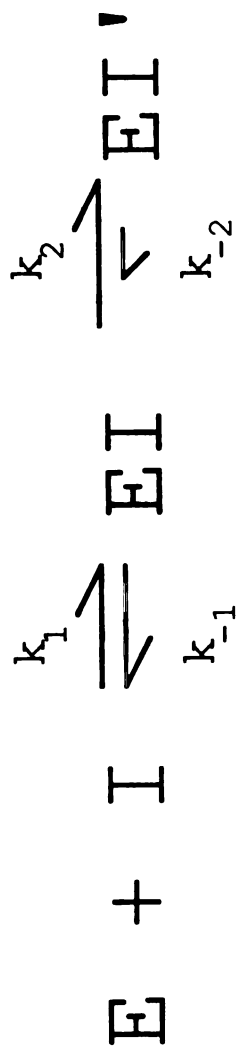
**Concentrations of MTX are as follows: (a) 0; (b) 5 nM; (c) 10 nM; (d) 15 nM; (e) 20 nM;**

**(f) 30 nM. B.) Reaction rates for the inhibition of D7BR1000 DHFR by MTX. Reactions**

**were started by addition of enzyme (3.6 nM). Concentrations of MTX are as follows: (a)**

**0; (b) 10 nM; (c) 20 nM; (d) 50 nM; (e) 100 nM.**





Scheme I



to equation 1:

$$[\text{NADP}] = v_f t - (v_f - v_i)(1 - e^{-kt})/k_{\text{obs}} \quad (1)$$

where  $v_i$  and  $v_f$  are the initial and final DHFR steady-state rates, and  $k_{\text{obs}}$  is the pseudo-first order rate constant. The reciprocal of the observed pseudo-first order rate constants were plotted vs. the reciprocal of the MTX concentration, employing eqn 2:

$$1/k_{\text{obs}} = (1/k_{\text{slowbind}}) + (K_i/k_{\text{slowbind}})[\text{MTX}] \quad (2)$$

where  $K_i$  is the equilibrium constant for the initial inhibition complex, and  $k_{\text{slowbind}}$  is the rate constant for the slow-binding process of inhibition. The  $k_{\text{slowbind}}$  for the wildtype enzyme was  $7.2 \pm 1 \text{ min}^{-1}$ , and  $K_i = 25 \text{ nM}$ ; these values were similar to the values reported for DHFR isolated from *Streptococcus faecium* A,  $5.1 \text{ min}^{-1}$  and  $23 \text{ nM}$ , respectively (20). When DHFR from D7BR1000 cells was used in these studies, both the appearance of the "progress curves" and the extent of inhibition at any given concentration of MTX were greatly changed (Fig 4B). , Although the steady-state rate was inhibited at high concentrations of MTX (above  $50 \text{ nM}$ ), this rate was linear; i.e., no time-dependent decrease in the reaction rate, which represents the slow-binding step of MTX inhibition, was detected with TS-DHFR from D7BR1000 cells. At  $10$  and  $20 \text{ nM}$  inhibitor, only a trace of the slow-binding inhibition was observed. Therefore, to determine an approximate value for  $K_i$  for MTX inhibition of the D7BR1000 enzyme, percent inhibition at the various MTX concentrations was determined, and assuming competitive inhibition, yielded a calculated value for  $K_i = 5 \text{ nM}$ .

We summarize the interaction between MTX and DHFR in Table III. When the overall inhibition constant is determined for the wildtype enzyme and compared with the

**Table III: Summary of interaction between MTX and DHFR from wildtype cells and from D7BR1000 cells.**

<b>process</b>	<b>wildtype DHFR</b>	<b>D7BR1000 DHFR</b>
<b>rate of [<sup>3</sup>H]MTX dissociation from the ternary complex</b>	$0.046 \pm 0.005 \text{ min}^{-1}$	$<0.3 \text{ min}^{-1}$
<b>rate of the slow-binding step of inhibition</b>	$7.2 \pm 1.0 \text{ min}^{-1}$	not detectable
<b>K<sub>i</sub> (overall)</b>	$0.14 \pm .05 \text{ nM}^{\text{a}}$	$5 \pm 1 \text{ nM}^{\text{b}}$

<sup>a</sup> the K<sub>i</sub> for the wildtype enzyme was determined by multiplying the K<sub>i</sub> for the initial inhibitory complex (23 nM) by the ratio of the rates for dissociation and association of the slow-binding complex.

<sup>b</sup>The K<sub>i</sub> D7BR1000 enzyme was determined by assuming competitive inhibition kinetics.

inhibition constant for the D7BR1000 enzyme, it is seen that D7BR1000 DHFR binds MTX less tightly by a factor of approximately 30. Because D7BR1000 TS-DHFR was actually a mixture of altered and wildtype enzymes, the difference in MTX affinity between wildtype and altered enzyme must be greater than 30. It should be noted that the overall inhibition constant determined in this study (0.14 nM) is the same as the value determined previously by a different approach (0.13 nM) (13). The difference in the overall inhibition appears to be divided into two effects: the initial competitive inhibition is approximately four times more tight in the D7BR1000 enzyme than in the wildtype enzyme, and the slow-binding step of MTX inhibition has been noticeably lessened in the D7BR1000 DHFR. Only at low MTX concentrations is a time-dependent decrease in the reaction rate observed, and this decrease is probably due to the wildtype enzyme that is present in the D7BR1000 preparation.

### Discussion

The data presented here demonstrate that D7B *Leishmania* resistant to high concentrations of MTX possess both amplified DNA and an altered TS-DHFR. The amplified DNA was shown to be the R-region DNA, which contains the gene for the bifunctional protein TS-DHFR. The R-region DNA has now been amplified in three resistant cell lines, albeit the size of the amplified unit is different in each cell line. More importantly, the present study shows that D7B *L. major* cells resistant to high concentrations of MTX contain an altered TS-DHFR as demonstrated by the following evidence. (1.) The ratio of DHFR to TS in crude extracts from D7B cells resistant to higher concentrations of MTX was significantly lower than the ratio that is measured in wildtype or previously-studied resistant cells (5, 13). This was in part due to the decrease

in the turnover number of the D7BR1000 DHFR. (2.) When crude extracts were electrophoresed in either 2-d gels or non-denaturing polyacrylamide gels, a band that was not present in wildtype cells was observed in D7BR1000 cells. This band represented a more negatively-charged molecule compared to wildtype TS-DHFR. Western blot analysis of the non-denaturing gel showed that the new band in D7BR1000 cells hybridized to a TS-DHFR antibody. (3.) Purified TS-DHFR from D7BR1000 cells showed a single band upon SDS-PAGE, which corresponded to the 56-kDa molecular weight for the wildtype TS-DHFR subunit. In contrast, there were two bands on urea-denaturing IEF gels. One band comigrated with wildtype enzyme; a second, more basic protein was approximately five times the wildtype enzyme. (4.) The D7BR1000 DHFR activity was approximately four times less efficient. The purified specific activity of DHFR was about 4000 u/mg (vs 15000 u/mg measured for the purified wildtype enzyme (13)); and the  $k_{cat}$  derived from the  $K_m$  studies was approximately  $7 \text{ sec}^{-1}$  (vs the wildtype enzyme's value of  $28 \text{ sec}^{-1}$ ). (5.) The rate of MTX dissociation from the MTX-NADPH- enzyme complex has been reduced from  $k=0.046 \text{ min}^{-1}$  to a rate that cannot be measured by the technique that we used ( $<0.3 \text{ min}^{-1}$ ). These experiments also suggested that a significant amount of wildtype TS-DHFR was present in the purified enzyme preparation, with an approximate ratio of altered to wildtype enzyme of 5:1. (6.) Steady-state rates showed a 30-fold increase in the concentration of MTX necessary to inhibit D7BR1000 DHFR, when compared with wildtype DHFR. (7.) These kinetics also demonstrated that the slow-binding process of MTX inhibition has been greatly reduced, if not completely removed, in the D7BR1000 enzyme. This will be discussed below. From these data we conclude that an alteration in the bifunctional TS-DHFR occurred that caused the following properties: (a) a reduction in the affinity of DHFR for MTX, (b) a decrease in the catalytic

efficiency of DHFR, and (c) a shift in the protein's pI toward a more basic molecule. The alteration did not cause any detectable change in the TS activity of the bifunctional protein.

We do not know what has caused the alteration in TS-DHFR. The most likely explanation is a point mutation within the gene for TS-DHFR (and probably, specifically within the DHFR portion), but other explanations are possible. We have results which suggest that the altered TS-DHFR is overproduced and thus is directly connected with the amplified R-region DNA. When D7BR1000 cells that have been in 1 mM MTX for 1 month are removed from drug for 80 generations, the amplified R-region DNA, as viewed by chromosome gels, decreases approximately 80% of the original value (8). TS-DHFR levels also drop by the same extent; however, the ratio of DHFR to TS also reverts back to the wildtype ratio of 1.5 (unpublished data). These data indicate that the altered TS-DHFR is overproduced, and that this overproduction is unstable (ie. the altered TS-DHFR is lost in the absence of drug selection pressure); this in turn suggests that the alteration occurs at the level of DNA sequence. We have recently determined the sequence for the bifunctional protein (10); we plan to sequence the gene for the D7BR1000 TS-DHFR in hopes of confirming the basis for the alteration in TS-DHFR.

An immediate question that arises is which came first, gene amplification or enzyme alteration. Although we cannot definitely answer this question at this time, we suspect that amplification of the R-region DNA occurred prior to alteration of TS-DHFR. In D7B cells resistant to 10  $\mu$ M MTX (the first selection step examined), there was a 25-fold increase in the R-region DNA copy number and also a 7-fold increase in the amount of TS-DHFR in crude extracts. In addition, the ratio of DHFR to TS in these cells was the same as the ratio in wildtype cells. Therefore, at least by first approximation, R10 cells possessed amplified DNA and overproduced a wildtype enzyme. Unfortunately, the

11  
12  
13  
14  
15  
16  
17  
18  
19  
20  
21  
22  
23  
24  
25  
26  
27  
28  
29  
30  
31  
32  
33  
34  
35  
36  
37  
38  
39  
40  
41  
42  
43  
44  
45  
46  
47  
48  
49  
50  
51  
52  
53  
54  
55  
56  
57  
58  
59  
60  
61  
62  
63  
64  
65  
66  
67  
68  
69  
70  
71  
72  
73  
74  
75  
76  
77  
78  
79  
80  
81  
82  
83  
84  
85  
86  
87  
88  
89  
90  
91  
92  
93  
94  
95  
96  
97  
98  
99  
100

cells resistant to 10  $\mu$ M MTX were lost, and therefore this viewpoint cannot be confirmed. Cells resistant to 50  $\mu$ M MTX appeared to represent an intermediate stage of resistance. Although R-region DNA was not quantitated in these cells, the level of TS-DHFR, and especially TS, indicated that the enzyme was still overproduced, possibly to a greater extent (TS level increased from 29 to 92 pmol/mg between R10 and R50 cells.) The R50 cells displayed the first decline in the DHFR/TS ratio (a decrease from 1.5 to 0.4); and, also possessed a structurally-altered TS-DHFR, as determined by non-denaturing polyacrylamide gels and subsequent Western blot analysis. Thus, of the cells we examined, R50 cells marked the first cell line that possessed an altered TS-DHFR. Cells resistant to 1000  $\mu$ M MTX represented the final stage of resistance. The copy number of the R-region DNA increased slightly from R100 to R1000 cells (15 to 30), and the altered TS-DHFR level showed a similar increase. Therefore, to our best understanding, the stepwise selection procedure produced the following responses: (1) amplification of the R-region DNA during the initial steps, (2) an alteration to the DHFR portion of the bifunctional protein that was somehow maintained at the R-region DNA level during the intermediate steps, and (3) a final resistant stage that was characterized by a mixed population of enzymes, and probably a mixed population of amplified R-region DNAs. We are in the process of cloning cells resistant to 1 mM MTX in an attempt to address this and other questions.

The altered DHFR has been shown to bind MTX less tightly by a factor of at least 30. The most interesting aspect of this altered binding is the significant reduction in the slow-binding step of MTX inhibition. This characteristic step in MTX inhibition has been thoroughly examined in DHFRs from *Streptococcus faecium* (20, 22), *E. coli*, and chicken (21). Because of this slow development of inhibition, MTX has been termed a slow-binding inhibitor. In addition, because the concentration of MTX necessary to inhibit

DHFR is comparable to that of the enzyme, MTX is further classified as a slow, tight-binding inhibitor (23). This type of inhibition is juxtaposed with classical, competitive inhibition which requires a significant excess of inhibitor over enzyme to effect inhibition, and produces only initial rates which are linear, albeit inhibited, upon binding to enzyme. The slow-binding process in MTX inhibition of DHFR has been attributed to a conformational change that the protein undergoes after MTX, NADPH, and protein have formed an initial, ternary complex (20, 21, 22). (A recent study has actually dissected this process into two measureable rates (22).) Williams et al. (20) proposed that, because MTX is such a good analogue of the substrate dihydrofolate, this conformational change might reflect a conformational change which mimics a conformational change that occurs during catalysis; hence, they termed MTX a pseudo-substrate. We present data here that demonstrate an alteration in *L. major* DHFR which relieves this slow-binding step in MTX inhibition, thereby changing MTX from a sub-nanomolar slow, tight-binding inhibitor into a nanomolar classical, competitive inhibitor. It is interesting to note that (1) neither of the  $K_m$ 's for the two DHFR substrates are significantly affected and that the initial inhibition complex between MTX and enzyme appears to have been unaltered; and (2) the slow-binding step of inhibition, and the catalytic efficiency of DHFR have been lessened. These observations are consistent with the proposal by Williams et al. (20) that the slow-binding process constitutes a conformational change that also occurs during catalysis. Finally, because the alteration has affected the overall charge of the protein, it is tempting to speculate that, in the wildtype TS-DHFR, an essential charged amino acid participates in an ionic bond interaction that locks the MTX-NADPH-enzyme complex in its final conformation. According to this hypothesis, this charged amino acid has been changed in the altered protein, thereby altering the protein's pI and removing the



slow-binding step of MTX inhibition.

Finally, we note the potential importance of the structurally-altered TS-DHFR to the field of molecular parasitology. If our suspicions prove correct and the alteration exists at the level of DNA sequence, then we will have an ideal unit of DNA to attempt to transform wildtype *Leishmania* promastigotes; a plasmid-like DNA that contains a DHFR which binds MTX less tightly by a factor of at least 30. No successful transformation studies have been done in *Leishmania* to date. The benefits derived from the transformation of these cells, about which only the most rudimentary genetics are understood, are both obvious and far-reaching.

#### References

1. Harrap, K.R., and Jackson, R.C. (1978) Antibiotics Chemother. **23**, 228-237.
2. Bruchovsky, N., and Goldie J.H. (1982) "Drug and Hormone Resistance in Neoplasia" Vol. 1 (CRC Press, Inc., Boca Raton, Fl.)
3. Coderre, J.C., Beverley, S.M., Schimke, R.T., and Santi D.V. (1983) Proc. Natl. Acad. USA **80**, 2132-2136.
4. Beverley, S.M., Coderre, J.C., Santi, D.V., and Schimke, R.T. (1984) Cell **38**, 431-439.
5. Garvey, E.P., Coderre J.C., and Santi, D.V. (1985) Mol. Biochem. Parasitol. **17**, 79-81.
6. Rainey, P., and Santi, D.V. (1984) Biochem. Pharmacol. **8**, 1374-1377.
7. Robinson, N., Kaur, K., Emmett, K. Iovannisci, D.M., Ullman, B. (1984) J. Biol. Chem. **259** 7637-7643.
8. Garvey, E.P., and Santi, D.V. (1986) submitted for publication.

9. Washtien, W.L., Grumont, R., and Santi, D.V. (1985) J. Biol. Chem. **260** 7809-7812.
10. Grumont, R., Washtien, W.L., and Santi D.V. (1986) submitted for publication.
11. Brown, P.C., Beverley, S.M., and Schimke, R.T. (1981) Mol. Cell Biol. **1** 1077-1083.
12. Maniatis, T., Fritsch, E.F., and Sambrook, J. (1982) Molecular cloning: a laboratory manual. Cold Spring Harbor Laboratory, C.S.H., New York.
13. Meek, T.D., Garvey, E.P., and Santi, D.V. (1985) Biochem **24**, 678-686.
14. Garvey, E.P., and Santi, D.V. (1985) Proc. Natl. Acad. Sci. USA **82**, 7188-7192.
15. O'Farrell, P.H. (1975) J. Biol. Chem. **250**, 4007-4021.
16. Garrett, C.E., Coderre, J.A., Meek, T.D., Garvey, E.P., Claman, D.M., Beverley, S.M., and Santi, D.V. (1984) Mol. Biochem. Parasitol. **11** 257-265.
17. Hillcoat, B., Nixon, P., and Blakley, R.L. (1967) Anal. Biochem. **21** 178-189.
18. Orsi B.A., and Tipton K.F. (1979) Methods in Enz. **63** 159-182.
19. Cha, S. (1975) Biochem. Pharmacol. **24** 2177-2185.
20. Williams, J.W., Morrison, J.F., and Duggleby, R.G. (1979) Biochem **18** 2567-2573.
21. Stone, S.R., Montgomery, J.A., and Morrison, J.F. (1984) Biochem. Pharmacol. **33**, 589-595.
22. Blakley, R.L., and Cocco, L. (1985) Biochem. **24**, 4772-4777.
23. Williams, J.W., and Morrison, J.F. (1979) Method in Enzymol. **63** 437-466.

### **Chapter 3**

## **Amplified DNA in Drug-Resistant *Leishmania* Exists As Extrachromosomal Circles**

### **Abstract**

**We had previously reported that the relative stability of amplified DNA in drug-resistant *Leishmania major* was dependent upon location: unstable amplified DNA was extrachromosomal and stable amplified DNA was chromosomal. We have now examined leishmanial chromosomes directly through the technique of orthogonal-field-alternation gel electrophoresis. The amplified DNAs in three resistant cell lines displayed unusual migration and were clearly extrachromosomal, regardless of whether the amplified DNAs were stable or unstable. To our knowledge, this is the first demonstration in eukaryotic cultured cells of stable, amplified DNA that is extrachromosomal. In addition, these amplified DNAs were shown to be circular on the basis of their resistant to exonuclease III digestion and their behavior upon OFAGE. Their mobility was also greatly changed after treatment with topoisomerase II, suggesting that the amplified DNAs were either supercoiled or concatenated circles.**

A basic tenet of gene amplification in drug-resistant cultured animal cells is that stability in the absence of continued drug pressure is determined by the location of the amplified gene (for review, see ref. 1). If the amplified gene occurs on acentromeric, extrachromosomal elements (double minute chromosomes), they segregate randomly in actively dividing cells and are eventually lost. If the amplified DNA resides on a chromosome, that DNA will be stable in the absence drug. We have previously reported on the stability of amplified DNA in drug-resistant *Leishmania major*, a parasitic protozoan (2,3,4). Results indicated that stability of gene amplification in this protozoan mimicked aspects of what had been found in cultured animal cells.

In our initial study of the molecular details of drug resistance in *Leishmania* (2), *L. major* promastigotes were selected for resistance against methotrexate (MTX), a potent inhibitor of dihydrofolate reductase. The resistant cell line overproduced the bifunctional protein thymidylate synthase-dihydrofolate reductase (TS-DHFR), with amplification of a 30-kilobase (kb) region of DNA (R-region DNA) (3) that contained the gene for TS-DHFR (5,6). The level of R-region DNA was approximately 100 times that of the wildtype copy number. The R-region was apparently generated by the joining of two regions of DNA separated by about 30-kb in wildtype organisms, yielding a rearranged "junctional" region in the amplified DNA. In cells grown in 1 mM MTX for three months (R1000-3 cells), a significant fraction of amplified R-region DNA existed as a 30-kb extrachromosomal, supercoiled circle, as shown by sedimentation in CsCl-ethidium bromide (EtBr) equilibrium gradients, and limited DNAase I digestion (3). When the resistant cells were grown in 1 mM MTX for 11 or more months (R1000-11 cells), most of the amplified DNA cosedimented with chromosomal DNA and, based on restriction site map analysis, was believed to have been incorporated into chromosomal DNA as a repetitive array of the 30-kb unit (3). In support of this belief, the R1000-11 amplified DNA persisted in leishmanial cells when MTX was withdrawn. In contrast, the R1000-3 amplified unit was

amplified DNA (H-region DNA) that was found in MTX-resistant cells has yet to be assigned a function. The amplified H-region DNA was also proposed to initially exist as an unstable, extrachromosomal circle in R1000-3 cells, and then to partly relocalize into chromosomes as stable DNA in R1000-11 cells.

*L. major* promastigotes were also selected for resistance against 10-propargyl-5,8-dideazafolate (CB3717) (4), an inhibitor of thymidylate synthase. These cells resembled the R1000 cells in that they overproduced TS-DHFR by amplification of the R-region DNA; however, CB3717-resistant cells did not possess amplified H-region DNA. The restriction-site map of the R-region DNA in these cells was nearly identical to the R1000 R-region map, except for a slight increase in size of the fragment that contains the rearranged junction of the R-region. When DNA was electrophoresed in 0.4% agarose, the R-region DNA from cells resistant to low levels of CB3717 (0.8 and 2  $\mu$ M) migrated with a similar mobility to the extrachromosomal circle found in R1000-3 cells. But in cells grown in 50  $\mu$ M CB3717 for 2 months (CB50-2 cells), the R-region DNA migrated in low-percentage agarose gels as higher molecular weight forms. Most, but not all, of the CB50-2 amplified DNA was shown to be unstable when CB3717 was removed from the medium; approximately 90% of the amplified DNA was lost in cells 125 generations removed from drug. Based on the electrophoretic properties, we assumed that the unstable amplified DNAs were high molecular weight, extrachromosomal forms, and that the stable DNA had been integrated into chromosome(s).

We now refine our earlier report concerning the location and nature of the stable amplified DNAs in R1000-11 cells, based on results we obtained when DNA from resistant cells was analyzed by orthogonal-field-alternation gel electrophoresis (OFAGE). This technique (7) is currently capable of fractionating high molecular weight DNAs up to 4000-kb. In addition, we have taken advantage of a gentle isolation procedure of DNA in which intact cells are embedded in agarose and then lysed *in situ* (8); breakage of DNA is

therefore greatly reduced. Enzymatic modifications of the DNA embedded in agarose blocks were permissible, thereby allowing the amplified DNA to be characterized.

**Wildtype *Leishmania* chromosomes.** DNAs from wildtype *L. major* promastigotes and from *S. cerevisiae* were electrophoresed in adjacent lanes (Fig. 1A). Most of the chromosomes of *L. major* are similar in size to those found in yeast. We used a number of different pulse times and were able to resolve 14 different EtBr-staining bands that ranged in size from approximately 300 to 2500-kb (Fig. 1B); this compares well with a recent report in which a similar technique, pulsed-field electrophoresis (8), was used to separate 17 leishmanial chromosomes (10). Some of the chromosomal bands were noticeably more intense than others, and were believed to either represent unresolved chromosomes or aneuploidism within *Leishmania*. When Southern blots were probed with the cDNA for the bifunctional protein TS-DHFR (6), a single chromosome (chromosome #4) displayed hybridization; likewise, only chromosome #6 hybridized when the H-region probe (3) was employed. Therefore, we concluded that these represented the chromosomal locus of the gene for TS-DHFR and the chromosomal location for the H-region DNA, respectively.

**Amplified DNA in drug-resistant *L. major* is extrachromosomal.**

When wild-type and R1000-11 DNA were analyzed by OFAGE, two bands absent in wild-type DNA were readily apparent in R1000-11 DNA (Fig 2A). When compared with the chromosomal DNA, these two new bands had an unusual banding pattern that was most apparent when they were actually superimposed on chromosomal DNA. The bands were tightly compressed and, in our system, skewed to the right side of the lanes when compared with linear chromosomes. We will refer to them as "tight bands." Upon probing the Southern blot with the cDNA for TS-DHFR, the faster-migrating tight band was identified as the R-region DNA (Figure 2B). It is not easily seen in this particular Southern blot, but several minor, slower-migrating bands also hybridized to the cDNA

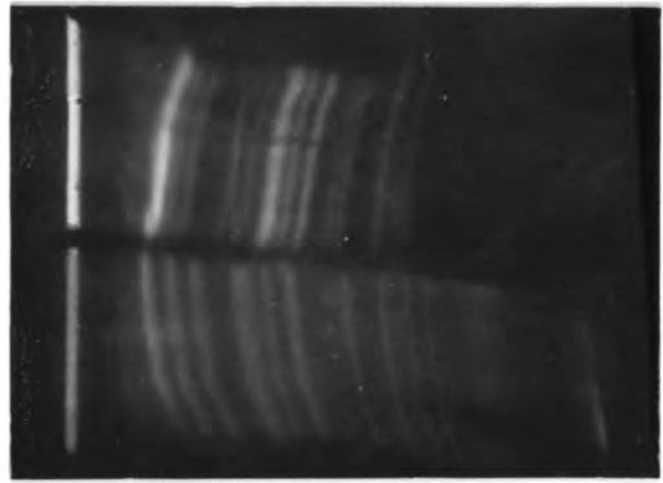
**Figure 1.**

**Chromosomal gel of wildtype *Leishmania*. (A) OFAGE of genomic DNAs (approx. 6 µg) from *S. cerevisiae* (left lane) and from wildtype *L. major* (right lane). Agarose blocks containing DNA from *L. major* were prepared by slightly modifying the cell-handling procedure of Schwartz and Cantor (8). *L. major* promastigotes grown to late log phase were harvested and washed once with PBS; the cells (approx.  $4 \times 10^7$ ) were then placed in 0.6 mls 0.6% low-melting agarose blocks (agarose from BioRad). The cells were lysed in 0.5 M EDTA, pH 9.0, 1% Lauroyl sarcosine, 1 mg/ml proteinase K for 2 d. at 50 °C. DNA blocks were washed thoroughly and stored at 4 °C in 0.2 M EDTA, pH 8.0. OFAGE was performed essentially as described by Carle and Olson (7). Electrophoresis was performed in 0.6 X TBE (56 mM tris, 56 mM boric acid, 1.2 mM EDTA, pH 8.4) for 22 hr: 40 sec pulse time for 9 hr, 80 sec pulse time for 11 hr, and 120 sec pulse time for 2 hr. In all OFAGE gels described in this report, the buffer was changed at approximately the half-way point of electrophoresis to achieve optimal resolution. Yeast DNA agarose blocks were a gift from F. Bayliss. Figure B shows an ideal composite of *L. major* chromosomes, drawn from several OFAGE gels in which various pulse times were used. Chromosomes are numbered from 1 to 14, with number 1 being the fastest-migrating chromosome. The approximate sizes were taken from the sizes of the yeast chromosomes (9).**



**A**

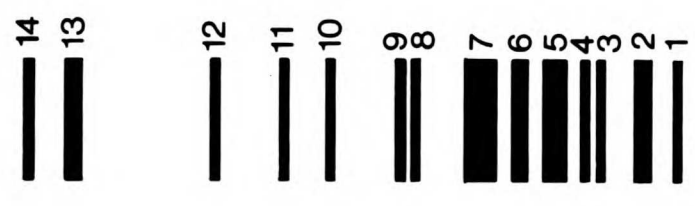
~kb



2000—  
1000—  
600—  
200—

**B**

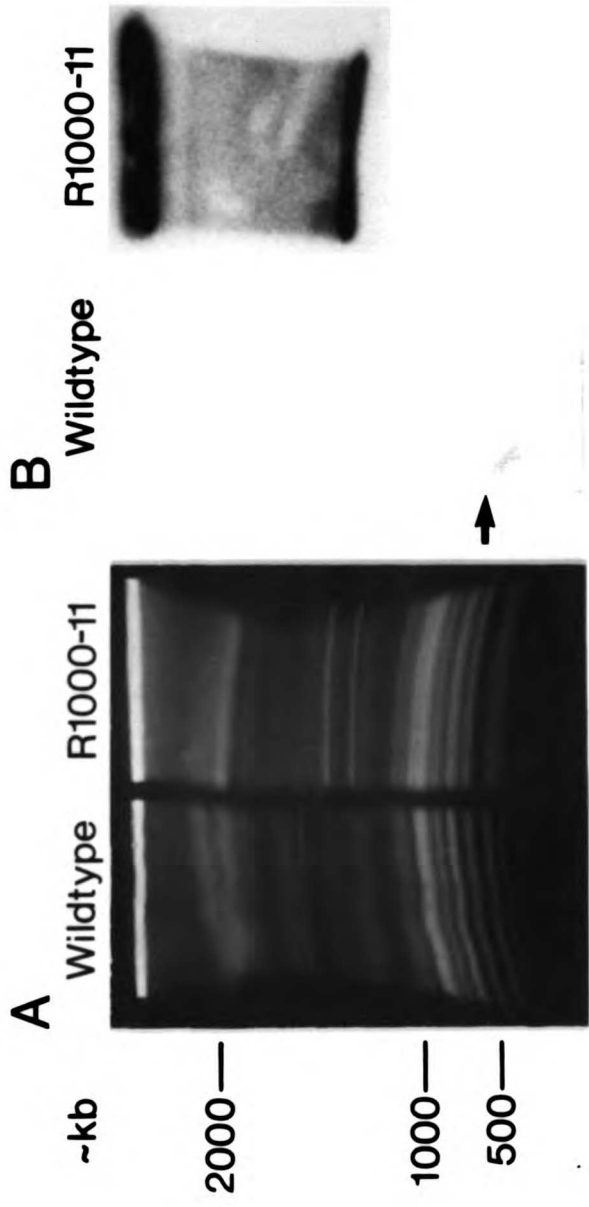
~kb  
2000—  
1800—  
1600—  
1400—  
1200—  
1000—  
800—  
600—  
400—  
200—



14  
13  
12  
11  
10  
9  
8  
7  
6  
5  
4  
3  
2  
1

**Figure 2.**

**Demonstration that stable amplified DNA in R1000-11 cells is extrachromosomal. OFAGE of genomic DNA (approx. 6  $\mu$ g) isolated from wild-type and R1000-11 *L. major*; (A) shows the EtBr-stained gel, and (B) shows the Southern transfer probed with the cDNA for TS-DHFR. The arrow denotes the location of the chromosomal locus for the gene for TS-DHFR. Experimental details same as described in Fig 1, except that OFAGE gel was run for 22 hr, at a 120 sec pulse time. After visualization by EtBr, gels were soaked in 0.5 N HCl (2X20 min.); 1 N NaOH, 1.5 M NaCl (2X20 min.); and 1 M tris, pH 8.0, 1.5 M NaCl (3X20 min.). Transfer to nitrocellulose and hybridizations were performed as described (11). Plasmid containing the cDNA for TS-DHFR was previously described (4).**

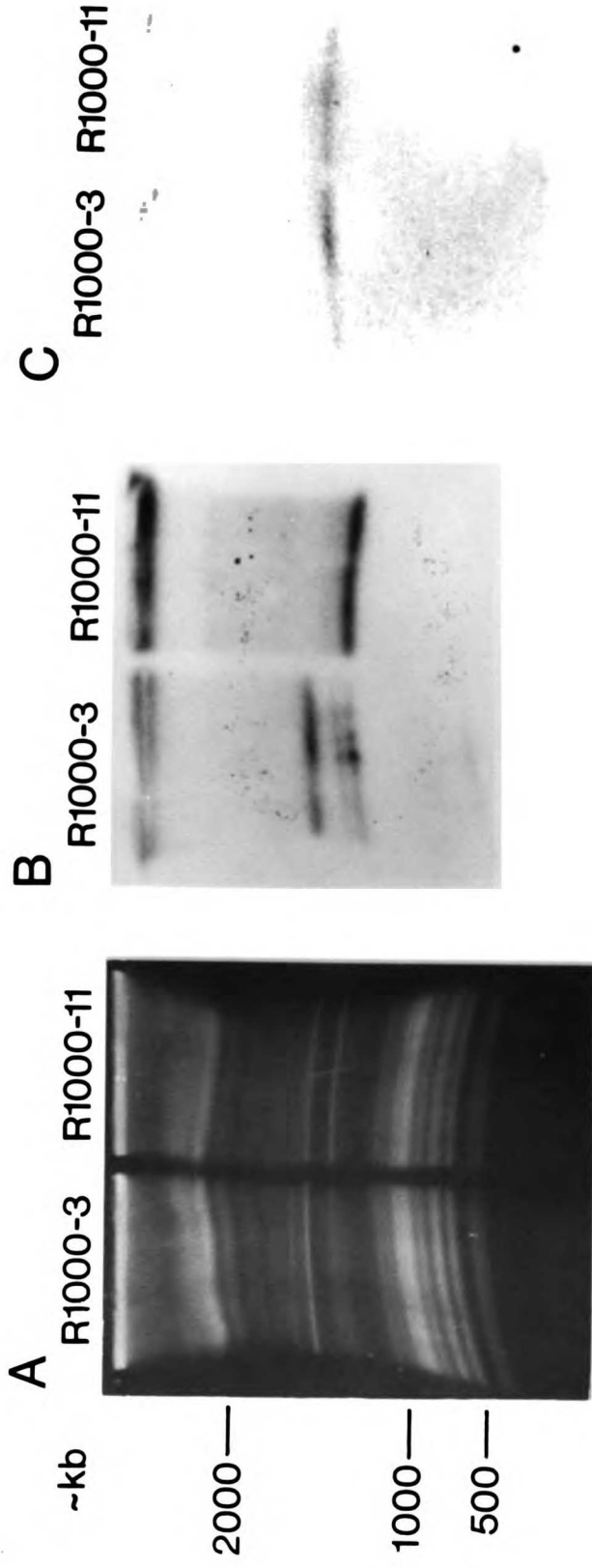


probe. The major band is approximately 30 times the wildtype copy number. The remainder of the amplified DNA remained in the gel slots (see comments below), so that the total R-region copy number was approximately 100. The cDNA probe also showed that the chromosomal locus for the TS-DHFR gene in wild-type cells remained present in the R1000-11 cells. When the Southern blot was reprobed with an H-region-specific probe (3), the slower-migrating tight band in the R1000-11 DNA was seen to be the amplified H-region. There is also a tight band in wild-type DNA; it is seen in Fig 2A, positioned above the tight bands in R1000-11 DNA. This tight band also hybridizes to the probe for the H-region DNA. We cannot explain this observation at the present time.

R1000-3 DNA, possessing unstable amplified R-region DNA, was directly compared to R1000-11 DNA (Figure 3A). The amplified R-region DNAs in the R1000-3 cells also appeared as extrachromosomal tight bands. When the Southern blot was probed with the cDNA for TS-DHFR (Fig 3B), three species of the R-region DNA were apparent. The major R-region tight band in R1000-3 cells moved noticeably slower than the major tight band in R1000-11 cells and was approximately 3 times more intense than were either of the two minor bands; the total cDNA hybridization indicated that the R-region copy number was approximately 75 times greater than in wildtype cells. A single H-region tight band was present in both resistant cell lines (Fig 3C). When this autoradiogram was further exposed, hybridization was also discernible to what we believe is the chromosomal locus of the H-region DNA (approx. chrom. 6). When DNA from R1000-3 cells that had been grown in MTX-free medium for 80 generations was analyzed, each of the three R-region tight bands was approximately 40% of the original level (data not shown), confirming that each of these amplified DNAs was unstable. TS-DHFR specific activity levels were approximately 30% of the original levels at the same point of MTX withdrawal. In contrast, when DNA from R1000-11 cells removed from selection pressure for 80 generations was electrophoresed, no differences were seen in the R-region

**Figure 3.**

**Comparison of R1000-3 amplified DNA (unstable) and R1000-11 amplified DNA (stable). OFAGE of genomic DNA (approx. 6  $\mu$ g) isolated from R1000-3 and R1000-11 cells; (A) shows the EtBr-stained gel, (B) shows the Southern transfer probed with the cDNA for TS-DHFR, and (C) shows the transfer reprobed with the H-region-specific probe. Experimental details are the same as described in Figure 2, except that after probing with the cDNA, the filter was placed in boiling water (2X10 min.) before probing with the H-region-specific probe.**



DNA when compared to R1000-11 R-region DNA (data not shown), and TS and DHFR levels were the same compared to R1000-11 enzyme levels. Thus, we concluded that both the stable amplified DNA in R1000-11 cells and the unstable amplified DNA in R1000-3 cells are extrachromosomal.

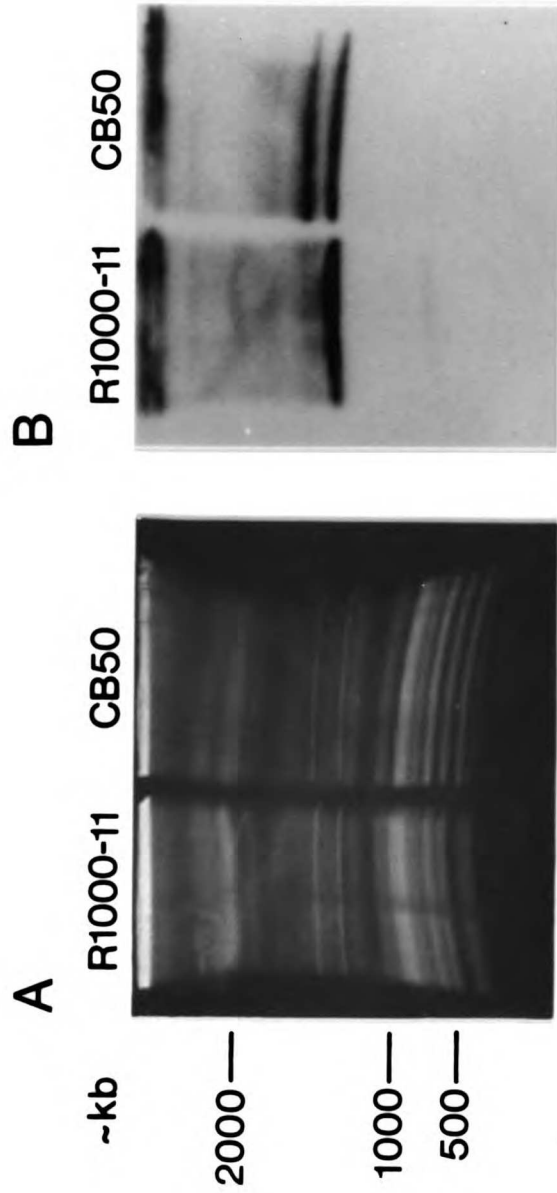
To establish similarities and differences between the amplified DNAs in two resistant lines that had been independently selected, DNAs from R1000-11 cells and from CB50-10 cells (cells grown in 50  $\mu$ M CB3717 for 10 months) were examined by OFAGE (Fig. 4A). CB50-10 cells possessed two tight bands of approximately equal molar amounts; the faster-moving band migrated with a mobility similar to the R1000-11 R-region DNA. Both of the CB50-10 tight bands hybridized to the cDNA for TS-DHFR (Fig. 4B). (The slower-migrating CB50-10 tight band moved with a mobility similar to the slowest-migrating, major tight band in R1000-3 cells.) The cDNA for TS-DHFR also hybridized to the chromosomal locus of TS-DHFR (chrom. 4). When the filter was washed and reprobbed with the H-region-specific probe, chromosome 6, the chromosomal locus for the H-region DNA, showed hybridization; no H-region tight band was observed in CB50 cells.

We had previously reported that CB50-2 cells (cells grown in 50  $\mu$ M CB3717 for 2 months) possessed relatively unstable DNA, although neither the amplified DNA nor TS-DHFR enzyme levels reverted completely back to wildtype levels (approx. 90% of the resistant levels are lost) (4). DNA from CB50-2 cells grown for 250 generations in the absence of CB3717 was examined by OFAGE, and subsequently showed cDNA hybridization to three locations: the chromosomal locus of TS-DHFR, the faster-migrating CB50 tight band, and the gel slot (data not shown). The total cDNA hybridization to the tight band and the gel slot positions was approximately 5 times that to the chromosomal locus, which is in agreement with the R-region DNA copy number reported previously in this cell line (4). Even when CB50 cells have been exposed to drug for 10 months, the

**Figure 4.**

**Comparison of amplified DNAs from two drug-resistant *L. major* : R1000-11 and CB50-10 DNAs. OFAGE of genomic DNA (approx. 6 µg) isolated from R1000-11 and CB50-10 cells; (A) shows the EtBr-stained gel, and (B) shows the transfer probed with the cDNA for TS-DHFR. Experimental procedure is the same as described in Fig 2.**





amplified R-region did not gain significant stability; this is compared with R1000-11 amplified DNA that had acquired stability. The amplified DNA from CB50-10 cells grown 85 generations in the absence of drug showed the same tight band and hybridization patterns as displayed in Fig. 4, but the relative amount was only 50% of that found in CB50-10 cells. TS and DHFR levels show a similar decrease: levels were approximately 70% at 50 generations removed and approximately 30% at 100 generations removed from drug.

A third independent resistant cell line possessing amplified R-region DNA has been examined by OFAGE. A cloned *L. major* cell line (D7B *L. major*) was used to select for resistance against MTX, and cells resistant to 1 mM MTX (D7BR1000 cells) have been obtained (12). The amplified R-region in D7BR1000 cells is considerably larger (approx. 37-kb) than either the original R1000 or CB50 R-regions (approx. 30-kb); this difference in size appears to be located in the rearranged junctional region (unpublished results). When DNA from D7BR1000 cells was examined by OFAGE, transferred to nitrocellulose, and probed with the cDNA for TS-DHFR, two R-region tight bands were seen by both EtBr-stain and Southern blot analysis (data not shown). The mobility of both tight bands was slightly decreased when compared to the R1000-11 R-region tight band. As is the case in all resistant cells, the chromosomal locus of TS-DHFR remained present in D7BR1000 cells. No amplified H-region DNA was apparent in D7BR1000 cells. Finally, the amplified R-region DNA in D7BR1000 cells grown in 1 mM MTX for 1 month was relatively unstable. After 80 generations in drug-free medium, approximately 80% of both the R-region copy number and TS-DHFR enzyme levels had been lost; when the DNA from these cells was examined by OFAGE, both tight bands showed the same decrease in the intensity of hybridization to the cDNA of TS-DHFR.

To summarize these results, we have shown that both stable and unstable amplified DNAs in three resistant cell lines are extrachromosomal, existing as

unusual-migrating bands. In addition, each cell line possesses more than one species of amplified DNA, based on the criterion of differing mobility upon OFAGE. Even though one predominant species of tight band exists in the R1000-11 cells that possess stable DNA, tight bands with a similar mobility show significant degrees of instability in both R1000-3 and CB50-10 cells. Therefore, at this time, we cannot equate mobility of DNA in OFAGE gels with stability (13).

**Characterization of the tight bands.** We wished to determine the size and structure of the stable amplified DNA in R1000-11 cells that migrated as tight bands. Unusual banding patterns have been observed when double-stranded (ds) RNA is analyzed by OFAGE (14). The tight bands were not ds RNA, because they were resistant to RNAase (as a positive control, dsRNA (15) was embedded in agarose and shown to be RNAase sensitive.) We noticed that when pulse times were shifted to resolve different chromosomes, the tight bands migrated aberrantly with respect to the chromosomal bands. At the 120 second pulse time shown in Figure 1, the amplified DNA containing the TS-DHFR gene migrated between chromosomes 11 and 12 (apparent size of 1300 kb). When gels were run at 45 seconds and then 90 seconds, this amplified DNA banded between chromosome 7 and 8 (approx. 800 kb). At a 40 second pulse time, the amplified DNA migrated between chromosome 4 and 5 (approx. 550 kb). Thus, at pulse times varying between 40 and 120 sec, the apparent size of the tight band changed some 700 kb. Subsequently, it was pointed out to us that supercoiled circles are not affected by a change in pulse times; they migrate as a function of electrophoretic duration and presumably size (16). We realized that the tight bands were behaving in a similar manner; they were not responding to the changes in pulse time, and that the apparent changes of size was in fact due to the differing mobilities of the chromosomes. Therefore, we attempted to demonstrate directly that the tight bands were circular DNA. When DNA agarose blocks from R1000-11 cells were incubated with exonuclease III and then analyzed by OFAGE,

there was seen a time-dependent disappearance of all chromosomal bands but not the two tight bands (Figure 5). By probing the Southern transfer with the TS-DHFR cDNA or the H-region probe, we confirmed that both amplified DNAs were resistant to exonuclease III activity. We therefore concluded that the tight bands were circular DNA.

In order to determine the size of the R1000-11 R-region tight band, DNA agarose blocks were incubated with limiting amounts of EcoR I. (EcoR I cleaves the 30-kb unit of R-region DNA twice, generating fragments of 28- and 2-kb (3)). If the tight band were the amplified 30-kb supercoiled circle, then the limited digest would produce only the linear 30-kb DNA and the 28-kb fragment. If the tight band were a circular multimer of the 30-kb unit, then a limited digest would show linear multiples of the unit size. If the 100 copies of the R-region DNA had been incorporated into chromosome(s) as a repetitive array (as was previously proposed for R1000-11 amplified DNA), then the digest would produce an extensive ladder of R-region DNA, consisting of multiples of 30 kb. The only significant R-region DNA generated from the limited digest appears to be the linear 30-kb unit and the 28-kb fragment (Fig. 6); a faint band that appears to be approximately 60-kb in size is seen when the autoradiogram is extensively exposed. (The minor bands of R-region DNA which migrate slower than the tight band, alluded to previously, are more noticeable in this figure.) The final time point shows complete digestion of the R-region DNA; only the 28-kb fragment remains. The above results were confirmed when R1000-11 DNA agarose blocks were digested with limited amounts of Not I (17) (data not shown), a restriction enzyme that cleaves the R-region DNA once (3); although slightly different results were observed. In addition to the predominant 30-kb linear DNA expected and a small amount of a 60-kb intermediate, an equally small amount of a second intermediate was produced (slightly larger and assumed to be approx. 90-kb). The ratio of intermediates to 30-kb R-region was 1:1.4. The above data suggests that the R1000-11 amplified DNA exists predominantly as a monomer of the 30-kb R-region, with small

**Figure 5.**

**Demonstration that R1000-11 amplified DNA is circular. OFAGE of indicated time points from a reaction of exonuclease III with R1000-11 DNA blocks. R1000-11 DNA blocks (approx. 2  $\mu$ g DNA/block) were equilibrated (3 X 3hr) with exo III buffer (66 mM tris, pH 8.0, 1 mM DTT, 0.66 mM  $MgCl_2$ ). Blocks were then added to 2.5 mls of buffer containing 130 units of exonuclease III (BRL), and incubated at 37 °C. Blocks were added to 0.2 M EDTA, pH 8.0 (to stop reaction) at indicated times.**

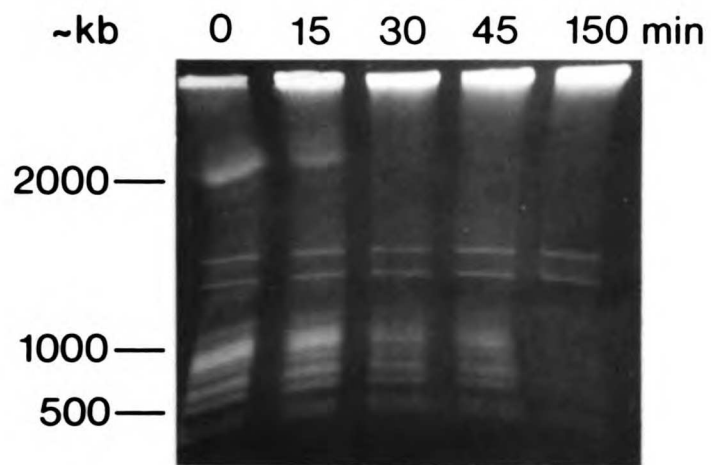
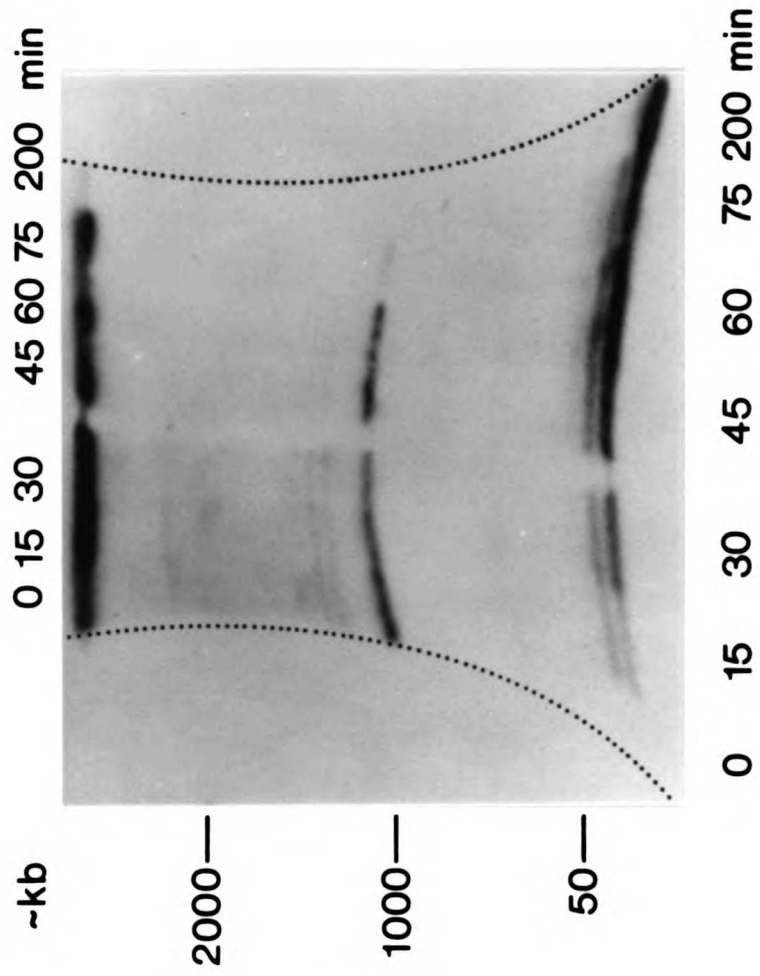


**Figure 6.**

**Determination of the size of the amplified DNA in R1000-11 cells. Indicated time points from a reaction of limiting amounts of EcoR 1 with R1000-11 DNA blocks were analyzed by OFAGE; the subsequent Southern transfer was probed with the cDNA for TS-DHFR. The times of digestion are noted both at the top and bottom, and the curvature of migration is outlined to aid in viewing. R1000-11 DNA blocks (approx. 2  $\mu$ g DNA/block) were equilibrated (3 X 3hr) with EcoR 1 buffer (33 mM tris acetate, pH 7.9, 66 mM potassium acetate, 10 mM magnesium acetate). Blocks were then added to 3 mls of buffer containing 30 units of EcoR 1 (New England Biolabs), and incubated at 37 °C. Blocks were placed into 0.2 M EDTA, pH 8.0 (to stop reaction) at indicated times. After 75 min., 100 units of EcoR 1 was added and the final DNA block was incubated for an additional 2 hr. The fragments generated after 15 min of digestion represent less than 5% of the total amplified DNA; this clearly shows that a limited digest was achieved. The EtBr-stained gel showed that all DNA was digested after the final time point. Uncut lambda DNA was electrophoresed in the center lane and migrated slower than both EcoR I-generated DNAs.**





amounts of multimeric forms (probably dimer and trimer).

There is considerable hybridization of the cDNA for TS-DHFR to the gel slots. Early in these studies, it was considered possible that the amplified DNA had been incorporated into a very large chromosome as a repetitive array, and that the chromosome does not migrate from the origin. However, because the EcoR I limited digest of R1000-11 DNA did not produce a ladder of R-region DNA, we have ruled out this explanation for the gel slot hybridization. More likely, the hybridization results in part from the random entrapment of DNA within the agarose block. (Many reports using either OFAGE (7,18) or pulsed-field electrophoresis (8,10,19) contain examples of non-specific sticking of DNA to the gel slots.) In addition, nicked circular DNA has a tendency to be entrapped in the agarose (20). The well hybridization, therefore, may represent nicked supercoiled circles. Finally, this lack of migration may result from a higher order structure of the amplified DNA (concatenated circles or a form unknown) that impedes movement out of the block. Clearly, more information concerning the species of DNA which remain at the origin in this system is needed.

In order to determine whether the structure of the R-region amplified DNA was either supercoiled or concatenated circles, we incubated R1000-11 DNA agarose blocks with topoisomerase II (21). This enzyme makes an opening in dsDNA that allows for both the relaxation of supercoiled circles and also the release of concatenated circles. In samples treated with topoisomerase II, both the R-region and H-region tight bands disappeared (by both EtBr-staining and hybridization criteria), with no effect on the chromosomal DNA, and the hybridization intensity at the gel slot increased by the amount that was originally present in the tight bands (data not shown). This particular experiment unfortunately does not clarify why the amplified R-region sticks to the gel slots. It does, however, suggest that the R- and H-region tight bands represent either supercoiled or concatenated circles.

These enzymatic modifications of the DNA entrapped in agarose blocks were also

employed to examine the tight bands found in the other resistant cell lines. In all cell lines, the tight bands were resistant to exonuclease III. When CB50-10 DNA blocks were digested with EcoR I, the reaction produced an intermediate (approx. 60-kb) in addition to the 30-kb and 28-kb R-region DNAs (Fig 7). The intermediate suggested that some of the amplified R-region DNA exists in a dimeric form, consistent with what had been previously proposed (4). When D7BR1000 DNA agarose blocks were digested, the results showed only the pattern expected of the monomeric R-region; no intermediate-sized DNAs were observed. And when R1000-3 DNA blocks were digested with Not I, a small amount of a 60-kb intermediate was observed in addition to the linear 30-kb DNA (ratio of 1 to 10 in favor of the monomer). Finally, when DNA blocks from R1000-3, CB50-10, or D7BR1000 cells were incubated with topoisomerase II, the tight bands were no longer visible, with no effect to the linear chromosomes; and the cDNA hybridization to the gel slots increased by the amount originally present in the tight band. We viewed these results as demonstration that the structure and size of the amplified DNAs in all three different resistant cells was qualitatively the same.

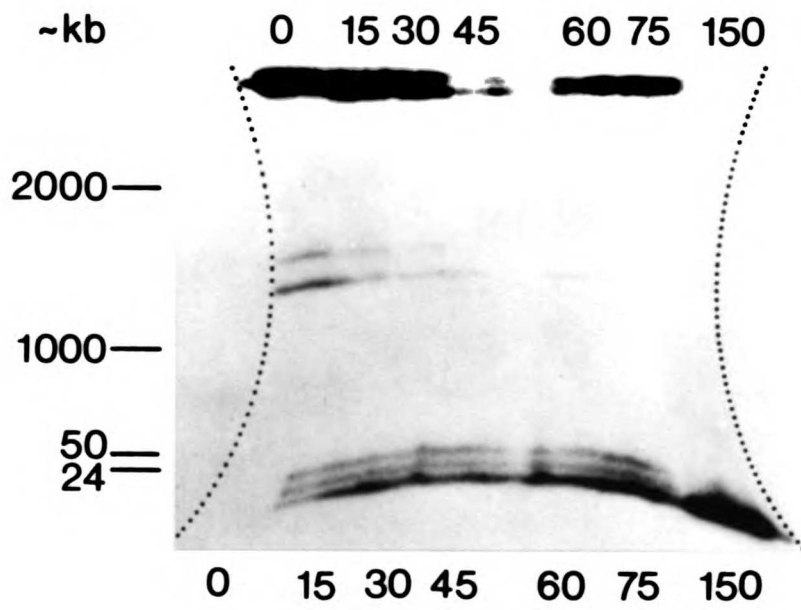
Finally, it should be noted that the amplified H-region DNA in the R1000-3 and R1000-11 cells which migrated as tight bands were resistant to exonuclease III, and remained in the well upon treatment with topoisomerase II. In addition, the H-region DNA appeared to consist only of a monomeric form. We have described two independent amplified DNAs in these cells, both of which are extrachromosomal and circular; these characteristics may be a signature for gene amplification in drug-resistant *L. major*.

#### **Additional alteration of chromosomal DNA in MTX-resistant cells.**

A final observation from the OFAGE analysis of these resistant cells is worth noting; when gels were run at short pulse times (data not shown), an EtBr-staining band was visible between chromosomes 1 and 2 (approx. 300-kb) in MTX-resistant cells that was absent in both wildtype and CB3717-resistant cells. The intensity of the EtBr stain was equal to the

**Figure 7.**

Determination of the size of the amplified DNA in CB50-10 cells. Experimental procedures and figure explanations are the same as described in Fig 6, except that the final time point indicates 75 min of incubation after 100 units of EcoR I was added to the initial 75 min incubation; and, in addition to uncut lambda DNA, a Hind III digest of lambda DNA was electrophoresed in the center of the gel to aid in the sizing of the DNAs generated by EcoR I.



intensity of any single chromosome. Not only was this band present in R1000-3, R1000-11, and D7BR1000 cells, but it was stable in these cells even when grown in the absence of MTX. This band did not have the unusual characteristics of the tight bands; it was sensitive to exonuclease III, and therefore linear, and its migration was unaffected by topoisomerase II. Also, the band did not hybridize to either the cDNA for TS-DHFR or the H-region-specific probe. In addition, in the MTX-resistant cell lines, assigned bands 5 and 7 (both of which appear to represent unresolved chromosomes in wildtype cells; see Fig 1B) have each been resolved into two chromosomes, which differ by about 100-kb in both instances. Thus, it appears that significant chromosomal alterations have occurred in the MTX-resistant cells, in addition to the rearrangements that led to the formation of the R-region DNA. At the present time, we do not know how these alterations originated or if they are functionally important to resistance.

**Conclusions.** The powerful tool of orthogonal-field-alternation gel electrophoresis which fractionates chromosomes has allowed us to directly examine the amplified DNA in anti-folate-resistant *L. major*. We have been able to both confirm and extend our previous observations regarding the size, structure, and location of the amplified DNAs. Although many questions still remain, we can conclude the following: 1.) Most significantly, both stable and unstable amplified DNAs in drug-resistant *L. major* are extrachromosomal. We had previously concluded that only unstable amplified DNA was extrachromosomal, and that the mechanism of mitotic stability of the amplified R-region DNA was insertion of the amplified DNA into a chromosomal locus as a repetitive array. This is not the mechanism by which stability is gained. Other possible explanations will be explored below. 2.) The amplified R-region unit that contains the gene for the bifunctional protein TS-DHFR exists as circular DNA. These circles may exist as individual supercoiled circles, or as concatenated circles, or as an unrecognized structure consisting of circles. Clearly, none of the resistant cells described here possess amplified

DNA that exists as a large, repetitive array. 3.) All resistant cells examined in this study have at least two different species of R-region DNA. R1000-11 cells have one predominant tight band (which is stable in the absence of MTX); the other cell lines, however, have significant amounts of amplified R-region that have slightly different mobilities on OFAGE. We hope to determine the structure of these different tight bands. Based on results from the limited endonuclease digests, one possible explanation is that the slower-migrating tight bands represent circular multimers of the 30-kb R-region unit (existing as a 60- or 90-kb circular DNA). 4.) Initially, the amplified R-region DNA possesses no inherent stability; stability must be acquired. Three independent selection procedures have led to a similar amplified unit, and none of these units is initially stable. In the original study stability was gained only after cells were grown for many months in drug. This acquisition of stability was not repeated when CB3717-resistant cells were grown in drug for a similar length of time. These CB50 cells are being maintained to determine if and when stability of the amplified DNA is acquired. 5.) In the resistant cell lines examined in this study, the wildtype chromosomal locus of TS-DHFR remains present. Therefore, the DNA rearrangements which generate the extrachromosomal circles appear to leave the chromosomal locus more or less intact.

To our knowledge, this is the first demonstration in eukaryotic cultured cells of stable, amplified DNA that is extrachromosomal and circular. The amplified DNA containing the gene for TS-DHFR can be viewed as a new, mini-chromosome. As such, factors must be present which permit autonomous replication and, in the stable R1000-11 cells, confer mitotic stability. Although we expect that the details of these factors may prove unique, insight is gained by consideration of better understood systems. As in other systems studied (22), the amplified extrachromosomal DNAs in *L. major* probably possess a sequence which is responsible for autonomous replication; the copy number increase during selection and is subsequently maintained through many generations of

growth. In other eukaryotic systems studies, stability of plasmids and chromosomes require mitotic stabilizing sequences. These are exemplified by sequences of the yeast 2 u circle (23), of the *S. cerevisiae* centromere (CEN) DNA (for reviews, see ref. 24), and of the bovine papilloma virus (25); CEN sequences also control segregation during meiosis. In some systems, copy number and size also play a role in stability of plasmids (19,25).

What can we say regarding the stability of the extrachromosomal circular DNA in *L. major* R1000-11 cells? (1) The stability is acquired. We have shown that upon continued selection in MTX, unstable amplified DNA changes to a stable form without major alteration in physical form. (2) The stability probably is not exclusively due to high copy number or size. The copy number and size of the amplified DNAs are similar in both the unstable and stable cell lines. (3) We propose that stability of MTX-resistance in *L. major* involves acquisition of mitotic-stabilizing sequences in the extrachromosomal, circular DNA. How similar such sequences would be to mitotic-stabilizing sequences such as CEN is unknown. Because amplified DNAs from both unstable and stable resistant cells are available, we hope to identify these sequences if they exist. Whatever the mechanism, the acquisition of stability is not as simple as previously envisioned.

#### References and Notes.

1. Schimke, R.T. *Cell* 37, 705 (1984).
2. Coderre, J. C., Beverly, S.M., Schimke, R.T., and Santi, D.V. *Proc. Natl. Acad. Sci. USA* 80, 2132 (1983).
3. Beverly, S.M., Coderre, J.C., Santi, D.V., and Schimke, R.T. *Cell* 38 431 (1984).
4. Garvey, E.P., Coderre, J.C., and Santi, D.V. *Mol. and Bioch. Parasit.* 17 79 (1985).
5. Washtien, W.L., Grumont, R., and Santi, D.V. *J. Biol. Chem.* 260 7809 (1985).
6. Grumont, R., Washtien, W.L., and Santi, D.V., manuscript submitted.
7. Carle, G.F. and Olson, M.V. *N.A.R.* 12 5647 (1984).

8. Schwartz, D.C. and Cantor, C.R. *Cell* 37 67 (1984).
9. Mortimer, R.K., and Schild, D. *Microbiol. Rev.* 49 181 (1985); Carle, G.F., and Olson, M.V. *Proc. Natl. Acad. Sci. USA* 82 3756 (1985)
10. Spithill, T.W. and Samaras, N. *N.A.R.* 13 4155 (1985)
11. Maniatis, T., Fritsch, E.F., and Sambrook, J. *Molecular cloning: a laboratory manual*. ( Cold Spring Harbor Laboratory, Cold Spring Harbor, N.Y., 1982).
12. Garvey, E.P. and Santi, D.V., unpublished work.
13. It should be noted that the multiplicity of tight bands in the various cells might reflect heterogeneous populations; of the resistant cells described in this report, only the CB50-10 have been cloned (CB50 cells were cloned on agar after 7 months of growth in 50  $\mu$ M CB3717).
14. Church, G.; Wang, C.C., personal communications.
15. Wang, A.L. and Wang, C.C. *J. Biol. Chem.* 260 3697 (1985).
16. Hui, C.F., Smith, C.L., and Cantor, C.R., personal communication.
17. Not I reaction: R1000-11 DNA agarose blocks were equilibrated (3 X 3hr washes) with Not I reaction buffer (150 mM NaCl, 6 mM tris HCl (pH 7.9), 6 mM MgCl<sub>2</sub>, 6 mM 2-mercaptoethanol, 100 ug/ml BSA, 0.01% triton X-100). Blocks were then added to 3mls of buffer containing 30 units of Not I (New England Biolabs), and incubated at 37 °C. Time points were taken by putting the DNA block into 0.2 M EDTA, pH 8.0.
18. Hieter, P., Mann C., Snyder, M., and Davis, R.W. *Cell* 40 381 (1985).
19. Van der Ploeg et al. *Cell* 37 77 (1984); Kemp et al. *Nature* 315 347 (1985).
20. Mickel, S., Arena, V., and Bauer, W. *N.A.R.* 4 1465 (1977).
21. Topoisomerase II reaction: R1000-11 DNA agarose blocks were equilibrated (3 X 3hr) with Topo II reaction buffer (40 mM tris, pH 7.8; 60 mM KCl; 10 mM MgCl<sub>2</sub>; 0.5 mM DTT; 0.5 mM EDTA; 0.5 mM ATP; and 30  $\mu$ g/ml BSA). Blocks were added to 1.5



mls of buffer containing 0.32 µg/ml topoisomerase II, and incubated at 30 °C for 120 min.

Reaction was stopped by adding block to 0.2 M EDTA, pH 8.0.

22. Stinchcomb, D.T., Struhl, K., and Davis, R.W. *Nature* **282** 39 (1979); Zakian, V.A., and Scott, J. *Mol. Cell. Biol.* **2** 221 (1982); Fangnan, W.L., Hice, R.H., and Chiebowicz-Stedziewska, E. *Cell* **32** 831 (1983).

23. M. Jayaram, Y.-Y. Li, and Broach, J.R. *Cell* **34** 95 (1983).

24. Szostak, J.W. and Blackburn, E. *Ann. Rev. Biochem.* **53** 163 (1984); Clarke, L., and Carbon, J. *Ann. Rev. Genet.* **19** 29 (1985).

25. Lusky, M., and Botchan, M.R. *Cell* **36** 391 (1984).

26. We thank F. Bayliss and R. Nelson for their valuable expertise and advice. We also thank F. Bayliss for supplying DNA agarose blocks of *S. cerevisiae*, B. Alberts for supplying Topoisomerase II from T4 bacteriophage, and C.C. Wang for supplying dsRNA from *Trichomonas vaginalis*.

## **Chapter 4**

# **Purification and Characterization of the Bifunctional Thymidylate Synthase-Dihydrofolate Reductase from Methotrexate-Resistant *Leishmania major***

### Abstract

Thymidylate synthase (TS) and dihydrofolate reductase (DHFR) in *Leishmania major* exist as a bifunctional protein. By use of a methotrexate-resistant strain, which overproduces the bifunctional enzyme, the protein was purified 80-fold to apparent homogeneity in two steps. The native protein has an apparent molecular weight of 110 000 and consists of two subunits with identical size and charge. The TS of the bifunctional protein forms a covalent 5-fluoro-2'-deoxyuridylate (FdUMP)- $(\pm)$ -5,10-methylenetetrahydrofolate-enzyme complex in which 2 moles of FdUMP are bound per mole of enzyme. In contrast, titration of DHFR with methotrexate indicated that only 1 mole of the inhibitor is bound per mole of dimeric enzyme. Both TS and DHFR activities of the bifunctional enzyme were inactivated by the sulfhydryl reagent *N*-ethylmaleimide. Substrates of the individual enzymes afforded protection against inactivation, indicating that each enzyme requires at least one cysteine for catalytic activity. Kinetic evidence indicates that most, if not all, of the 7,8-dihydrofolate produced by TS is channeled to DHFR faster than it is released into the medium. Although the mechanism of channeling is unknown, the possibility that the two enzymes share a common folate binding site has been ruled out.

Thymidylate synthase (TS<sup>1</sup>; EC 2.1.1.45) and dihydrofolate reductase (DHFR; EC 1.5.1.3) catalyze sequential reactions in the de novo synthesis of dTMP. TS catalyzes the conversion of dUMP and (±)-5,10-methylenetetrahydrofolate (CH<sub>2</sub>H<sub>4</sub>folate) to dTMP and H<sub>2</sub>folate; it is unique among enzymes that utilize folate cofactors in that H<sub>4</sub>folate is oxidised in the course of the one-carbon transfer reaction. DHFR catalyzes the subsequent NADPH-dependent reduction of the H<sub>2</sub>folate produced by TS to regenerate H<sub>4</sub>folate, which serves as a carrier of one-carbon units in a number of metabolic processes. Because blocking either TS or DHFR results in depletion of dTMP and subsequent cessation DNA synthesis, these enzymes have been studied extensively and exploited as targets for chemotherapeutic agents for a number a diseases.

TS and DHFR are distinct and readily separable in sources as varied as bacteria, bacteriophage, yeast, and vertebrates. Usually, TS is a dimer of identical subunits with a native molecular weight of about 70 000 and DHFR is a monomer with a molecular weight of about 20 000 [for reviews see Blakely (1984) and Santi & Danenberg (1984)]. In contrast, TS and DHFR have recently been reported to exist as a bifunctional protein in a number of protozoa that span a diverse group of the subkingdom (Ferone & Roland, 1980; Garrett et al., 1984). Depending upon the species, the bifunctional TS-DHFRs have apparent native molecular wieghts ranging from 100 000 to 240 000 as determined by gel filtration chromatography.

Because of their unique structures, bifunctional TS-DHFRs in protozoa represent interesting proteins for kinetic and structural characterization. Further, many parasitic protozoa are major health problems, and the bifunctional protein is a promising target for selective chemotherapeutic agents. In this regard, pyrimethamine, a species-specific inhibitor of DHFR, has been extensively used to treat malaria (Rollo, 1980).

Thus far, the only protozoan TS-DHFR that has been purified to homogeneity and

partially characterized is that from *Crithidia fasciculata* (Ferone & Roland, 1980), a non-pathogenic trypanosomatid that can be cultivated in large quantities. In general, purifying sufficient amounts of TS-DHFR from pathogenic protozoa has been impractical because of source limitations. We recently reported the development of a methotrexate (MTX)-resistant strain of the parasitic protozoan *Leishmania major* (Coderre et al., 1983); this strain overproduces TS-DHFR to the extent that milligram amounts of the bifunctional protein are obtainable. In this paper we describe the purification and characterization of TS-DHFR from MTX-resistant *L. major*.

### Materials and Methods

Folic acid, H<sub>4</sub>folate, dUMP, FdUMP, pyridoxal phosphate, protease inhibitors, and all buffers were obtained from Sigma. H<sub>2</sub>folate (Friedkin, 1959), CH<sub>2</sub>H<sub>4</sub>folate, and (6R)-L-CH<sub>2</sub>H<sub>4</sub>folate (Bruce and Santi, 1982) were prepared as described and stored under argon at -80 °C. Concentrations of H<sub>2</sub>folate and CH<sub>2</sub>H<sub>4</sub>folate were determined enzymatically with DHFR and TS, respectively. MTX was obtained from the Lederle Parenterals, Inc. [6-<sup>3</sup>H]FdUMP (20 Ci/mmol) and [3',5',7'-(N)-<sup>3</sup>H]MTX were purchased from Moravsek Biochemicals. [6-<sup>3</sup>H]-L-Serine was an Amersham product. Sephadex G-15, Sephadex G-25, DEAE-Sepharose CL-6B, and Sepharose CL-6B were from Pharmacia. Cibracon Blue F3GA-agarose was obtained from Pierce Corp. PteGluL4P-lysine-Sepharose was a gift from Dr. Roy L. Kisliuk. MTX-Sepharose was prepared by coupling MTX to aminohexyl-Sepharose CL-6B (Dann et al., 1976), which was prepared according to the method of Bethell (1979); spectrophotometric assay of the digested resin (Failla and Santi, 1973) indicated that the preparation contained 0.6 umol of MTX/ml of wet gel. Reagents and protein standards for NaDodSO<sub>4</sub>-PAGE and Bio-Gel P-300 were from Bio-Rad. Ampholines were LKB products. *L. casei* TS and DHFR

were prepared from a MTX-resistant strain (Crushberg et al., 1970) as described (Wataya and Santi, 1977; Dann et al., 1976). The following buffers were used: buffer A, 50 mM Tes (pH specified in the text), 75 mM b-mercaptoethanol, 1 mM EDTA; buffer B 50 mM Tes (pH 7.4), 5 mM DTT, 1 mM EDTA; buffer C, 10 mM potassium phosphate (pH 7.0).

**Growth of organisms.** *L. major* promastigotes (strain 252, Iran), obtained from S. Meshnik (Cornell University Medical College), were cultured in M199 medium (Gibco) containing Earl's buffered saline salts, 20 % fetal calf serum, 25 mM Hepes (pH 7.4), and 50 µg/ml gentamicin. The MTX-resistant strain of *L. major* (Coderre et al., 1983) was maintained in the same media containing 1 mM MTX. For large-scale preparations of the latter, cells were grown to stationary phase (approximately  $2 \times 10^7$  cell/ml) and harvested by centrifugation (1550g, 5 min); the medium containing MTX was removed, and the cells were seeded at about  $10^6$  cells/ml into larger volumes (1-10 L) of medium not containing MTX and incubated by stirring in Bellco spinner flasks at 26 °C. Organisms were harvested at late log phase [ $(1.0-1.5) \times 10^7$  cells/ml] by centrifugation (1500g, 5 min) and washed twice with ice-cold phosphate-buffered saline. If cell pellets were not used immediately, they were stored at -80 °C, although freezing resulted in some loss of enzyme activity.

**Purification of TS-DHFR from *L. major*.** The following protocol was used to purify the enzyme from 1-10 L cultures of wildtype or MTX-resistant cells. All steps were performed at 4 °C, and the entire procedure was performed without interruption.

**Step I: preparation of cell extracts.** Packed cell pellets of *L. major* were suspended at a density of approximately  $3 \times 10^9$  cells/ml in buffer B, which contained 10% glycerol and the following protease inhibitors: 1 mM 1,10-phenanthroline, 1 mM benzamidine, 50 µM phenylmethanesulfonyl fluoride, 20 µg/ml leupeptin, 50 µg/ml crude soybean trypsin inhibitor, and 50 µg/ml aprotinin. The cells were disrupted by sonication (Bronwill Biosonic IV; 5-s bursts at 100 W with intermittent 30-s cooling periods) and

centrifuged at 48000g for 70 min.

**Step II: DEAE-Sepharose chromatography.** The supernatant was applied to a column of DEAE-Sepharose CL-6B (2.5x8.6 cm) previously equilibrated with buffer B. The column was washed with the equilibration buffer (~25 ml) until protein was undetectable in the effluent, and the enzyme was eluted with 30 ml of 0.15 M KCl in buffer B. Alternatively, a 200-ml linear gradient of 0-0.2 M KCl in buffer B was applied to the equilibrated column, and the enzyme eluted at 75 mM salt.

**Step III: MTX-Sepharose affinity chromatography.** The fractions containing TS-DHFR from Step II were pooled and applied to a column of MTX-Sepharose (1.0x2.5 cm) that had been equilibrated with buffer C. The enzyme was applied by circulating the protein solution through the column with a peristaltic pump (flow rate=0.3 ml/min) for 4-6 hr or until less than 5% of the DHFR activity remained in the reservoir. The column was washed with buffer C, containing 1 M KCl, until protein was undetectable in the effluent, and then washed with 10 ml of buffer C. One column volume of buffer B, containing 1 mM H<sub>2</sub>folate, was applied to the column, allowed to equilibrate for 30 min, and then eluted with the same buffer. Fractions of 1.0 ml were collected, and the enzyme eluted in the first 4 mls.

Fractions containing the enzyme were pooled; H<sub>2</sub>folate was removed by filtration through a column of Sephadex G-15 (120 mesh; 1x10 cm), equilibrated with buffer B. TS-DHFR eluted in 5-7 ml and H<sub>2</sub>folate eluted in 15-21 ml. Alternatively, pooled fractions were applied to a small DEAE-Sepharose column (0.4x8 cm) previously equilibrated with buffer B. After the column was washed with about 20 ml of buffer B, TS-DHFR was eluted in about 2 ml of buffer containing 0.15 M KCl.

**Enzyme Assays.** DHFR activity was determined spectrophotometrically at 25 °C (Hillcoat et al., 1967). The standard assay mixture (1.0 ml), contained buffer A (pH

7.0), 1 mg/ml BSA, 0.1 mM NADPH, 0.1 mM H<sub>2</sub>folate, and limiting enzyme; controls included 2 μM MTX. TS activity was determined spectrophotometrically (Wahba and Friedkin, 1961) at 25 °C. The standard assay mixture (1.0 ml) contained buffer A (pH 7.8), 5 mM H<sub>2</sub>CO, 1 mg/ml BSA, 0.2 mM CH<sub>2</sub>H<sub>4</sub>folate, 0.1 mM dUMP, and limiting enzyme; controls included 2 μM FdUMP. Serine transhydroxymethylase activity was determined at 37 °C as reported by Taylor and Weissback (1965), except the reaction mixture (0.1 ml) contained buffer A (pH 8.0), 1 mg/ml BSA, 0.2 mM pyridoxal phosphate, 1.7 mM H<sub>4</sub>folate, 1.9 μM [<sup>3</sup>H]-L-serine (28 Ci/mmol), and appropriate amounts of enzyme; controls omitted enzyme. One unit of enzyme activity is defined as that amount of enzyme that produces 1 nmol of product/min.

DHFR and TS were quantitated by binding assays in which we used the active-site titrants MTX and FdUMP, respectively. For DHFR, 0.1 ml solutions containing 0.25-4 μg of protein in buffer B were incubated with 0.4 μM [<sup>3</sup>H]MTX (28 Ci/mmol) and 0.5 mM NADPH for 20 min. Macromolecular-bound radioactivity was separated from free [<sup>3</sup>H]MTX by gel filtration on small columns of Sephadex G-15 (Garrett et al., 1984). For TS, the [6-<sup>3</sup>H]FdUMP-CH<sub>2</sub>H<sub>4</sub>folate-enzyme complex was formed in buffer B and was quantitated by the nitrocellulose filter binding assay as previously described (Santi et al., 1974) or isolated by gel filtration through Sephadex G-25 (Washtien and Santi, 1979).

The TS and DHFR coupled system was assayed by monitoring the decrease in NADPH absorbance at 340 nm in the absence of added H<sub>2</sub>folate. The assay mixture (1.0 ml), containing buffer A (pH 7.8), 5 mM H<sub>2</sub>CO, 1 mg/ml BSA, 30 μM NADPH, 28 μM CH<sub>2</sub>H<sub>4</sub>folate, and specified amounts of both enzymes, was incubated at 25 °C to enzymatically reduce traces of endogenous H<sub>2</sub>folate. When the absorbance at 340 nm was stable, the reaction was initiated by addition of 0.02 ml of 5 mM dUMP to give a final



concentration of 0.1 mM. The TS and DHFR rates required to analyze the coupled system were obtained by initial velocity determinations under conditions of the coupled assay, with the following modifications: for DHFR, CH<sub>2</sub>H<sub>4</sub>folate and dUMP were omitted and 100 μM H<sub>2</sub>folate was included; for TS, NADPH was omitted and the formation of H<sub>2</sub>folate was monitored spectrophotometrically.

**Electrophoretic methods.** NaDod SO<sub>4</sub>-PAGE was performed on slab gels 0.15 cm thick and 14.5 cm long; stacking gels (3.5 cm) were 4.5% polyacrylamide, and separating gels (11 cm) were 8.5-12.5% polyacrylamide. Procedures used were those described by Laemmli (1970). Gels containing the [6-<sup>3</sup>H]FdUMP-cofactor-TS complex were cut in 1-mm strips, treated with 1 ml of Protosol at 60 °C for 20 min, neutralized with 0.1 ml of HOAc, and counted.

Nondenaturing isoelectric focusing was performed in cylindrical polyacrylamide gels (0.25x10 cm) prepared with 4.7% acrylamide, 0.15% *N,N'*-methylene-bis(acrylamide), 10 % glycerol, 2% ampholines (pH 5-8, 1.5%; pH 3-10, 0.5%). 0.02% ammonium persulfate, and 0.001% TEMED. The pH gradient was determined by electrophoresis of colored protein standards with known isoelectric points (pI=4.7-10.6) (BDH Chemicals, Poole, England). Electrophoresis was performed at 400 V for 7000-8000 V h, and gels were subsequently fixed and stained with Coomassie blue as described by Winter et al. (1977). Denaturing isoelectric focusing gels were prepared and conducted according to the method of O'Farrell (1975). Isoelectric focusing gels that contained urea were fixed for 6-8 hr in 10% trichloroacetic acid and then washed for 12 hr in 25% 2-propanol/10% HOAc and for 2 hr in H<sub>2</sub>O. The gels were stained for 10 min at 60 °C in a solution containing 0.12% Coomassie Blue R-250 in 25% EtOH/10% HOAc and destained overnight with a solution of 25% EtOH/10% HOAc.

**Analytical Gel Filtration.** Gel filtration of *L. major* TS-DHFR was

performed on a 2x56 cm column of Bio-Gel P-300 (100-200 mesh) at a flow rate of 3 ml/hr. The column was calibrated by separate determinations with the following protein standards: catalase (Stokes radius,  $a = 5.2$  nm), aldolase ( $a = 4.8$  nm), bovine serum albumin ( $a = 3.6$  nm), and ovalbumin ( $a = 3.1$  nm).

**Density Gradient Centrifugation.** Glycerol density gradients (6.7-20% v/v) were prepared in 4.5 ml of 50 mM Tes (pH 7.2) and 5 mM DTT in cellulose nitrate tubes. A solution (0.10 ml) containing 8  $\mu$ g of yeast alcohol dehydrogenase, 5  $\mu$ g of beef catalase, 6  $\mu$ g of *Escheichia coli* alkaline phosphatase ( $s = 7.4, 11.3,$  and  $6.4$  S, respectively), and 1.5  $\mu$ g of TS-DHFR was added to two of the above tubes, which were then centrifuged at 38 000 rpm for 18 hr with a SW 50.1 rotor in a Bechman Model L2-65B ultracentrifuge. Samples were collected and the protein standards were assayed as described by Martin and Ames (1961); the TS and DHFR activities were assayed as described above.

**Protein Analysis.** Protein concentrations were determined by the method of Read and Northcote (1981) using BSA as a standard. Purified TS-DHFR was submitted to high-performance liquid chromatography on a  $C_4$  reverse-phase column (Vydac Model 214TP54; 0.4x25 cm) prior to amino acid analysis. A 40-min linear gradient was run at 0.5 ml/min from 24-95% acetonitrile in aqueous 0.1% trifluoroacetic acid, and protein was detected by its absorbance at 220 nm. TS-DHFR eluted in a single peak with a retention volume of 12.0 ml (70% acetonitrile). Protein samples were hydrolyzed for 24, 48, and 72 hr in 6 M HCl at 110 °C; amino acid compositions were determined in duplicate on a Beckman 6300 amino acid analyzer. Tryptophan content was determined by hydrolyzing TS-DHFR in 4 M methanesulfonic acid (Simpson and al., 1978); the hydrolysate was analyzed on a Beckman 121 amino acid analyzer.

## Results

**Purification of TS-DHFR from MTX-Resistant *L. major*.** Most freshly prepared crude extracts from MTX-resistant *L. major* possess 20-40-fold higher levels of TS-DHFR than extracts of wild-type organisms. Early in this work we found that storage of either frozen cells or crude extracts resulted in loss of TS and DHFR activities and that during purification the TS activity decreased disproportionately to that of DHFR, presumably because of proteolysis. Ultimately, we obtained optimal yields when harvested cells were immediately lysed in the presence of a mixture of protease inhibitors and when purification steps were performed without interruption.

Preliminary studies were performed to evaluate a number of affinity chromatography matrices that have been used to purify TS or DHFR from other sources. In these experiments, crude extracts were applied to small columns containing the affinity matrix. After the column was washed with salt to remove nonspecifically bound protein, the enzyme was eluted biospecifically. First, we examined MTX-Sepharose, an affinity matrix that has been used extensively to purify a number of DHFRs (Kaufman, 1974). As shown in Figure 1A, both activities were retained on this column and coeluted when treated with 1.0 mM H<sub>2</sub>folate; the TS-DHFR was obtained in about 75% yield and was about 100-fold purified. Second, we examined Cibacron Blue-agarose, a matrix that has affinity for some enzymes that bind to nicotinamide cofactors and that has also been used to purify DHFR (Johnson et al., 1980). In our initial experiments, the *Leishmania* TS-DHFR did not elute with buffers containing 1 M KCl, 0.1 mM dUMP, or 0.5 mM NADPH but did elute with buffer containing 0.5 mM H<sub>2</sub>folate. In the final protocol, we included 0.5 mM NADPH in the loading buffer in an attempt to prevent binding of other enzymes that use NADPH. After the column was washed with salt, TS and DHFR activities were eluted with H<sub>2</sub>folate in 50% overall yield with a 20-fold purification (Figure



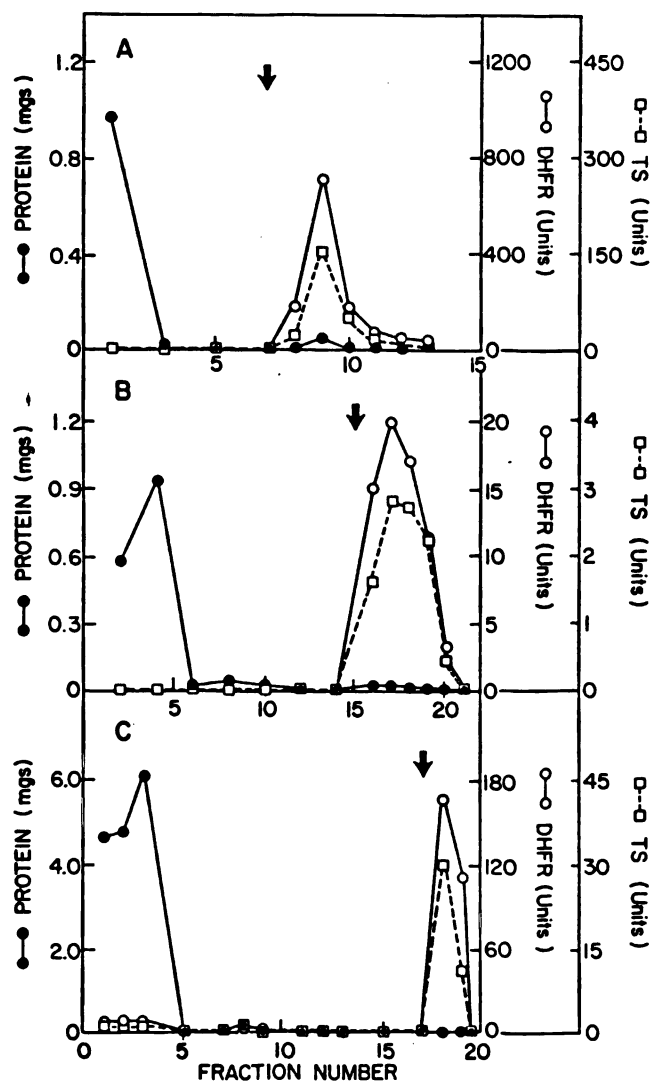


Figure 1: Affinity chromatography of TS-DHFR. (A) The extract was applied to a column containing MTX-Sepharose (0.1 x 2.5 cm) equilibrated with buffer C. The column was washed with buffer C containing 1 M KCl, and TS-DHFR was eluted with buffer B containing 1 mM H<sub>2</sub>folate (arrow). (B) The extract in buffer B containing 0.5 M NaCl and 0.5 mM NADPH was applied to a column containing Cibacron Blue-agarose (0.5 x 4 cm) equilibrated with the same buffer. The column was washed with 10 ml of loading buffer and 5 ml of buffer B containing 0.5 M NaCl; TS-DHFR was eluted with

buffer B containing 0.5 M NaCl and 0.5 mM H<sub>2</sub>folate (arrow). (C) The extract was applied to a column of PteGlu<sub>4</sub>-lysine-Sepharose (0.5 x 3 cm) equilibrated with buffer B. The column was washed with 15 ml of buffer B containing 0.5 M NaCl, and TS-DHFR was eluted with buffer B containing 1 M NaCl and 0.5 mM H<sub>2</sub>folate (arrow).

1B). The third affinity column was PteGlu<sub>4</sub>-lysine-Sepharose, an affinity resin that has been used to purify TS (Rao & Kisliuk, 1983). However, unlike previously reported uses of this matrix, the *Leishmania* TS-DHFR bound tightly to the resin in the absence of dUMP and was eluted with 0.5 mM H<sub>2</sub>folate (Figure 1C). The enzyme was obtained in 65% yield and was about 100-fold purified compared with the crude extract. Of the affinity columns described, MTX-Sepharose and PteGlu<sub>4</sub>-lysine-Sepharose were clearly the most effective; because of its availability, MTX-Sepharose was chosen for further study.

The TS-DHFR from MTX-resistant *L. major* was purified by sequential DEAE-Sepharose chromatography and MTX-Sepharose affinity chromatography (Table I). Early in this work DEAE-Sepharose chromatography was performed with a linear gradient; both enzymes activities coeluted at about 0.07 M salt, and pooled fractions were about 8-fold purified. Subsequently, we found it more convenient to elute the enzyme activities with a single salt concentration of 0.15 M KCl. This provided a 3-4-fold purification, which was sufficient to provide homogenous enzyme after affinity chromatography on MTX-Sepharose. The highly purified TS-DHFR exhibited a single band on NaDodSO<sub>4</sub>-PAGE (Figure 2) and a single band upon isoelectric focusing under both denaturing and nondenaturing conditions. The isoelectric point of the native protein was  $6.4 \pm 0.1$ .

**Serine Transhydroxymethylase.** Crude extracts of wild-type and MTX-resistant *L. major* possessed 0.003 and 0.001 unit/ml serine transhydroxymethylase, respectively. The enzyme coeluted with TS-DHFR from DEAE-Sepharose upon elution with 0.15 M salt but separated from TS-DHFR during MTX-Sepharose chromatography.

Table I. Purification of TS-DHFR from *Leishmania tropica* (R1000)<sup>a</sup>

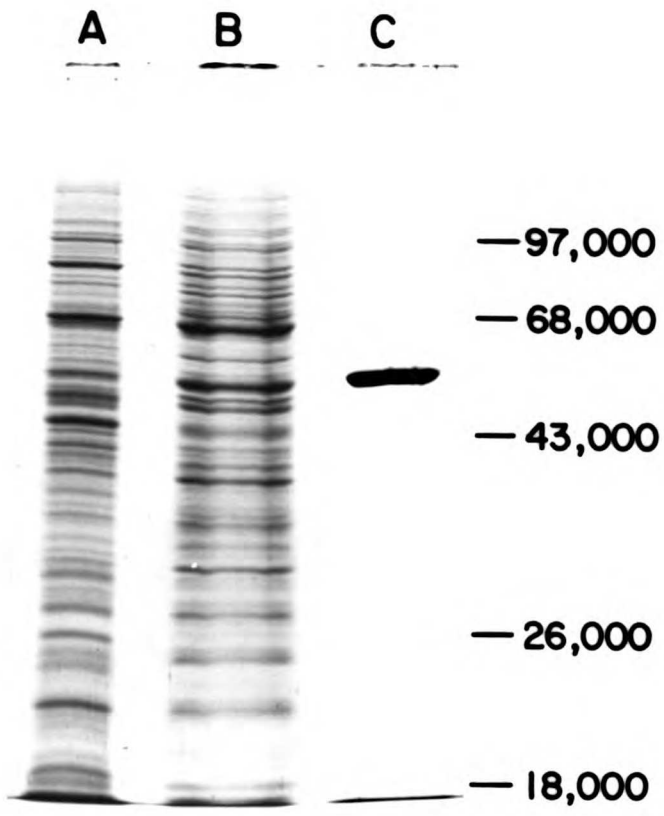
purification step	total protein (mg)	DHFR		TS		total purification yield (x-fold) <sup>b</sup>	purification yield (%)
		specific activity (U/mg)	total units	specific activity (U/mg)	total units		
I. crude extract	48.7	179	8700	40.6	1980	1.0	100
II. DEAE-Sephadex chromatography	10.9	631	6880	192	2091	3.5	80
III. MTX-Sephadex chromatography	0.41	14620	6000	3620	1480	82	69

<sup>a</sup>Prepared from  $4 \times 10^{10}$  cells. <sup>b</sup>Based on DHFR activity.



Figure 2.

NaDodSO<sub>4</sub>-PAGE (12.5% polyacrylamide) of *L. major* TS-DHFR following each step of protein purification : (A) crude extract (30 µg); (B) after DEAE-Sepharose column chromatography (30 µg); (C) after MTX-Sepharose column chromatography (3 µg). The molecular weight standards were phosphorylase *b* (97 000), bovine serum albumin (68 000), ovalbumin (43 000), alpha-chymotrypsinogen (26 000), and beta- lactoglobulin (18 000).



### **Native and Subunit Molecular weights of *L. major* TS-DHFR.**

NaDodSO<sub>4</sub>-PAGE of the purified TS-DHFR showed a single protein band (over 99% of the total protein by densitometric scanning) with a molecular weight of 56 2000 ±200 (eight determinations with 8.5%, 9%, 10%, and 12.5% polyacrylamide gels). A single radioactive peak corresponding to a molecular weight of 56 400 was observed upon NaDodSO<sub>4</sub>-PAGE of the complex formed with [<sup>3</sup>H]FdUMP and CH<sub>2</sub>H<sub>4</sub>folate. Gel filtration of the purified protein on Bio-Gel P-300 resulted in coelution of TS and DHFR activities in a single peak that corresponded to an apparent molecular weight of 150 000 and a Stokes radius of 4.4 nm. Glycerol density gradient centrifugation of the purified TS-DHFR indicated a sedimentation coefficient of 6.0 S. Using the data and a partial specific volume of 0.734 cm<sup>3</sup>/g determined as described below, we calculated a molecular weight of 110 000 and a frictional coefficient of 1.40 (Siegel & Monty, 1966).

**Amino Acid Analysis.** The amino acid composition of *L. major* TS-DHFR is given in Table II. Using the nearest integer of the experimentally determined values, we calculated that the native protein has 988 amino acids and a molecular weight of about 108 800. The extinction coefficient calculated from the tyrosine and tryptophan content (Edelhoch, 1967) was  $E_{280} = 87\,600\text{ M}^{-1}\text{cm}^{-1}$ , which agreed with the value of  $83\,600\text{ M}^{-1}\text{cm}^{-1}$  determined by the method of Scopes (1974). From the amino acid composition the partial specific volume for TS-DHFR was calculated to be 0.734 cm<sup>3</sup>/g (Cohn & Edsall, 1943).

**Interaction of TS-DHFR with MTX and FdUMP.** MTX was a potent inhibitor of DHFR activity and FdUMP was a potent inhibitor of TS activity in the bifunctional protein; both compounds exhibited patterns characteristic of stoichiometric inhibition (Ackerman & Potter, 1949). However, MTX did not inhibit TS and FdUMP did not inhibit DHFR. When 1.0 μM MTX was added to on-going reactions, DHFR was rapidly inhibited, but the rate of dTMP formation was unchanged. Similarly, in the

Table II. Amino Acid Composition of *L. tropica* TS-DHFR

Amino acid	Residue/dimer
Asx	89.1
Thr	55.1
Ser	58.1
Glx	117.8
Pro	52.9
Gly	79.6
Ala	104.4
Cys <sup>a, b</sup>	6.1
Val <sup>b</sup>	49.8
Met	29.6
Ile <sup>b</sup>	38.2
Leu <sup>b</sup>	105.1
Tyr	24.3
Phe	37.9
His	16.0
Lys	53.5
Arg	60.7
Trp <sup>c</sup>	9.6

<sup>a</sup>Determined as cysteic acid. <sup>b</sup>Data obtained from 72-h hydrolyses. <sup>c</sup>Obtained from protein hydrolysis in 4 M methanesulfonic acid.

presence of 25  $\mu\text{M}$  CH<sub>2</sub>-H<sub>4</sub>folate, adding 2.0  $\mu\text{M}$  FdUMP rapidly inhibited TS but did not affect the rate of DHFR-catalyzed reduction of H<sub>2</sub>folate.

The inhibitory properties of MTX and FdUMP were analyzed by the method of Cha (1975). This method requires determining the concentration of inhibitor necessary for 50% inhibition ( $I_{50}$ ) at several concentrations of enzyme ( $E_i$ ) and, from eq 1, permits approximations of both the  $K_i$  of the inhibitor and the stoichiometry of binding. The  $I_{50}$

$$I_{50} = 0.5E_i + K_i \quad (1)$$

values for MTX inhibition of DHFR in the presence of 0.10 mM NADPH were determined under standard assay conditions with 0.32-1.6 nM TS-DHFR; similarly,  $I_{50}$  values for FdUMP inhibition of TS in the presence of 0.24 mM CH<sub>2</sub>-H<sub>4</sub>folate were determined with 2.0-6.0 nM bifunctional protein. Plots of  $I_{50}$  values ( $n = 5$ ) of the inhibitors vs. the concentration of TS-DHFR gave  $K_i$  values of  $0.13 \pm 0.04$  nM for MTX and  $0.3 \pm 0.1$  nM for FdUMP; the stoichiometry determined from the slopes of such plots indicated that 0.98 mole of MTX and 1.44 mole of FdUMP were bound per mole of dimeric enzyme. The stoichiometry of binding was also directly determined by forming the [<sup>3</sup>H] MTX-enzyme and [<sup>3</sup>H] FdUMP-CH<sub>2</sub>H<sub>4</sub>folate-enzyme complexes, as described under Materials and Methods, and then isolating the complexes by Sephadex G-25 chromatography at 4 °C. With crude extract, 316 pmole of [<sup>3</sup>H] FdUMP and 163 pmol of [<sup>3</sup>H] MTX were bound per milligram of protein. After the protein was purified to homogeneity, 2.20 mole of [<sup>3</sup>H] FdUMP and 1.05 mole of [<sup>3</sup>H] MTX were bound per mole of enzyme.

The rates of dissociation of MTX and FdUMP from purified TS-DHFR were determined by a previously described method (Santi et al., 1974). In separate solutions, [<sup>3</sup>H] MTX-enzyme and [<sup>3</sup>H] FdUMP-CH<sub>2</sub>H<sub>4</sub>folate-enzyme complexes were formed as described under Materials and Methods. A 500-fold excess of unlabeled inhibitor was

added to each solution and the solutions were incubated at 25 °C. At intervals, aliquots were removed and assayed for enzyme-bound [<sup>3</sup>H]FdUMP by the nitrocellulose-binding assay or enzyme-bound [<sup>3</sup>H] MTX by gel filtration. In each case, loss of bound radioactivity was first order for at least 3 half-lives; FdUMP dissociated with  $k = 0.0056 \text{ min}^{-1}$  and MTX dissociated with  $k = 0.033 \text{ min}^{-1}$ .

#### **Inactivation of TS-DHFR by NEM and Protection by Substrates.**

Treatment of TS-DHFR with NEM resulted in a time-dependent loss of both activities. In a typical experiment, the enzyme was incubated with the specified amount of NEM in 50 mM Tes (pH 7.4), 1 mM EDTA, and 0.5 mM DTT; at various time intervals, 50  $\mu$ l aliquots were removed and added to 0.95 ml of the standard assay mixture, and the initial velocity was determined. With 15 units/ml TS and 0.2 mM NEM, there was first-order loss of enzyme activity with  $t_{1/2} = 9 \text{ min}$ . When 1.0  $\mu$ M dUMP was included in the incubation mixture there was no loss in activity for as long as 15 min. Similarly, treatment of 60 units/ml DHFR with 0.01 mM NEM resulted in a first-order loss of DHFR activity with  $t_{1/2} = 17 \text{ min}$ . The presence of 1.0  $\mu$ M NADPH afforded complete protection for up to 30 min; with 1.0  $\mu$ M H<sub>2</sub>folate, 85% of the activity remained after 30 min. Treatment of the FdUMP-CH<sub>2</sub>H<sub>4</sub>folate-enzyme complex with 0.01 mM NEM for 30 min resulted in a 90% loss in DHFR activity, which was identical with a control in which the enzyme was not bound to FdUMP.

Kinetic constants of the *L. major* TS-DHFR were determined from double-reciprocal plots in experiments in which the nonvaried substrate was kept at a fixed, saturating concentration. For DHFR, apparent  $K_m$  values for H<sub>2</sub>folate and NADPH were  $1.5 \pm 0.1 \mu\text{M}$  and  $2.7 \pm 0.1 \mu\text{M}$ , respectively, at pH 7.0 and 25 °C in the presence of 100  $\mu$ M fixed substrate. For TS at pH 7.8 and 25 °C, the apparent  $K_m$  for

dUMP was  $4.7 \pm 0.9 \mu\text{M}$  with  $1.7 \text{ mM CH}_2\text{H}_4\text{folate}$  and the  $K_m$  for (6*R*)-L- $\text{CH}_2\text{H}_4\text{folate}$  was  $35 \pm 4 \mu\text{M}$  with  $0.1 \text{ mM dUMP}$ . The  $K_m$  for the diastereomeric mixture of  $\text{CH}_2\text{H}_4\text{folate}$  was  $65 \pm 8 \mu\text{M}$ , twice that of the natural isomer, indicating the inactive 6*S* diastereomer does not significantly inhibit TS. Our most active preparations of the bifunctional enzyme gave  $V_{\text{max}}$  values of  $19 \pm 2 \mu\text{mol min}^{-1} \text{ mg}^{-1}$  for DHFR and  $4.5 \pm 0.4 \mu\text{mol min}^{-1} \text{ mg}^{-1}$  for TS.

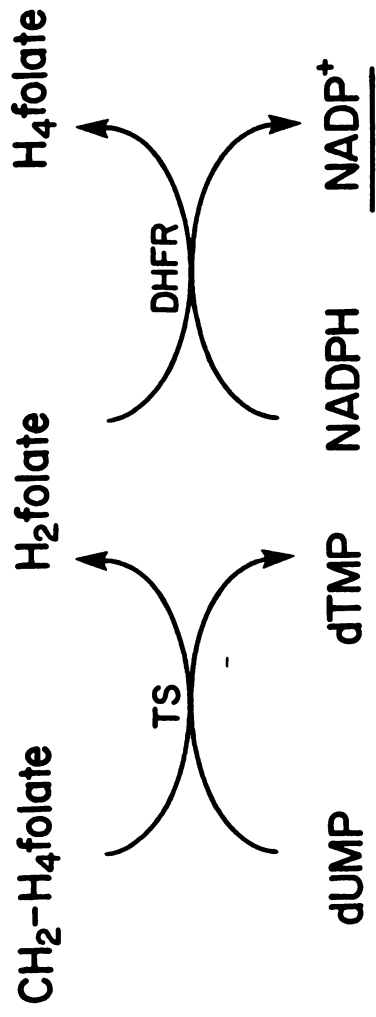
To obtain kinetic parameters of DHFR required for the coupled TS-DHFR assay (see below), initial velocities were determined in buffer A (pH 7.8), which contained  $100 \mu\text{M NADPH}$ ,  $5 \text{ mM formaldehyde}$ , and limiting *L. major* TS-DHFR or *L. casei* DHFR. For the bifunctional protein, the apparent  $K_m$  for  $\text{H}_2\text{folate}$  was  $0.6 \pm 0.1 \mu\text{M}$  and  $V_{\text{max}}$  was  $18 \pm 1 \mu\text{mol min}^{-1} \text{ mg}^{-1}$ . The *L. casei* DHFR showed an apparent  $K_m$  for  $\text{H}_2\text{folate}$  of  $1.5 \pm 0.2 \mu\text{M}$  and  $V_{\text{max}} = 17 \pm 1 \mu\text{mol min}^{-1} \text{ mg}^{-1}$ .

**Coupled Assay for TS and DHFR.** The coupled assay depicted in Scheme I was used to monitor the DHFR-catalyzed reduction of  $\text{H}_2\text{folate}$  formed by TS. With certain assumptions (Easterby, 1973; Rudolph et al., 1979), eq 2 depicts the time course of NADP formation. Here,  $K_m$  is the

$$[\text{NADP}] = v_1 t + (v_1/v_2) K_m (e^{-v_2/K_m} - 1) \quad (2)$$

Michaelis constant for  $\text{H}_2\text{folate}$ ,  $v_1$  is the rate ( $\mu\text{M min}^{-1}$ ) of TS under conditions of the coupled assay, and  $v_2$  is the rate of DHFR using near-saturating concentrations of substrates. In the experiments described below, extrapolation of the linear portion of plots of NADP to the horizontal axis ( $K_m/v_2$  provided the lag time that precedes attainment of a

Scheme I





steady-state concentration of H<sub>2</sub>folate, and extrapolation to the vertical axis ( $v_1 K_m / v_2$ ) provided the steady-state concentration of H<sub>2</sub>folate.

Early in these studies, we found that CH<sub>2</sub>H<sub>4</sub>folate inhibited DHFR of the bifunctional enzyme ( $K_i = 150 \mu\text{M}$ ) and cause concentration-dependent increases in the lag time of NADP production. To minimize this effect, we used a low concentration of CH<sub>2</sub>H<sub>4</sub>folate (30  $\mu\text{M}$ ) in the coupled assays. Although this amount was insufficient to saturate TS, the necessary data could be obtained over a period of time where only a small fraction of the cofactor was consumed (<10%), so  $v_1$  closely approximates a zero-order reaction.

The validity of eq 2 under the coupled assay conditions of TS and DHFR was confirmed by using mixtures of the individual enzymes for *L. casei*. In contrast to the bifunctional enzyme, CH<sub>2</sub>H<sub>4</sub>folate showed no inhibition of *L. casei* DHFR at concentrations 80-fold higher than that of the substrate H<sub>2</sub>folate. With limiting TS, the production of NADP shows a lag as expected of two noninteracting enzymes in a coupled assay system; this closely corresponds to the curve simulated from eq 2 (Figure 3A). As shown in Table III, both the lag times of NADP formation and steady-state concentrations of H<sub>2</sub>folate agree with those calculated from eq 2 by using  $K_m = 1.5 \mu\text{M}$  for H<sub>2</sub>folate and specified values for  $v_1$  and  $v_2$ . The results also show that we were able to detect lag times as low as 12 s and steady-state concentrations of H<sub>2</sub>folate as low as 0.10  $\mu\text{M}$ .

Figure 3B shows the experimental and simulated time course of NADP production in the coupled assay using a preparation of TS-DHFR that had a TS rate ( $v_1$ ) of 0.11  $\mu\text{M min}^{-1}$  and a DHFR rate ( $v_2$ ) of 0.57  $\mu\text{M min}^{-1}$ . When  $K_m = 0.6 \mu\text{M}$  for H<sub>2</sub>folate was

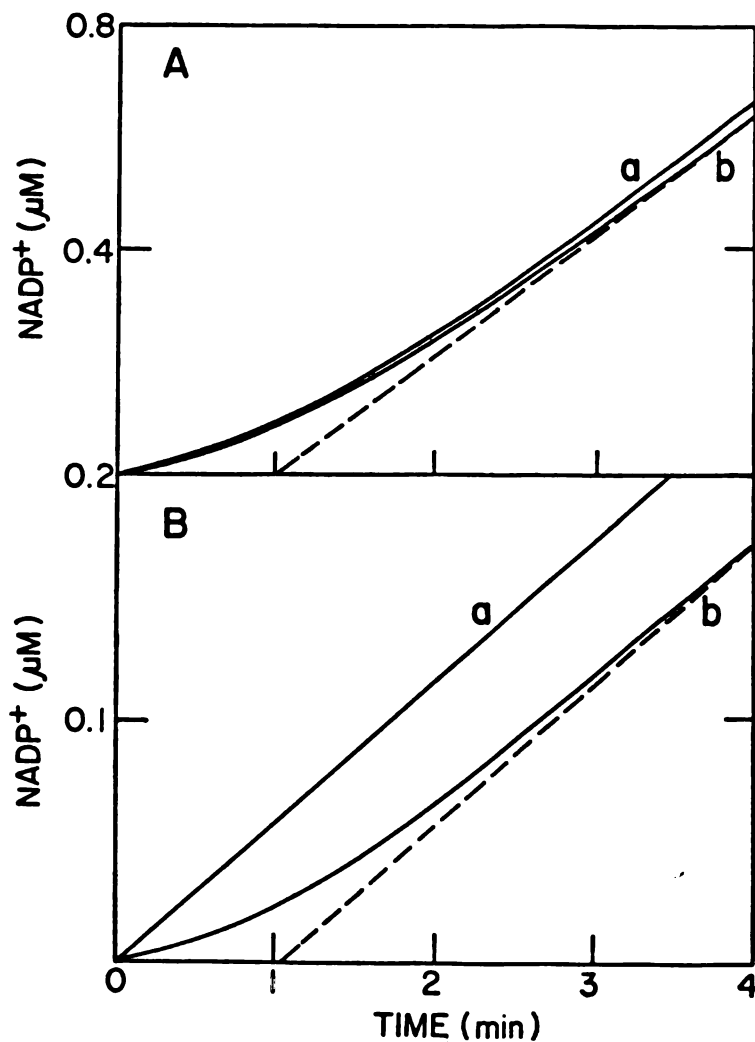


Figure 3: Experimental and simulated time courses for NADP formation in the TS-DHFR coupled assay using the enzymes from L. casei and L. major. Reactions were performed as described under Materials and Methods, and simulations were computer generated from eq. 2. (A) Curve a is the observed time course using  $0.3 \text{ uM min}^{-1}$  TS and  $1.5 \text{ uM min}^{-1}$  DHFR from L. casei. Curve b is the time course simulated from the aforementioned values, and  $K_m=1.5 \text{ uM}$ . (B) Curve a is the observed time course using the bifunctional enzyme from L. major, which had  $0.11 \text{ uM min}^{-1}$  TS and  $0.57 \text{ uM min}^{-1}$  DHFR; curve b is the time course simulated ( $K_m=0.6 \text{ uM}$ ).

Table III. Coupled TS/DHFR Assays Using Mixtures of TS and DHFR from *L. casei* and the Bifunctional TS-DHFR from *L. tropica*

Source	rate ( $\mu\text{M min}^{-1}$ ) TS	rate ( $\mu\text{M min}^{-1}$ ) DHFR	lag time (sec)		steady state $\text{H}_2$ folate ( $\mu\text{M}$ )	
			Calc.	Exp.	Calc.	Exp.
<i>L. casei</i>	1.0	9.0	10	12	0.17	0.10
	0.30	3.0	30	35	0.15	0.16
	0.30	1.5	60	65	0.30	0.24
<i>L. tropica</i>	0.11	0.57	63	<sup>a</sup>	0.12	-
	0.22	1.1	33	-	0.12	-
	0.33	1.7	21	-	0.12	-

<sup>a</sup>Not detectable.

used and inhibition of DHFR by  $\text{CH}_2\text{H}_4\text{folate}$  was ignored, eq 2 predicts a 63-s lag time and  $0.12 \mu\text{M}$  steady-state concentration of  $\text{H}_2\text{folate}$ . However, no lag in NADP production was observed. Since we could experimentally detect lag times as low as 12 s, this result indicates that at least 80% of the  $\text{H}_2\text{folate}$  produced by TS in the bifunctional protein is channeled to DHFR faster than it is released into the medium. Similar experiments that used higher concentrations of the bifunctional TS-DHFR resulted in expected increase in the steady-state rate of NADP production, but lag periods and  $\text{H}_2\text{folate}$  could not be detected (Table III). If inhibition of *L. major* DHFR by  $\text{CH}_2\text{H}_4\text{folate}$  is taken into consideration, the simulated lag periods and steady-state concentrations of  $\text{H}_2\text{folate}$  would be even greater than the values used here.

**TS-DHFR from Wild-Type *L. major*.** It has been previously reported that TS-DHFR from wild-type and MTX-resistant *L. major* is inhibited to the same extent by MTX (Coderre et al., 1983). For additional characterization, TS-DHFR from wild-type *L. major* was purified as described for the MTX-resistant organisms except that a linear gradient of 0-0.2 M KCl was used in the DEAE-Sepharose step. From  $4 \times 10^{10}$  cells possessing 8.9 units of DHFR and 4.0 units of TS per milligram of protein, the enzyme was purified 1500-fold and obtained in 46% yield. The purified protein had specific activities similar to those of purified TS-DHFR from MTX-resistant organisms, eluted from gel filtration chromatography with an apparent molecular weight of 150 000, and showed a single band on NaDodSO<sub>4</sub>PAGE corresponding to a molecular weight of 56 000. The  $K_m$  ( $1.0 \pm 0.2 \mu\text{M}$ ) and  $V_{\max}$  ( $23 \mu\text{mol min}^{-1} \text{mg}^{-1}$ ) of  $\text{H}_2\text{folate}$  at pH 7.0, as well as the rate of dissociation of the [<sup>3</sup>H] MTX-enzyme complex ( $k = 0.038 \text{ min}^{-1}$ ), were similar to the values obtained for TS-DHFR from MTX-resistant cells.

## Discussion

TS and DHFR have been shown to exist as a bifunctional protein in diverse species of protozoan (Ferone & Rowland, 1980; Garrett et al., 1984). We have initiated investigations of this unusual protein in protozoan that are pathogenic to man. However, in most cases, studies of TS-DHFR from such organisms are limited by the amount of protein that can be obtained; the TS-DHFRs are present in relatively low abundance, and it is impractical to obtain large quantities of pathogenic protozoa. Recently, we developed a MTX-resistant strain of *L. major* promastigotes that, by DNA amplification, overproduces TS-DHFR (Coderre et al., 1983). The bifunctional protein represents about 1% of the soluble protein in these organisms, and milligram amounts of purified protein can be obtained from a few liters of organisms grown in tissue culture. A comparison of kinetic parameters of DHFR, MTX, binding and native and subunit molecular weights of TS-DHFR from resistant and parent cell lines revealed no differences; unless otherwise specified, we used the protein from MTX-resistant *L. major*.

The bifunctional TS-DHFR has been purified to homogeneity by ion-exchange chromatography on DEAE-Sepharose and affinity chromatography on MTS-Sepharose. As indicated in Table I, only an 80-fold purification was required, and the homogenous protein was obtained in about 70% yield. By use of a similar procedure, TS-DHFR from wild-type organisms was purified 1500-fold and obtained in 46% yield. Two additional affinity chromatography systems were effective in purifying TS-DHFR: the bifunctional protein bound avidly to PteGlu<sub>4</sub>-lysine-Sepharose and Cibacron Blue-agarose and, after elution of nonspecifically bound proteins, was obtained by biospecific elution with H<sub>2</sub>folate. The major difficulty encountered in purifying TS-DHFR was loss of enzyme activities, particularly TS, which occurred upon storage of cells or crude extracts and during purification. We attributed this problem in part to proteolysis and were able to circumvent it to a great extent by using freshly harvested cells, including protease

inhibitors during cell lysis, and performing the purification without interruption. When the purified protein was used, it was subsequently found that TS but not DHFR activity was extremely sensitive to a variety of endopeptidases as well as carboxypeptidase A (see Chapter 2).

The purified protein migrated as a single band on native isoelectric focusing gels with  $pI = 6.4$  and on NaDodSO<sub>4</sub>-PAGE with an apparent molecular weight of 56 200. The molecular weight of the native enzyme appeared to be 150 000 as determined by gel filtration chromatography. However, using the Stokes radius, sedimentation coefficient, and partial specific volume, we calculated a molecular weight of 110 000, which agrees with the value of 108 800 calculated from the amino acid composition. These parameters closely resemble those reported for the bifunctional protein from *C. fasciculata* (Ferone & Rowland, 1980) and demonstrate that the *L. major* TS-DHFR is a dimer of subunits with identical size. In addition, the homogenous protein showed a single band upon isoelectirc focusing under denaturing conditions, demonstrating that the subunits also have identical charge. The probability is very low that two different subunits of the protein would have both identical molecular weights and charge (O'Farrell, 1975), and it is reasonable to conclude that the subunits are identical, each possessing TS and DHFR.

It has been suggested that additional enzymes might be associated with the TS-DHFR of protozoa (Ferone & Rowland, 1980). In particular, serine transhydroxymethylase would be an attractive candidate because it catalyzes the conversion of H<sub>4</sub>folate to CH<sub>2</sub>-H<sub>4</sub>folate and completes the cycle necessary for continuing dTMP synthesis. However, *L. major* TS-DHFR and serine transhydroxymethylase are readily separable upon MTX-Sepharose, and if an association does exist, it must be weak. Further, serine transhydroxymethylase levels are not increased in MTX-resistant cells, indicating that the gene that codes for this protein is not present in the amplified region of DNA that possesses the TS-DHFR gene.

FdUMP was a potent inhibitor of TS activity in the bifunctional protein, showing an apparent  $K_i$  of 0.3 nM. As with TS from other sources, covalent [ $^3\text{H}$ ]FdUMP- $\text{CH}_2\text{H}_4\text{folate}$ -enzyme complexes were formed that could be isolated and quantitated and were stable upon NaDodSO<sub>4</sub>-PAGE. Similarly, MTX was a potent inhibitor of DHFR activity with an apparent  $K_i$  of 0.1 nM, and [ $^3\text{H}$ ]MTX-enzyme complexes were formed that were sufficiently stable for isolation for isolation and quantitation. Kinetic analysis indicated that about 1.5 mole of FdUMP was bound per mole of enzyme, but direct binding experiments that used [ $^3\text{H}$ ]FdUMP as an active-site titrant for TS clearly demonstrated that 2 mole of inhibitor was bound per mole of TS-DHFR. In contrast, kinetic analysis and binding experiments demonstrated that only 1 mole of MTX was bound per mole of dimeric enzyme. We interpret this result to indicate that two DHFR active sites interact in such a manner that when one is bound to MTX, the other is both catalytically incompetent and unable to bind to MTX. Whether an interaction between the DHFR sites is important in the catalytic reaction was not revealed by the kinetic experiments performed in the present study.

Studies of TS from a variety of sources revealed that a cysteine residue is essential in catalysis; an early event in the reaction involves attack of a sulfhydryl group of the enzyme at the 6-position of dUMP, which activates the 5-position for reaction with the cofactor,  $\text{CHL}_2\text{-H}_4\text{folate}$  [for a review, see Santi & Danenberg (1984)]. This aspect of the mechanism has been verified by studies of the interaction of TS with the mechanism-based inhibitor, FdUMP, which forms a covalent FdUMP- $\text{CH}_2\text{-H}_4\text{folate}$ -TS complex in which the 6-position of the inhibitor is covalently attached to the catalytic cysteine residue [for a review, see Maley et al. (1984)]. As shown here, treatment of the bifunctional protein with the sulfhydryl reagent NEM resulted in rapid inactivation of TS activity that was prevented by the substrate dUMP. By analogy to what is known of the

enzyme from other sources, it is reasonable to assume that a cysteine residue of the bifunctional enzyme serves as a nucleophilic catalyst in the TS reaction and is directly involved in forming the covalent FdUMP-CH<sub>2</sub>-H<sub>4</sub>folate-enzyme complex. Cysteine residues are also found in a number of DHFRs, but available evidence indicates that they do not play a direct role in catalysis (Williams & Bennett, 1977; Blakley, 1984). The DHFR activity of the bifunctional protein was also inactivated by NEM. This inactivation also occurred with the FdUMP-CH<sub>2</sub>-H<sub>4</sub>folate-enzyme complex, demonstrating that the susceptible sulfhydryl group in DHFR is distinct from that in TS. Although NADPH and, to a lesser extent, H<sub>2</sub>folate protected DHFR from inactivation, it is not known whether the modified cysteine is within the active center and is directly protected by substrate binding or whether substrate binding causes a conformational change that results in protection of a thiol remote from the active center. Nevertheless, both DHFR and TS domains of the bifunctional protein appear to possess at least one cysteine residue that is essential for catalytic activity.

One of the possible biological advantages of the bifunctional TS-DHFR is channeling of the H<sub>2</sub>folate produced in the TS reaction to the substrate binding site of DHFR. To test this, we used a couple assay system containing all substrates except H<sub>2</sub>folate and monitored the formation of NADP that occurred upon DHFR-catalyzed reduction of the H<sub>2</sub>folate generated in situ. Equations that describe the kinetics of a coupled system containing two enzymes predict that channeling of H<sub>2</sub>folate would be manifested by a decrease in the lag period that precedes linearity of the rate of the second enzyme, DHFR. As a model system, mixtures of the individual TS and DHFR from *L. casei* were used to verify that these enzymes followed the expected kinetic behavior of two separate sequential enzymes under the conditions of the coupled assay; both lag times for



NADP production and steady-state concentrations of H<sub>2</sub>folate closely matched predicted values for two noninteracting enzymes. In contrast, under similar conditions with the *L. major* TS-DHFR there was no observable lag time preceding NADP production and H<sub>2</sub>folate was undetectable. Since we could experimentally detect lag times as low as 12 s and predicted lag times were as high as 63 s for the bifunctional assay, we conclude that at least 80% of the H<sub>2</sub>folate produced by TS was channeled to DHFR faster than it was released into bulk solvent.

Although unlikely, TS and DHFR might share a common folate binding site. However, when TS activity was completely inhibited by formation of the FdUMP-CH<sub>2</sub>-H<sub>4</sub>folate-enzyme complex, DHFR remained active. Conversely, complete inhibition of DHFR by MTX did not significantly affect TS activity. Together with the aforementioned disproportionate sensitivity of TS toward proteolysis, these results clearly demonstrate that TS and DHFR have autonomous binding sites.

**Acknowledgements.** We thank W. Hensell, R. Harkins, and D. Hardman for performing the amino acid analysis.

#### References.

- Ackerman, H.W., and Potter V.R. (1949) Proc.Soc.Exp.Biol.Med. **72**, 1-9.
- Bethell, G.S., Ayers, J.S., and Hancock, W.S. (1979) J.Biol.Chem. **254**, 2572-2574.
- Blakley, R.L. (1984) in Folates and Pteridines (Blakley, R.L., and Benkovic, S.J., Eds.) Vol. 1, pp 191-253, Wiley, New York.
- Bruice, T.W., and Santi, D.V. (1982) Biochem. **21**, 6703-6709.
- Cha, S. (1975) Biochem.Pharmacol. **24**, 217-2185.
- Coderre, J.A., Beverley, S.M., Schimke, R.T., and Santi, D.V. (1983)

- Proc.Natl.Sci.USA **80**, 2132-2136.
- Cohn, E.J., and Edsall, J.T. (1943) in Proteins. Amino Acids, and Peptides as Ions and Dipolar Ions (Cohn, E.J., and Edsall, J.T., Eds.) pp 370-381, Reinhold, New York.
- Crushberg, T.C., Leary, R., and Kisliuk, R.L. (1970) J.Biol.Chem. **245**, 5292-5296.
- Dann, J.G., Ostler, G., Bjur, R.A., King, R.W., Scudder, P., Turner, P.C., Roberts, G.C.K., and Burgen, A.S.V. (1976) Biochem.J. **157**, 559-571.
- Easterby, J.S. (1973) Biochim.Biophys.Acta **293**, 552-558.
- Edelhoch, H. (1967) Biochem. **6**, 1948-1954.
- Failla, D., and Santi, D.V. (1973) Anal.Biochem. **52**, 363-368.
- Ferone, R., and Roland, S. (1980) Proc.Natl.Acad.Sci.USA **77**, 5802-5806.
- Garrett, C.E., Coderre, J.A., Meek, T.D., Garvey, E.P., Claman, D.M., Beverley, S.M., Santi, D.V. (1984) Mol. Biochem.Parasitol. **11**, 257-265.
- Hillcoat, B., Nixon, P., and Blakley, R.L. (1967) Anal. Biochem. **21**, 178-189.
- Johnson, S.J., Stevenson, K.J., and Gupta, V.S. (1980) Can.J. Biochem. **58**, 1252-1257.
- Kaufman, B.T. (1974) Methods Enzymol. **34**, 272-281.
- Laemmli, U.K. (1970) Nature **227**, 680-685.
- Maley, F., Belfort, M., and Maley, G. (1984) Adv.Enzyme Regul. **22**, 413-430.
- Martin, R.G., and Amers, B.N. (1961) J.Biol.Chem. **236**, 1372- 1379.
- Monod, J., Wyman, J., and Changeux, J.-P. (1965) J.Mol.Biol. **12**, 88-118.
- O'Farrell, P.H. (1975) J.Biol.Chem. **250**, 4007-4021.
- Rao, N.K., and Kisliuk, R.L. (1983) Pro.Natl.Acad.Sci.USA **80**, 916-920.
- Read, S.M., and Northcote, D.H. (1981) Anal.Biochem. **116**, 53-64.
- Rollo, I.M. (1980) in The Pharmacological Basis of Therapeutic (Gilman, A.G., Goodman, L.S., and Gilman, A., Eds.) 6th ed.,pp 1038-1069, Macmillan, New York.
- Rudolph, F.B., Baugher, B.W., and Bessiner, R.S. (1979) Method Enzymol. **63**, 22-42.

- Santi, D.V., and Danenberg, P.V. (1984) in Folates and Pteridines (Blakley, R.L., and Benkovik, S.J., Eds.) Vol. 1, pp343-396, Wiley, New York.
- Santi, D.V., McHenry, C.S., and Periard, E.R. (1974) Biochem. **13**, 467-470.
- Scopes, R.K. (1974) Anal. Biochem. **59**, 277-282.
- Siegel, L.M., and Monty, K.J. (1966) Biochim. Biophys. Acta **112**, 346-362.
- Simpson, R.J., Neuberger, M.R., and Liu, T.Y. (1978) J. Biol. Chem. **253**, 1936-1940.
- Steitz, T.A., Fletterick, R.J., and Hwang, K.J. (1973) J. Mol. Biol. **78**, 551-561.
- Taylor, R.T., and Weissbach, H. (1965) Anal. Biochem. **13**, 80-84.
- Wahba, A.J., and Friedkin, M. (1961) J. Biol. Chem. **236**, PC11.
- Washtien, W.L., and Santi, D.V. (1979) Cancer Res. **39**, 3397-3403.
- Wataya, Y., and Santi, D.V. (1977) Methods Enzymol. **46**, 307-312.
- Williams, M.N., and Bennett, C.D. (1977) J. Biol. Chem. **252**, 6871-6877.
- Winter, A., Ek, K., and Anderson, U-B. (1977) LKB Appl. Note #250.

**Chapter 5****Limited Proteolysis of the Bifunctional Thymidylate Synthase-  
Dihydrofolate Reductase from Leishmania tropica**

1950

—state that it is not intended to be a general statement  
regarding the fact that an amount of money

### Abstract

The structure and activity of the bifunctional thymidylate synthase-dihydrofolate reductase (TS-DHFR) from the protozoan parasite Leishmania major were examined by limited proteolysis with five different endopeptidases. Each reaction resulted in a rapid time-dependent loss of TS activity and no effect on DHFR activity. The proteolytic products were examined under denaturing conditions; each digest produced a fragment that was ~35-kDa, and three of the five digests generated a fragment that was ~20-kDa. Attempts to separate the fragments under native conditions failed, suggesting that the proteolyzed protein remains a dimer with the gross structure of the subunits more or less undisturbed. In contrast, kinetic data indicate that some aspects of higher order structure in the native protein are affected by proteolysis. The fragments (36.6-kDa and 20-kDa) generated by Staphylococcus aureus V-8 protease were subjected to sequence analysis. Whereas neither the native protein nor the 36.6-kDa fragment yielded an N-terminus amino acid, we obtained the sequence of the first 28 amino acids of the 20-kDa fragment. This sequence bore strong homology with sequences situated within four thymidylate synthases. These and other data indicate that the TS-DHFR polypeptide consists of a DHFR sequence at the blocked N-terminal and a TS sequence at the C-terminal end of the protein. The region that is the target of the five proteases corresponds to a highly variable region within the sequences of the four thymidylate synthases. We suggest that an insertion occurs within the TS-DHFR sequence, positioned on the surface of the protein, and quite vulnerable to the action of endopeptidases.

The first part of the document discusses the general principles of the project, including the objectives and the scope of the work. It also outlines the methodology used for the data collection and analysis.

The second part of the document presents the results of the study, including the data collected and the analysis performed. It also discusses the implications of the findings and the conclusions drawn from the study.

The third part of the document discusses the limitations of the study and the areas for future research. It also provides a list of references and a list of figures and tables.

The fourth part of the document discusses the conclusions of the study and the implications of the findings. It also provides a list of references and a list of figures and tables.

The fifth part of the document discusses the conclusions of the study and the implications of the findings. It also provides a list of references and a list of figures and tables.

The sixth part of the document discusses the conclusions of the study and the implications of the findings. It also provides a list of references and a list of figures and tables.

The seventh part of the document discusses the conclusions of the study and the implications of the findings. It also provides a list of references and a list of figures and tables.

The eighth part of the document discusses the conclusions of the study and the implications of the findings. It also provides a list of references and a list of figures and tables.

The ninth part of the document discusses the conclusions of the study and the implications of the findings. It also provides a list of references and a list of figures and tables.

The tenth part of the document discusses the conclusions of the study and the implications of the findings. It also provides a list of references and a list of figures and tables.

Thymidylate synthase and dihydrofolate reductase catalyze consecutive reactions in the de novo synthesis of dTMP. In sources as varied as bacteriophage, bacteria, and vertebrates, these two enzymes exist as distinct and readily separable enzymes (for reviews see refs. 3,4). In contrast, a bifunctional protein, thymidylate synthase-dihydrofolate reductase (TS-DHFR)<sup>1</sup>, has been identified in a number of genera of protozoa which span a diverse group of the subkingdom (1,2). This protein ranges in molecular weight from about 110,000 to 140,000, with subunits of molecular weight 55,000 to 65,000. As has been noted (1), the subunit size of the protozoan TS-DHFR is close to the sum of the subunit size of TS (~35-kDa) and DHFR (~20-kDa) found in most other sources, suggesting that the TS-DHFR gene may have resulted from the fusion of independent TS and DHFR genes. TS-DHFR from a MTX-resistant cell line of the protozoan parasite Leishmania major has been purified to homogeneity and was found to be a dimer of apparently identical subunits of molecular weight 56,000 (5). To date, there has been no direct evidence for either homology or lack of homology between L. major TS-DHFR and the two individual enzymes from any non-protozoan species.

Limited proteolysis has been used to examine the structure of a number of multifunctional proteins. Results of these studies have led to proposals for the arrangement of the various functions on the polypeptide (6,7) and have produced evidence that many multifunctional proteins exist as a series of separate, independent domains (each domain reflecting a function) (7-9). We undertook the limited proteolysis of L. major TS-DHFR in hopes of separating the two activities as proteolytic fragments, the size of each approximating



The first part of the document discusses the importance of maintaining accurate records of all transactions and activities. It emphasizes the need for transparency and accountability in financial reporting. The second part details the various methods used to collect and analyze data, including surveys, interviews, and focus groups. The third part presents the findings of the study, highlighting key trends and insights. The final part concludes with recommendations for future research and practical applications of the findings.

The study was conducted over a period of six months, starting in January and ending in June. Data was collected from a sample of 100 participants, representing a diverse range of backgrounds and experiences. The results indicate that there is a significant correlation between the variables studied, suggesting that the factors investigated have a strong influence on the outcomes. These findings have important implications for both theory and practice, and provide a foundation for further exploration in this field.

In conclusion, the research has provided valuable insights into the complex relationships between the variables under investigation. The findings suggest that a comprehensive understanding of these relationships is essential for developing effective strategies and interventions. Further research is needed to explore the underlying mechanisms and to test the generalizability of the results. The authors hope that this study will contribute to the advancement of knowledge in this area and inform future research and practice.

their non-protozoan counterparts (i.e., TS ~35-kDa and DHFR ~20-kDa). We report here the results of the limited proteolysis of L. major TS-DHFR. We propose an arrangement of the enzymatic activities on the TS-DHFR polypeptide, and suggest a structural model of the region that is selectively cleaved by the five different endopeptidases.

### Materials and Methods

**Enzymes and Activity Measurements.** The bifunctional TS-DHFR from 10-propargyl-5,8-dideazafolate-resistant L. tropica (32) was purified to homogeneity by MTX-Sepharose CL-6B chromatography, as previously described (5). TPCK-treated trypsin, TLCK-treated  $\alpha$ -chymotrypsin, Staphylococcus aureus V-8 protease, Streptomyces griseus type-XIV protease, elastase, and soybean trypsin inhibitor were purchased from Sigma. Rabbit antiserum to L. major TS-DHFR was obtained after injecting 150  $\mu$ g of pure TS-DHFR mixed 1:1 with Freund's complete adjuvant, followed by a boost of 100  $\mu$ g TS-DHFR mixed 1:1 with Freund's incomplete adjuvant. Rabbit antiserum raised against Escherichia coli TS was provided by Dr. F. Maley; rabbit antiserum against E. coli RT 500 DHFR was provided by Dr. D. Baccanari. Goat anti-rabbit antibody-alkaline phosphatase conjugate was from Boehringer Mannheim Biochemicals.

DHFR activity (10) and TS activity (11) were determined spectrophotometrically at 25°C. Also, DHFR was quantitated by binding to [ $^3$ H]MTX (1), and TS was quantitated by binding to [ $^3$ H]FdUMP and CH<sub>2</sub>-H<sub>4</sub>folate (12), as previously described.

... ..  
... ..  
... ..  
... ..

... ..

... ..  
... ..  
... ..  
... ..

... ..  
... ..  
... ..  
... ..

... ..  
... ..  
... ..  
... ..

... ..  
... ..  
... ..  
... ..

**Gel Electrophoresis.** SDS-PAGE (10-15% polyacrylamide) was performed as described by Laemmli (13). Non-denaturing PAGE (12.5% polyacrylamide) was performed as reported by Davis (14). Proteins were transferred from polyacrylamide gels to nitrocellulose filters according to the procedure of Towbin et al. (15). The transferred proteins were probed with antibody, according to the method of Fisher et al. (16); the alkaline phosphatase conjugate was assayed as described by Blake et al. (17). Peptides were isolated from polyacrylamide gels for peptide mapping by the method of Fischer (18) and for N-terminus sequence analysis by the procedure of Hunkapiller et al. (19).

**Limited Proteolysis.** TS-DHFR, 0.1-0.5 mg/ml, in 50mM TES (pH 7.4), 2mM DTT, 1mM EDTA, 5% glycerol, was digested with 1% (wt/wt) endopeptidase or 5-10% (wt/wt) exopeptidase at 25°C. To monitor enzymatic activities, aliquots (2-10 ul) were added directly to 1 ml assay solutions. DEAE-Sepharose chromatography was performed as reported (5), eluting the bound proteolyzed TS-DHFR with a linear gradient of 0-0.2 M KCl. Likewise, MTX-Sepharose chromatography was as described (5), except for the following additional washes of the bound proteolyzed TS-DHFR before elution: 0.1% triton X-100 in 10mM potassium phosphate (pH 7.0) and 0.1% NP-40 in 10mM potassium phosphate (pH 7.0). Enzyme was eluted with 1mM 7,8-dihydrofolate in 50mM TES (pH 7.4), 2mM DTT, 1mM EDTA. G-150 Sephadex (40-120  $\mu$ m; 14 x 56 cm) was equilibrated and analysis was performed with 50mM TES (pH 7.4), 2mM DTT, 1mM EDTA, 10% glycerol. In each chromatographic technique, the elution of the proteolyzed TS-DHFR was monitored by DHFR activity assay and by SDS-PAGE.

The American Red Cross is a national organization that provides humanitarian relief to people in need. It is a voluntary organization that has been serving the community since 1881. The organization's primary focus is on providing relief to people who are suffering from natural disasters, war, and other crises. The organization also provides a wide range of services, including blood donation, disaster relief, and social services. The organization's work is supported by the generosity of millions of people who donate their time and money to help those in need. The organization's success is a testament to the power of volunteerism and the human spirit.

Financial Summary

The American Red Cross has a long history of financial success, and its 1945-1946 annual report shows a record year for the organization. Total revenue for the year was \$100,000,000, a significant increase from the previous year. This revenue was used to fund a wide range of programs and services, including disaster relief, blood donation, and social services. The organization's expenses for the year were \$90,000,000, leaving a net income of \$10,000,000. This net income was used to fund the organization's operations and to provide relief to people in need. The organization's financial success is a result of the generosity of its donors and the dedication of its staff and volunteers. The organization's financial strength allows it to continue its work and to provide relief to people in need for many years to come.

**N-terminus Sequence Analysis.** Sequential Edman degradation was performed by R. Harkins of Genentech, Inc. An Applied Biosystems model 470A vapor-phase sequencer was equipped with a "mini" Conversion Flask and updated with the "no vacuum" program. Polybrene (1.5 mg) was used as a carrier in the cup. In addition, the sequencer has been modified for automatic on-line HPLC separation of the phenylthiohydantoin (PTH) - amino acids as described by H. Rodriguez (20). Sequence data were interpreted with the aid of a Nelson Analytical model 6000 Data Acquisition system, which was interfaced to the HPLC detector. The PTH-amino acids were resolved on a Microsorb 5  $\mu\text{M}$   $\text{C}_8$  column (4.6 mm x 25 cm). The column was operated at a temperature of 42°C. The mobile phases consisted of (A) 20%  $\text{CH}_3\text{CN}$  in 10mM sodium phosphate, pH 4.5, and (B) 70%  $\text{CH}_3\text{CN}$  in water. The flow rate was 1.5 ml  $\text{min}^{-1}$  and a gradient from 100% A to 100% B was generated over 22 min.

### Results

The bifunctional TS-DHFR from L. major was subjected to limited proteolysis by use of five different endopeptidases: S. aureus V-8 protease, trypsin,  $\alpha$ -chymotrypsin, elastase, or S. griseus type XIV protease (Table I). Each of the five proteolytic reactions was monitored for enzymatic activities; in each digest there was a relatively rapid, time-dependent inactivation of TS that followed apparent first order kinetics for at least two half-lives ( $t_{1/2} < 20$  min), and, under the conditions used, no loss of DHFR activity. Curiously, in each of the five digests, the rate of TS inactivation was approximately twice the rate of proteolysis (Table I); when TS was



Table I. Summary of limited proteolysis of *L. tropica* TS-DHFR

Protease	Specificity	Loss of enzymatic activity ( $t_{1/2}$ , min)		Loss of 56-kDa subunit ( $t_{1/2}$ , min) <sup>a</sup>	Predominant fragments generated by protease (kilodaltons) <sup>a</sup>
		TS	DHFR		
<u><i>S. aureus</i></u> V-8 protease	Glu-x, Asp-x	18	no loss (225 min)	40	37.3 → 36.6 <sup>b</sup> 20
trypsin	Arg-x, Lys-x	6	no loss (200 min)	16	34.5 → 33.1 → 31.6 21 → 19
$\alpha$ -chymotrypsin	Tyr-x, Trp-x, Phe-x, Leu-x	20	no loss (90 min)	35	quartet @ 37 19
elastase	uncharged, non-aromatic	5	no loss (135 min)	10	35 m.n.s. <sup>c</sup>
<u><i>S. griseus</i></u> type XIV protease	non-specific	10	no loss (200 min)	14	36 m.n.s.

<sup>a</sup> determined by SDS-PAGE<sup>b</sup> arrows denote fragment generated from previous fragment during course of reaction<sup>c</sup> multiple non-specific bands



completely inactivated, approximately 50% of the 56-kDa subunit remained intact. The extent of proteolysis was also measured by assaying the ability of TS or DHFR to bind their respective stoichiometric inhibitors, [ $^3\text{H}$ ]FdUMP or [ $^3\text{H}$ ]MTX. V-8 protease caused a time-dependent loss in the ability of TS to bind  $^3\text{H}$  FdUMP and  $\text{CH}_2\text{H}_4$  folate, with the rate of loss occurring approximately twice as slowly as the rate of loss in catalytic activity ( $t_{1/2} \sim 35$  min vs. 18 min), and at approximately the same rate as proteolysis ( $t_{1/2} \sim 35$  min vs. 40 min). When TS-DHFR was digested with trypsin, there was no loss in the ability of DHFR to bind MTX; instead the amount of MTX bound to DHFR increased 2.3-fold after proteolysis was complete (that is, after >95% of the 56-kDa subunit had disappeared, as visualized by SDS-PAGE). The kinetic  $K_i$  for MTX inhibition of DHFR was the same for both the native and trypsin-digested protein.

Figure 1A shows the five individual 2-hr proteolytic digests, electrophoresed on a SDS-polyacrylamide gel. Each protease produced a fragment that was  $\sim 35$ -kDa, as visualized on SDS-PAGE. V-8 protease, trypsin, or  $\alpha$ -chymotrypsin also generated a polypeptide that was 20-kDa. When these various fragments were transferred to nitrocellulose and probed with antiserum raised against E. coli TS, only the 56-kDa subunit and the  $\sim 20$ -kDa fragments resulting from the V-8 protease, trypsin, or chymotrypsin digests showed reactivity (Fig. 1B). When the fragments from a V-8 digest were probed with L. major TS-DHFR antibody, both the 36.6-kDa and the 20-kDa fragments as well as the 56-kDa subunit bound the antibody. Antiserum raised against E. coli DHFR showed no reactivity to the native TS-DHFR and was not used in Western blot analysis. To test the assumption that all five

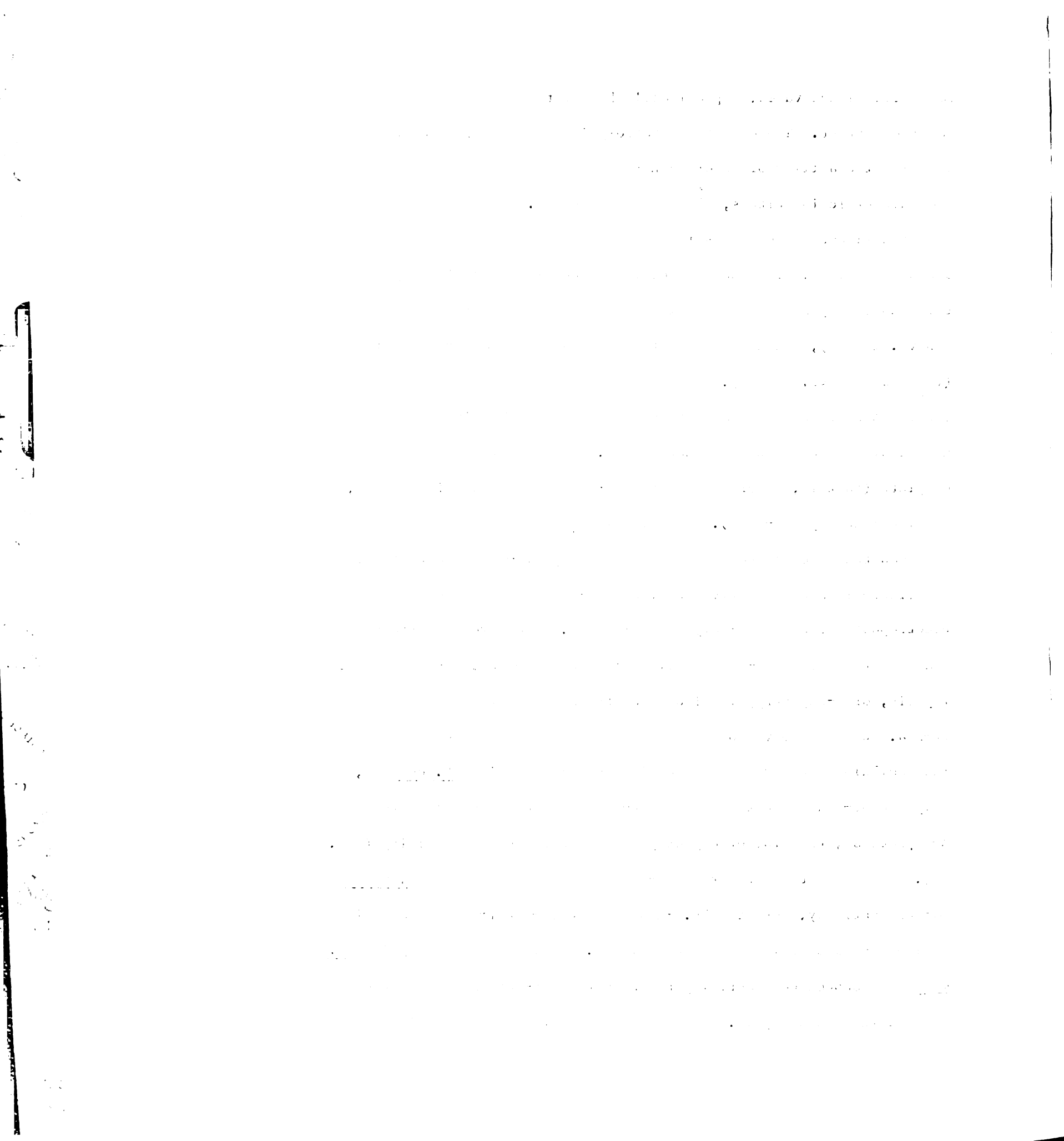
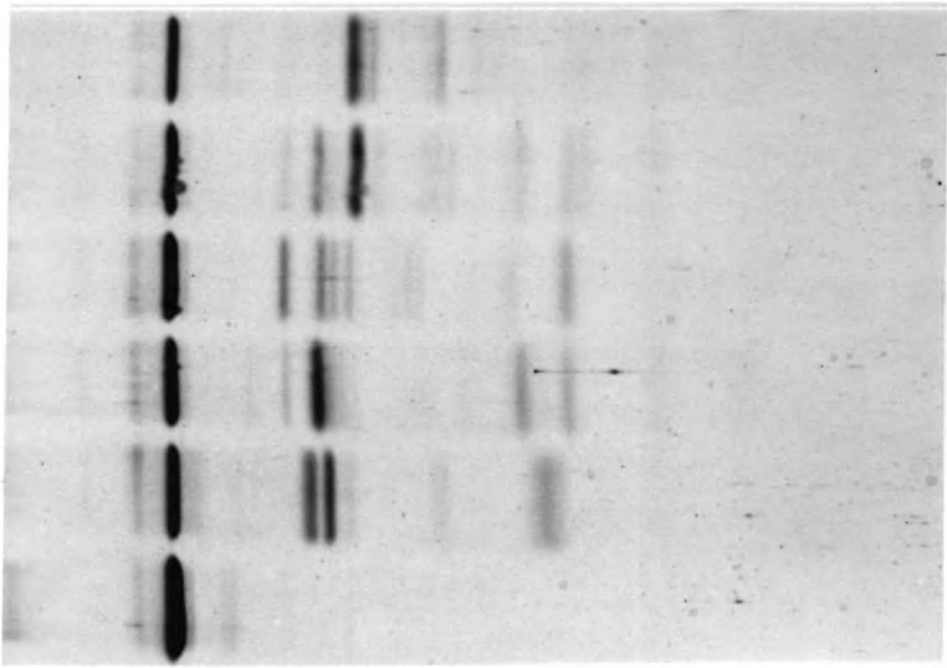


## Figure 1

Limited proteolysis (1% wt/wt) of L. major TS-DHFR by five different endopeptidases. Figure A shows a SDS-polyacrylamide gel in which aliquots from five different 2-hr proteolytic digests were electrophoresed (details of reaction are in Experimental Procedures). Lane a contains 5  $\mu$ g of intact subunit. Lanes b-f contain an equivalent amount of subunit, digested with the V-8 protease, trypsin,  $\alpha$ -chymotrypsin, elastase, the S. griseus protease, respectively. Figure B shows a Western blot analysis of a gel identical to the one shown in A; the antibody used was raised against the TS from L. casei.

1950  
1951  
1952  
1953  
1954  
1955  
1956  
1957  
1958  
1959  
1960  
1961  
1962  
1963  
1964  
1965  
1966  
1967  
1968  
1969  
1970  
1971  
1972  
1973  
1974  
1975  
1976  
1977  
1978  
1979  
1980  
1981  
1982  
1983  
1984  
1985  
1986  
1987  
1988  
1989  
1990  
1991  
1992  
1993  
1994  
1995  
1996  
1997  
1998  
1999  
2000  
2001  
2002  
2003  
2004  
2005  
2006  
2007  
2008  
2009  
2010  
2011  
2012  
2013  
2014  
2015  
2016  
2017  
2018  
2019  
2020  
2021  
2022  
2023  
2024  
2025

**A**



**B**



97K —  
68K —  
43K —  
25K —  
18K —  
12K —

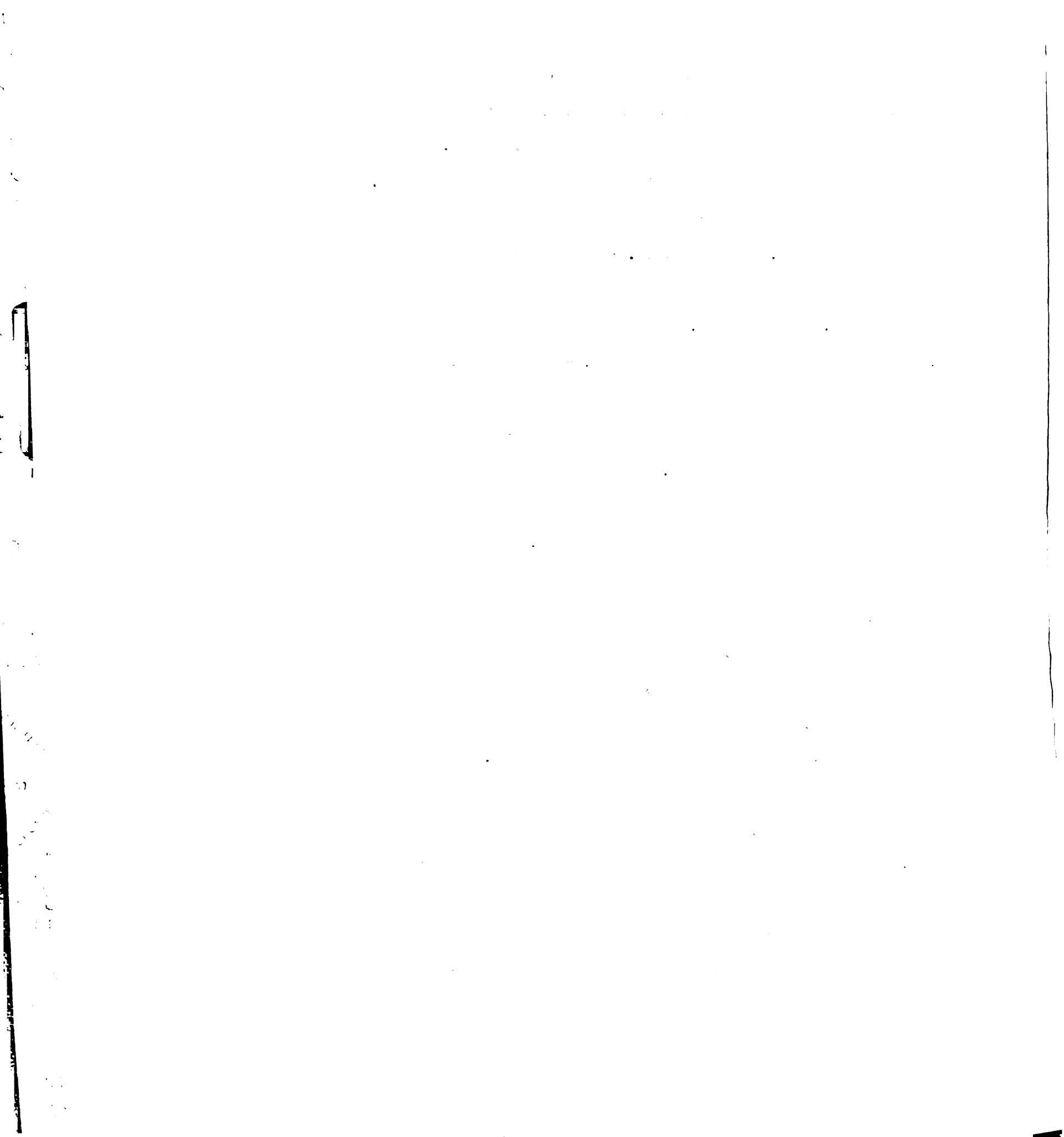
a b c d e f a b c d e f

35-kDa fragments were formed by cleavage in a common region of the protein, these larger fragments were isolated from gels and exposed to further proteolysis (10% wt/wt, V-8 protease in 0.1% SDS). The resulting peptide maps were essentially the same (data not shown).

The time course of the V-8 protease reaction with TS-DHFR is shown in Figures 2A and 2B. Initially, 37.3-kDa and 20-kDa fragments were produced; the larger fragment was further proteolyzed, resulting in a more stable 36.6-kDa fragment. At longer reaction times, the entire 37.3-kDa fragment was converted to the 36.6-kDa fragment.

Densitometry readings of each time point showed a constant amount of total protein, indicating that the 36.6-kDa and 20-kDa fragments were resistant to further proteolysis. After 220 min, approximately 10% of the 56-kDa subunit remained, illustrating that both subunits of the native protein were cleaved during the reaction.

To further characterize the fragments produced by V-8 protease digestion, we attempted to separate the polypeptides under non-denaturing conditions, using four chromatographic techniques: non-denaturing gel electrophoresis, anionic-exchange chromatography (DEAE-Sepharose), DHFR-specific affinity chromatography (MTX-Sepharose), and gel permeation (G-150 Sephadex). With all four approaches, the two fragments (which could be separated by SDS-PAGE) comigrated or coeluted, and behaved identically to the intact native dimer. With each approach, DHFR activity also comigrated or coeluted with the two fragments. 1) The proteolyzed TS-DHFR appeared as a single band upon non-denaturing PAGE; 2) the digested protein bound to DEAE-Sepharose and was eluted at 75mM KCl by use of a 0-200 mM linear gradient; 3) the proteolyzed TS-DHFR absorbed to MTX-Sepharose, was



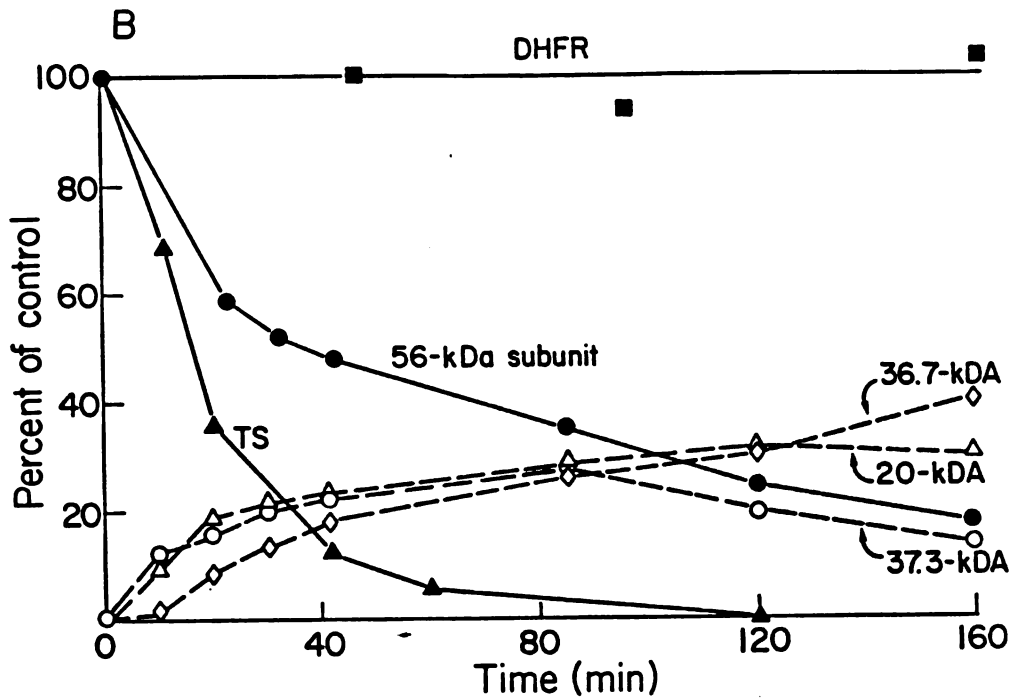
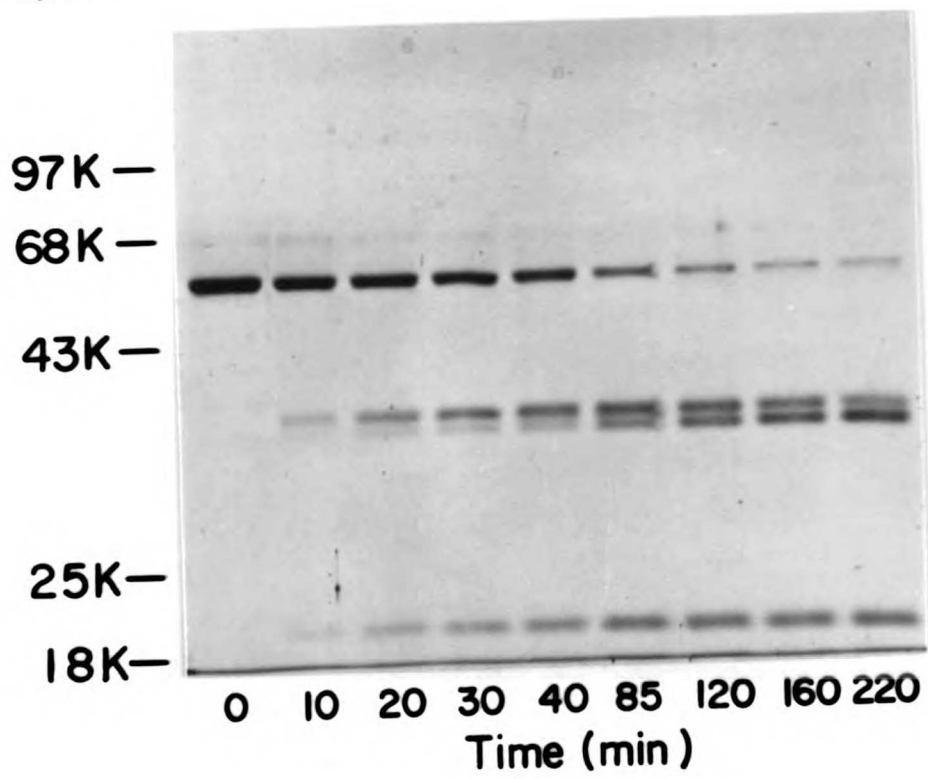


Figure 2

Time course of limited proteolysis (1% wt/wt) of *L. major* TS-DHFR by the V-8 protease. A shows the progression of the V-8 reaction with TS-DHFR, as analyzed by SDS-PAGE. Aliquots were taken out at indicated times. Molecular weight standards are as described in Figure 1. B shows the time course of digest as monitored by SDS-PAGE and DHFR and TS activity. Protein bands were scanned by densitometry. Activity assays are described in Materials and Methods.



A



not removed by either high salt or mild detergents, and was competitively eluted with 7,8-dihydrofolate; and 4) the proteolyzed protein migrated with an apparent molecular weight of 150-kDa upon G-150 Sephadex chromatography, the same apparent molecular weight as the native protein.<sup>2</sup> In order to determine if a disulfide bond held the fragments or the subunits together, the V-8 proteolytic reaction and SDS-PAGE analysis were performed in the absence of thiols; the fragments observed on the gel were identical to those shown in Fig. 2A, showing a lack of a disulfide either between fragments or between subunits.

TS-DHFR was also treated with various exopeptidases. With 10% (wt/wt) leucine aminopeptidase, aminopeptidase M, or pyroglutamate aminopeptidase (alone or in conjunction with aminopeptidase M), neither TS nor DHFR activity was affected after 2 hr. In contrast, 5% (wt/wt) carboxypeptidase A rapidly reduced TS activity in a time-dependent manner to 20% of control after 60 min; DHFR was 90% of control at this time. Upon SDS-PAGE, no difference in mobility of the 56-kDa subunit could be seen after any of the above exopeptidase digestions.

Previous attempts to determine the N-terminus sequences of native TS-DHFR resulted in no derivatized amino acids (5), suggesting that the N-terminus was blocked. We isolated (from a SDS-polyacrylamide gel) the stable 36.6-kDa and 20-kDa fragments produced by the V-8 protease and subjected the peptides to automated Edman sequence analysis. The 36.6-kDa fragment failed to yield any sequence, indicating that this fragment possessed the blocked N-terminus of the native protein. Because the 36.6-kDa fragment was derived from an

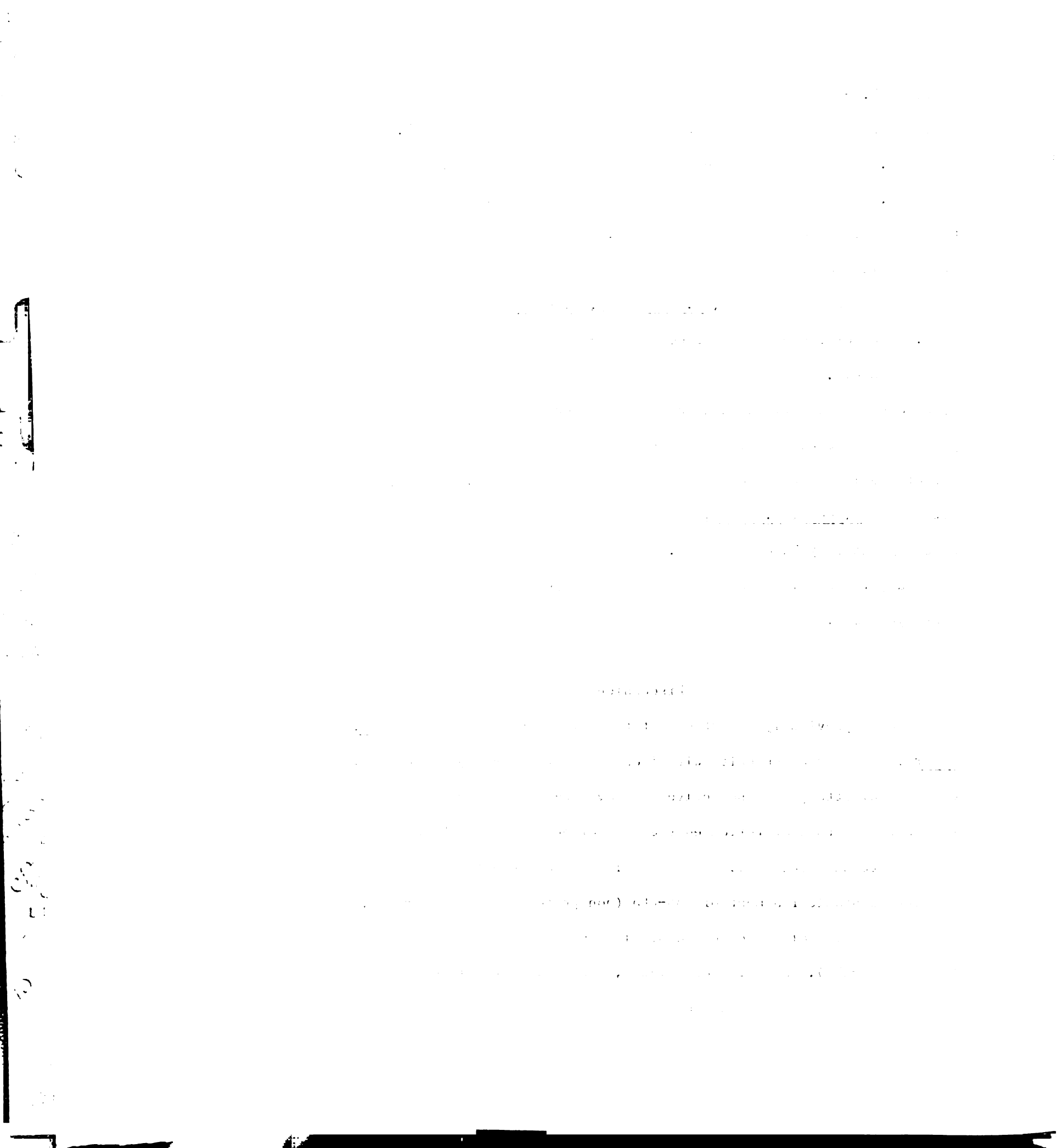
MEMORANDUM FOR THE HONORABLE SECRETARY OF THE INTERIOR  
SUBJECT: [Illegible]

[The remainder of the page contains extremely faint and illegible text, likely a memorandum or report.]

initial 37.3-kDa fragment, the secondary cleavage by V-8 protease must have occurred less than 1-kDa from the C-terminal end of the 37.3-kDa fragment. In contrast to the blocked N-terminus of the 36.6-kDa fragment, we obtained the sequence of the first 28 amino acids (with three omissions) of the 20-kDa fragment. Figure 3 shows this sequence aligned with sequences of TS from the four synthases that have been fully sequenced human (21), E. coli (22), L. casei (23), and T4 phage (24). Each of these sequences occurs 20-kDa from the C-terminal end of the protein. A striking degree of homology occurs among these sequences when the first 12 amino acids are compared; 11 of the 12 positions are conserved in at least four of the five synthases, with 7 out of the 12 positions conserved in all five synthases. The gaps within the E. coli, L. casei, and T4 phage sequences shown in Figure 3 were suggested by Takeishi et al. (21), and reflect the alignment necessary for continued homology among the reported sequences of the four synthases.

#### Discussion

We have previously reported that the bifunctional TS-DHFR from L. major is a dimer of subunits with identical size (56-kDa) and charge. Our initial attempts to selectively cleave TS-DHFR and generate two stable fragments that reflected the size of non-protozoan TS and DHFR appeared to be successful. Not only did five different endopeptidases generate a stable fragment of ~35-kDa (non-protozoan TS is ~35-kDa), but V-8 protease also produced a stable 20-kDa fragment (non-protozoan DHFR is ~20-kDa). As data accumulated, however, we realized that our initial assignment of TS to the ~35-kDa fragments and DHFR to the



<u>L. tropica</u>	Met-Asp-Leu-Gly-Pro-Val-Tyr-Gly-Phe-Gln-Trp-Arg-
	129
Human	Gly-Asp-Leu-Gly-Pro-Val-Tyr-Gly-Phe-Gln-Trp-Arg-
	88
<u>E. coli</u>	Gly-Asp-Leu-Gly-Pro-Val-Tyr-Gly-Lys-Gln-Trp-Arg-
	140
<u>L. casei</u>	Gly-Asp-Leu-Gly-Leu-Val-Tyr-Gly-Ser-Gln-Trp-Arg-
	103
T4 phage	Gly-Glu-Leu-Gly-Pro-Ile-Tyr-Gly-Lys-Gln-Trp-Arg-
<u>L. tropica</u>	Gly-Phe- X -Ala-Asp-Tyr-Lys- X -Phe-Glu-Ala-Asn-
	141
Human	His-Phe-Gly-Ala-Glu-Tyr-Arg-Asp-Met-Glu-Ser-Asp-
	100
<u>E. coli</u>	Ala-Trp-Pro - - - - - Thr-
	152
<u>L. casei</u>	Ala-Trp-His - - - - - Thr-
	115
T4 phage	Asp-Phe-Gly - - - - -
<u>L. tropica</u>	Tyr- X -Gly-Glu
	153
Human	Tyr-Ser-Gly-Gln-Gly-Val-Asp-Gln-Leu-
	104
<u>E. coli</u>	Pro-Asp-Gly-Arg-His-Ile-Asp-Gln-Ile-
	156
<u>L. casei</u>	Ser-Lys-Gly-Asp-Thr-Ile-Asp-Gln-Leu-
T4 phage	- - - - Gly-Val-Asp-Gln-Ile-

Figure 3

Comparison of the N-terminus sequence at the 20-kDa fragment from L. major TS-DHFR, generated by the V-8 protease, and homologous sequences found within TS from human (21), E. coli (22), L. casei (23), and T4 phage (24). The number above the first amino acid indicates the position of that amino acid in the complete primary sequence. X indicates that the amino acid at that position was not identified. The alignment of the human, E. coli, L. casei, and T4 phage sequences are taken from Takeishi et al (21).

20-kDa fragment should in fact be reversed, and we concluded that the various proteases did not make a scission directly between domains.

Data from the limited proteolysis of TS-DHFR indicate that DHFR and TS sequences are arranged in a linear fashion on the polypeptide, with DHFR at the blocked N-terminal and TS at the C-terminal end of the protein. First, TS, but not DHFR, activity is lost upon digestion with carboxypeptidase A. This inactivation of TS results from the hydrolysis of only a few C-terminal amino acids since the migrations of the carboxypeptidase A-treated and native proteins could not be differentiated upon SDS-PAGE. (A similar inactivation of TS from L. casei by carboxypeptidase A has been reported (25).) Second, because attempts to sequence the N-terminus of both the native TS-DHFR and the 36.6-kDa fragment generated by the V-8 protease failed to produce derivatized amino acids, and the V-8-generated 20-kDa fragment yielded a free N-terminus, we concluded that the 36.6-kDa fragment possesses the blocked N-terminus of TS-DHFR and the 20-kDa fragment represents the C-terminus of the protein. Third, when TS-DHFR was digested with either elastase or the S. griseus type XIV protease, only the larger 35-kDa fragments were stable, during which time the DHFR activity was unaffected and the TS activity was completely lost. More extensive proteolysis of the ~35-kDa fragments showed that these larger fragments were essentially the same. The larger fragments, and therefore the N-terminal end of TS-DHFR, possess DHFR. Finally, there is a large degree of homology between the N-terminus sequence of the 20-kDa fragment and sequences found ~20-kDa from the C-terminal end of TS from four sources. Also, only the smaller ~20-kDa fragments hybridized with an E. coli TS antibody. Therefore, part of TS resides

1

2

3

4

5

6

7

8

9

10

11

12

13

14

15

16

17

18

19

20

21

22

23

24

25

26

27

28

29

30

31

32

33

34

35

36

37

38

39

40

41

42

43

44

45

46

47

48

49

50

51

52

53

54

55

56

57

58

59

60

61

62

63

64

65

66

67

68

69

70

71

72

73

74

75

76

77

78

79

80

81

82

83

84

85

86

87

88

89

90

91

92

93

94

95

96

97

98

99

100



on the 20-kDa fragment, and consequently at the C-terminal end of TS-DHFR.

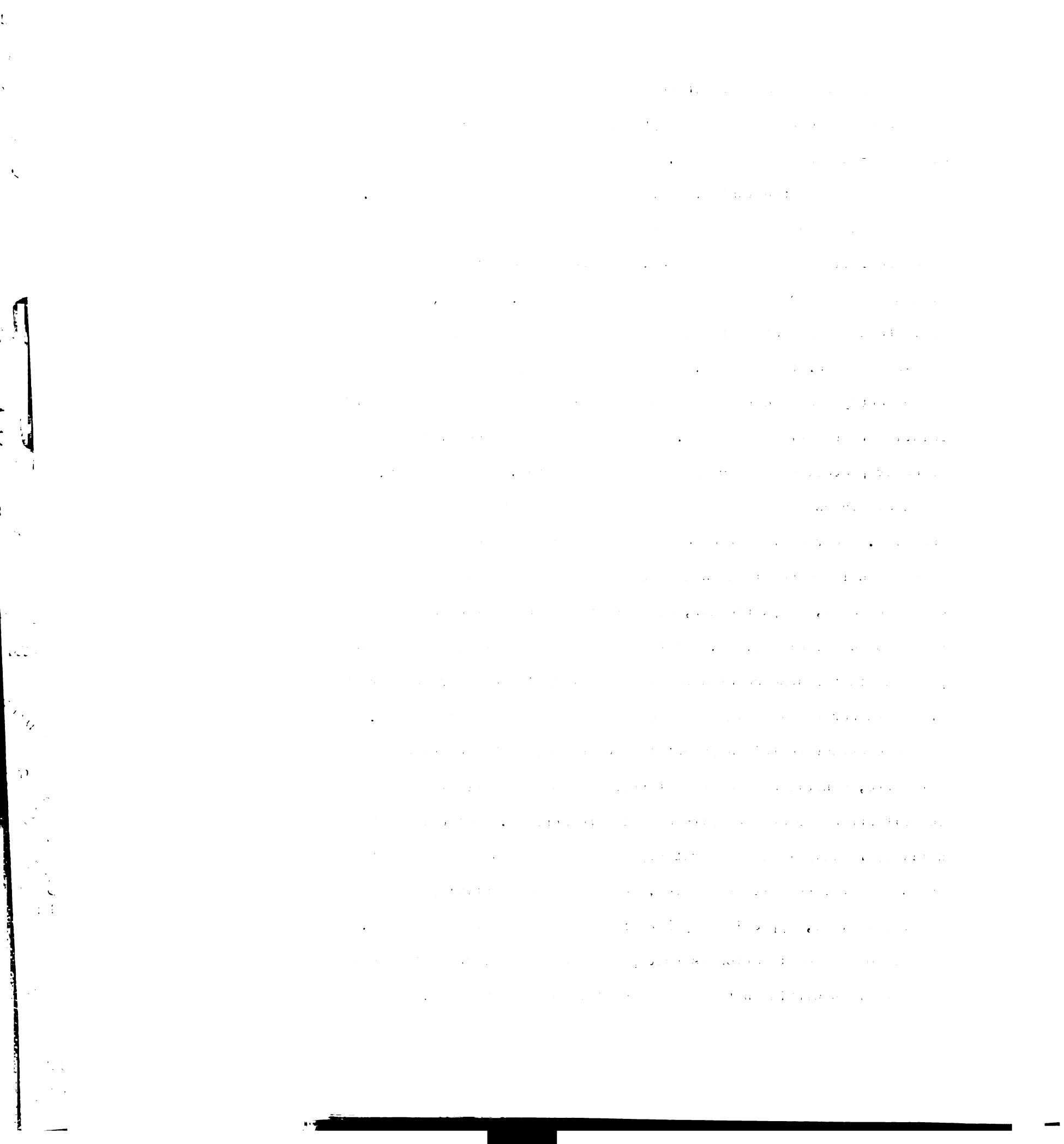
Some of the above data also verify that the two subunits of L. major TS-DHFR, which have the same size and charge (5), are indeed identical. Selective proteolysis of non-identical subunits is unlikely to occur in the same position of each polypeptide, as occurs in the V-8 protease reaction. More emphatically, non-identical subunits are extremely unlikely to have an identical 28-amino acid internal sequence at the same position of the polypeptide. The bifunctional TS-DHFR is found in a wide variety of protozoa. These proteins are dimers of subunits of identical size (1,2), and it is likely that the subunits are also identical.

The model presented above of a DHFR sequence followed by a TS sequence, with at least some homology between the L. major TS and non-protozoan TS, supports the suggestion that the L. major TS-DHFR gene, and most likely the TS-DHFR genes from other protozoa, resulted from the fusion of independent TS and DHFR genes. In E. coli, the genes encoding for TS and DHFR map far apart on the chromosome (26,27), but recent reports have shown a close arrangement of the two separate genes in Bacillus subtilis (28) and T4 phage (24,29). Interestingly, in T4 phage, the codon for the C-terminus of DHFR overlaps the codon for the N-terminus of TS by a single base pair (24,29), resulting in the biosynthesis of separate proteins. The introduction of a single nucleotide into this overlap region found in T4 phage would lead to synthesis of a bifunctional TS-DHFR.

The first part of the document discusses the importance of maintaining accurate records of all transactions. It emphasizes that every entry should be supported by a valid receipt or invoice. This not only helps in tracking expenses but also ensures compliance with tax regulations. The second part of the document provides a detailed breakdown of the company's financial performance over the last quarter. It includes a comparison of actual results against budgeted figures, highlighting areas of both strength and weakness. The third part of the document outlines the company's strategic goals for the upcoming year. It focuses on increasing operational efficiency, expanding market reach, and investing in research and development. The final part of the document provides a summary of the key findings and recommendations. It suggests that the company should continue to focus on cost reduction and revenue growth while also prioritizing employee development and customer satisfaction.

Many reports on multifunctional proteins that have used limited proteolysis have revealed a susceptible hinge region between catalytic or ligand-binding domains (6-9). The cleavage of such hinge regions has often allowed the isolation of functionally active domains (9). Although the data in this report show that TS-DHFR consists of a DHFR sequence followed by a TS sequence, we have been unable to separate distinct enzymatic domains by limited proteolysis. Rather, the data indicate that upon digestion the subunits are initially severed within the TS domain of the protein. With V-8 protease, a second cleavage is subsequently made about 1-kDa toward the N-terminal end of the protein relative to the first cleavage. Under the selective conditions used, no other proteolysis by V-8 protease was detected. Surprisingly, these cleavages do not disrupt the gross, overall integrity of the subunits. Four different chromatographic techniques under non-denaturing conditions failed to separate fragments; gel permeation chromatography, in particular, demonstrated that the proteolyzed subunits do not dissociate. Proteolysis and analysis of proteolytic products in the absence of a reducing agent indicated that neither the fragments nor the subunits were held together by a disulfide bond.

In contrast to this apparent lack of effect on higher order structure, kinetic data show that proteolysis does disrupt some subunit structure and subunit-subunit interactions. Not only is TS activity rapidly lost upon proteolysis, it is lost approximately twice as fast as the subunit is cleaved, so that when TS activity is completely lost, approximately 50% of the subunits are not cleaved. One reasonable explanation is that proteolysis of one subunit causes perturbations within that subunit and also between subunits,



inactivating TS in both; hence, the twofold difference in rates. Curiously, the disturbance of quarternary structure does not affect the ability of TS to bind its stoichiometric inhibitor FdUMP in the presence of cofactor; that is, TS loses this ability at the same rate as V-8 protease cleaves TS-DHFR and at about one-half the rate of TS inactivation. A second possible effect of proteolysis on quarternary structure is the increase of MTX bound after digestion. Previously, we showed that only one mole of the DHFR inhibitor MTX bound per mole of TS-DHFR dimer (5). As shown here, the amount of MTX bound per mole of TS-DHFR dimer increased twofold after proteolysis by trypsin. Proteolysis appears to disrupt the negative cooperativity observed between subunits in the intact dimer and to free a second MTX-binding site.

A large degree of homology exists among the complete primary structures of TS from human (21), E. coli (22), L. casei (23), and T4 phage (24); 45-60% homology is found when any two sequences are compared. The 28-amino acid internal sequence of TS-DHFR aligns with internal sequences found at approximately the same position in the four TS sequences. The first 12 positions of these five sequences show striking homology; 7 of the 12 positions are identical and only 1 position shows even moderate variability. The TS-DHFR sequence shows the highest degree of homology when compared with human TS: 11 of the first 12 positions are identical, 17 of the total 28 positions are identical, and, where differences occur, only a few are significant. When the last 16 positions of the 28- amino acid sequence are compared, the L. major sequence only shows homology with human TS. Both sequences appear to possess insertions in this region relative to

The first part of the document discusses the importance of maintaining accurate records of all transactions. It emphasizes that every entry should be supported by a valid receipt or invoice. This ensures transparency and allows for easy verification of the data. The text also mentions that regular audits are necessary to identify any discrepancies or errors in the accounting process. Furthermore, it highlights the role of technology in streamlining financial operations and reducing the risk of human error. The document concludes by stating that a robust accounting system is essential for the long-term success and stability of any business organization.

The second part of the document provides a detailed overview of the company's financial performance over the past year. It includes a comprehensive analysis of the income statement, balance sheet, and cash flow statement. The analysis shows that the company has achieved a steady increase in revenue, primarily driven by the expansion of its product line and the entry into new markets. However, it also notes that operating expenses have risen significantly, which has impacted the overall profit margin. The document further discusses the company's debt-to-equity ratio and its ability to service its obligations. Finally, it offers strategic recommendations for the upcoming year, focusing on cost optimization and investment in research and development to drive future growth.

the sequences of the three prokaryotic synthases. Interestingly, the human TS sequence possesses two consecutive glutamate residues just prior to the sequence that aligns with the internal 28-amino acid sequence of TS-DHFR; the specificity of V-8 protease (which generated the 20-kDa fragment) is for acidic amino acids. Therefore, it is likely that the L. major sequence also shows a glutamate at this position.

Insertions of polypeptide are found within the TS primary structures when the four sequences are compared. One of the most striking examples is found relative to the E. coli sequence. A 51-amino acid insertion between amino acids 87 and 88 of E. coli occurs within the L. casei TS (20). A 13-amino acid insertion is found at the same point within the human TS sequence. Finally, a 9-amino acid insertion is found within the T4 phage sequence. Curiously, the N-terminus of the 20-kDa fragment generated by the V-8 protease coincides with position 88 of the E. coli TS, and precisely at the C-terminal end of the insertions found in L. casei, human, and T4 phage TS. In addition, the molecular mass of each TS, measured from these positions to the C-terminus, is approximately 20-kDa. Because the five proteases used in this study initially cleave TS-DHFR in the same region (V-8 protease cleaves a second time in this area), this region most likely resides as a highly exposed sequence on the surface of the protein. Upon cleavage TS-DHFR remains a dimer and does not dissociate into fragments, indicating that the bulk of inter- and intra-subunit forces are unaffected by proteolysis of this region. Given this model, an insertion is also likely to occur within the L. major TS, positioned at the surface of the protein, vulnerable

Faint, illegible text, possibly bleed-through from the reverse side of the page. The text is arranged in approximately 20 horizontal lines across the page.

Handwritten notes or markings on the left margin, including what appears to be a circled number '2' and some illegible scribbles.



to the action of endopeptidases, but not affecting overall subunit stability. It is not known if these various insertions represent functional peptide, but we suggest two possibilities. First, these insertions might fold into a functional higher order structure and enable TS to bind within a multi-enzyme complex; TS activity has been reported to be associated with such a complex in T4 phage (30) and mammalian cells (31). Second, as we previously reported, TS activity was exceedingly labile during preparation of crude extracts from L. major when protease inhibitors were omitted (5). This important metabolic enzyme activity may be regulated in vivo through proteolysis, with these insertions providing a target for endopeptidases.

#### Acknowledgement

We thank Ric Harkins of Genentech, Inc., for performing the N-terminal sequence analysis.

#### References

1. Garrett, C.E., Coderre, J.A., Meek, T.D., Garvey, E.P., Claman, D.M., Beverley, S.M., and Santi, D.V. (1984) Mol. Biochem. Parasitol. 11, 257-265.
2. Ferone, R., and Roland, S. (1980) Proc. Natl. Acad. Sci. U.S.A. 77, 5802-5806.
3. Blakely, R.L. (1984) in Folates and Pteridines (Blakely, R.L., and Benkovic, S.J., Eds.) Vol. 1, pp. 191-253, Wiley, New York.

Faint, illegible text at the top of the page, possibly a header or introductory paragraph.

Introduction

Faint text block following the 'Introduction' header.

Conclusion

Faint text block following the 'Conclusion' header, ending with a signature or date.

4. Santi, D.V., and Danenberg, P.V. (1984) in Folates and Pteridines (Blakely, R.L., and Benkovic, S.J., Eds.) Vol. 1, pp. 343-396, Wiley, New York.
5. Meek, T.D., Garvey, E.P., and Santi, D.V. (1985) Biochem. 24, 678-686.
6. Mattick, J.S., Tsukamoto, Y., Nickless, J., and Wakil, S.J. (1983) J. Biol. Chem. 258, 15291-15299.
7. Walker, M.S., and DeMoss, J.A. (1983) J. Biol. Chem. 258, 3571-3575.
8. Matthews, R.G., Vanoni, M.A., Hainfeld, J.F., and Wall, J. (1984) J. Biol. Chem. 259, 11647-11650.
9. Grayson, D.R., and Evans, D.R. (1983) J. Biol. Chem. 258, 4123-4129.
10. Hillcoat, B., Nixon, P., and Blakely, R.L. (1967) Anal. Biochem. 21, 178-189.
11. Wahba, A.J., and Friedkin, M. (1961) J. Biol. Chem. 236, PC 11.
12. Santi, D.V., McHenry, C.S., and Sommer, H. (1974) Biochem. 13, 471-481.
13. Laemmli, U.K. (1970) Nature (London) 227, 680-685.
14. Davis, B.J. (1964) Ann. N.Y. Acad. Sci. 121, 404-421.
15. Towbin, H., Staehelin, T., and Gordon, J. (1979) Proc. Natl. Acad. Sci., U.S.A. 76, 4350-4354.
16. Fisher, P.A., Berrios, M., and Blobel, G. (1982) J. Cell. Biol. 92, 674-686.
17. Blake, M.S., Johnston, K.H., Russell-Jones, G.J., and Gotschlich, E.C. (1984) Anal. Biochem. 136, 175-179.
18. Fischer, S.G. (1983) Methods Enzymol. 100, 424-430.

.....

.....

.....

.....

.....

.....

.....

.....

.....

.....

19. Hunkapiller, M.W., Lujan, E., Ostrander, F., and Hood, L.E. (1983) Methods Enzymol. 91, 227-236.
20. Rodriguez, H., Kohr, W.J., and Harkins, R.N. (1985) Anal. Biochem., in press.
21. Takeishi, K., Kaneda, S., Ayusawa, D., Shimizu, K., Gotoh, O., and Seno, T. (1985) Nucleic Acids Res. 13, 2035-2043.
22. Belfort, M., Maley, G., Pedersen-Lane, J., and Maley, F. (1983) Proc. Natl. Acad. Sci. U.S.A. 80, 4814-4918.
23. Maley, G.F., Bellisario, R.L., Guarino, D.U., and Maley, F. (1979) J. Biol. Chem. 254, 1301-1304.
24. Chu, F.K., Maley, G.F., Maley, F., and Belfort, M. (1984) Proc. Natl. Acad. Sci. U.S.A. 81, 3049-3053.
25. Aull, J.L., Loebler, R.B., and Dunlap, R.B. (1974) J. Biol. Chem. 249, 1167-1172.
26. Taylor, A.L., and Trotter, C.D. (1967) Bacteriol. Rev. 31, 332-353.
27. Breeze, A.S., Sims, P., and Stacey, K.A. (1975) Genet. Res., Camb. 25, 207-214.
28. Myoda, T.T., Lowther, S.V., Fananage, V.L., and Young, F.E. (1984) Gene 29, 139-147.
29. Purohit, S., and Mathews, C.K. (1984) J. Biol. Chem. 259, 6261-6266.
30. Allen, J.R., Reddy, G.P.V., Lasser, G.W., and Mathews, C.K. (1980) J. Biol. Chem. 255, 7583-7588.
31. Reddy, G.P.V., and Pardee, A.B. (1980) Proc. Natl. Acad. Sci. U.S.A. 77, 3312-3316.
32. Garvey, E.P., Coderre, J.A., and Santi, D.V. (1985) Mol. Biochem. Parasitol. 17, 79-91.

1. The first part of the document discusses the importance of maintaining accurate records of all transactions and activities. It emphasizes the need for transparency and accountability in financial reporting.

2. The second part of the document outlines the various methods and techniques used to collect and analyze data. It highlights the importance of using reliable sources and ensuring the accuracy of the information gathered.

3. The third part of the document focuses on the interpretation and analysis of the collected data. It discusses the various statistical and analytical tools used to identify trends and patterns in the data.

4. The fourth part of the document provides a detailed overview of the results of the study. It includes a comprehensive analysis of the findings and their implications for the field of research.

5. The fifth part of the document discusses the limitations of the study and the areas for future research. It identifies the strengths and weaknesses of the methodology used and suggests ways to improve the study in the future.

6. The sixth part of the document provides a summary of the key findings and conclusions of the study. It emphasizes the importance of the research and its contribution to the field of study.

7. The seventh part of the document includes a list of references and a bibliography. It provides a comprehensive list of the sources used in the study and the works cited in the document.

8. The eighth part of the document includes a list of appendices and a glossary. It provides additional information and definitions for the terms used in the study.

9. The ninth part of the document includes a list of figures and tables. It provides a visual representation of the data and the results of the study.

10. The tenth part of the document includes a list of footnotes and a list of errata. It provides additional information and corrections for the document.

**Footnotes**

<sup>1</sup> The abbreviations used are: TS-DHFR, thymidylate synthase-dihydrofolate reductase; SDS-PAGE, sodium dodecyl sulfate-polyacrylamide gel electrophoresis; MTX, methotrexate; FdUMP, 5-fluoro-2'-deoxyuridylate; CH<sub>2</sub>H<sub>4</sub> folate, (+)-5,10-methylenetetrahydrofolate.

<sup>2</sup> From amino acid analysis, the native TS-DHFR has a molecular weight of 108,800. Upon gel filtration, the native protein has an apparent molecular weight of 150,000 and a Stokes radius of 4.4 nm (5).

1940

1. The first part of the report deals with the general situation in the country. It is noted that the economy is in a state of depression and that the government is facing a serious financial crisis. The report also mentions that the population is suffering from unemployment and poverty.

2. The second part of the report discusses the political situation. It is noted that the government is unstable and that there is a lack of confidence in the leadership. The report also mentions that there are rumors of a coup d'état.



## Chapter 6

### A Unique Substrate-Enzyme Binary Complex: Deoxyuridylate-Thymidylate Synthase from *Leishmania major*

### Abstract

The thymidylate synthase (TS) activity in *Leishmania major* resides on the bifunctional protein thymidylate synthase-dihydrofolate reductase (TS-DHFR). We have isolated, either by Sephadex G-25 chromatography or by nitrocellulose filter binding, a binary complex between the substrate deoxyuridylate (dUMP) and the TS from *L. major*. The kinetics of binding support a mechanism in which dUMP binds to TS in a rapid and reversible pre-equilibrium step, followed by a slower step which resulted in the isolable complex; the rates of association and dissociation of dUMP from this complex were  $3.5 \times 10^{-3} \text{ sec}^{-1}$  and  $2.3 \times 10^{-4} \text{ sec}^{-1}$ , respectively. The stoichiometry of dUMP to enzyme appears to be one mol of nucleotide bound per one mol of dimeric TS-DHFR. Binary complexes between the stoichiometric inhibitor 5-fluorodeoxyuridylate (FdUMP) and TS, and between the product deoxythymidylate (dTMP) and TS were also isolated by nitrocellulose filter binding. Competition experiments indicated that the three nucleotides were binding to the same site on the enzyme, and that this site was the same as that occupied by the nucleotide in the FdUMP-cofactor-TS ternary complex. Thus it appeared that the binary complexes were occupying the active site of TS. In contrast, the preformed dUMP-TS complex did not inhibit TS; even though the dissociation rate of dUMP is slower than catalytic turnover ( $\sim 3 \text{ sec}^{-1}$ ) by several orders of magnitude. We discuss the characterization of these complexes and the discrepancies which evolve from it.

Thymidylate synthase (TS) (1) catalyzes the reductive methylation of dUMP to produce dTMP, with the cofactor  $\text{CH}_2\text{H}_4\text{folate}$  being converted to  $\text{H}_2\text{folate}$  and serving as both the one-carbon donor and the reductant. The production of dTMP is essential for the biosynthesis of DNA; this enzyme has therefore been extensively studied as a target for chemotherapy against diseases which involve rapidly growing cells, e.g., cancer and infectious diseases (for reviews, see ref. 2-4). In protozoa, TS resides with the activity of DHFR on a bifunctional protein, TS-DHFR (5,6). We have extensively characterized TS-DHFR from *Leishmania major*, a protozoan parasite (7,8), and this laboratory has recently determined the DNA (and predicted amino acid sequence) of this bifunctional protein (9). The protein is a dimer, consisting of identical subunits that each possess both activities. When the amino acid sequence of the TS domain is compared with the known sequences of three other synthases, a striking degree of homology is observed (39-59% identical residues) (9). In addition, a certain degree of homology also occurs between the DHFR domain and other reductases (9). These observations, coupled with the similarity of kinetic parameters found when the *L. major* enzymatic activities (7) are compared with their nonprotozoan counterparts (2), argue that the protozoan TS and DHFR are indeed very similar, in most respects, to the enzymes found in other sources. The one dramatic difference, which arises from the bifunctional nature of this protein, is that  $\text{H}_2\text{folate}$ , the product of the TS reaction and substrate of the DHFR reaction, is channeled between active sites (7).

From all sources yet examined outside protozoa, TS has been found to be a dimer of apparently identical subunits (2), approximately 30-35 kDa in size. Much is known concerning the mechanism of this enzyme (2). An early event in the reaction involves attack of a sulfhydryl group of the enzyme at the 6-position of dUMP, which activates the 5-position for reaction with the cofactor  $\text{CH}_2\text{H}_4\text{folate}$ . This mechanism has been

supported by the observation that the stoichiometric inhibitor FdUMP (when in the presence of  $\text{CH}_2\text{H}_4\text{folate}$ ) is covalently attached via its 6-position to the catalytically essential cysteine of TS. Thus, many studies have shown that FdUMP can be physically isolated as a covalent ternary complex with TS and  $\text{CH}_2\text{H}_4\text{folate}$  (for review, see ref. 10), and that dUMP can likewise be isolated as a relatively less stable ternary complex with TS and certain folate analogues (11,12). Consistent with the above mechanism are the studies that have shown ordered binding in both the kinetic mechanism (13) and the binding of FdUMP and  $\text{CH}_2\text{H}_4\text{folate}$  to the enzyme (14); both studies demonstrated that nucleotide binds prior to cofactor. Only two reports have been published (15,16) that describe the isolation of a nucleotide-enzyme binary complex (between FdUMP and the TS from *L. casei*), and only one description of the isolation of a dUMP-enzyme complex (29) has been reported. In contrast, there are many descriptions of the existence of a binary complex (2). Spectroscopic (17) and  $^{19}\text{F}$  NMR (18) studies suggest that the FdUMP-TS binary complex displays a certain degree of covalency between the 6-position and the enzyme.

We describe here the physical isolation of the binary complex between dUMP and the TS activity of the bifunctional TS-DHFR from *L. major*. In addition, binary complexes between enzyme and FdUMP, and between enzyme and product, dTMP, have also been isolated. We describe the partial characterization of these complexes, and discuss the implications of these results.

### Materials and Methods

[6- $^3\text{H}$ ]dUrd (18 Ci/mmol), [6- $^3\text{H}$ ]FdUMP (20 Ci/mmol), [2- $^{14}\text{C}$ ]FdUMP (52 mCi/mmol), and [5- $^3\text{H}$ ]dCMP (14 Ci/mmol) were all obtained from Moravsek Biochemicals. [2- $^{14}\text{C}$ ]dTMP (43 mCi/mmol) was purchased from Amersham.

[6-<sup>3</sup>H]dUMP was prepared and purified as reported (19). The [6-<sup>3</sup>H]CH<sub>2</sub>H<sub>4</sub>folate used in this study was prepared previously in the laboratory by T.W. Bruice (20). CB3717 was a gift from A.H. Calvert, Institute of Cancer Research, Sutton, Surrey, U.K.

Nitrocellulose B45A membranes were from Schleicher and Schuell. Other materials were of the highest grade commercially available.

**Enzymes.** TS-DHFR was purified from CB3717-resistant *L. major*, as previously described (21). The concentration of active TS binding sites could not be determined by knowledge of the protein concentration, because of the inherent lability of TS during purification and storage (7,8); it was therefore determined by nitrocellulose binding assays (22), with [6-<sup>3</sup>H]FdUMP as an affinity label. TS from methotrexate-resistant *L. casei* was purified as previously reported (12).

**Enzyme Assays.** TS activity (23) and DHFR activity (24) were determined spectrophotometrically at 25 °C, as previously modified (7).

Nitrocellulose binding assays of all binary and ternary complexes were performed by slightly modifying the earlier reported procedure for assaying the FdUMP ternary complex (22). Solutions containing enzyme, nucleotide, and, if used, cofactor or CB3717 were incubated at 25 °C in Buffer A (50 mM TES, pH 7.8, 75 mM 2-mercaptoethanol, 5 mM H<sub>2</sub>CO, 1 mM EDTA). Unless specified otherwise in the text, the specific activity of [6-<sup>3</sup>H]dUMP was 15 Ci/mmol, and the specific activity of [6-<sup>3</sup>H]FdUMP was 20 Ci/mmol. In a standard reaction solution which would include TS-DHFR (20-100 nM FdUMP ternary complex sites) and 0.5-2 μM labeled nucleotide, the binary complex would be fully formed by 3 hr. Cofactor, if included, was added at a concentration of 0.2 mM. To filter either binary or ternary complexes, 50-100 μl aliquots were applied to moist filters and washed with six 1-ml portions of 20 mM potassium phosphate (pH 7.4). The filters were dissolved in 10 ml of ACS (Amersham), and the radioactivity was determined; dpm values were determined by the external standard ratio method. In the

experiments which utilized double label, samples were recycled for 5 x 20 min counts, so that minimally 30,000 cpms of  $^{14}\text{C}$  were collected. In experiments in which rates of dissociation were determined from a given complex, the complex was preincubated for 3 hr, a length of time in which all complexes examined had fully formed, and then a 500-fold excess of the unlabeled nucleotide was added to the reaction mixture; filter assays were performed over at least 3  $t_{1/2}$ 's.

**Limited proteolysis of TS-DHFR.** The bifunctional protein was digested with 1% (wt/wt) amounts of either the V-8 protease or trypsin, as previously described (8).

**Chromatography.** Protein-bound ligand was isolated at 4 °C by Sephadex G-25, as previously described (21). The column (1.0 x 22 cm) was equilibrated and chromatography was performed with a buffer of 25 mM potassium phosphate (pH 7.0), containing 10 mM 2-mercaptoethanol. Fractions (0.54 ml) were analyzed by directly counting 90  $\mu\text{l}$ , and by nitrocellulose filtration of 50  $\mu\text{l}$ . Fractions were kept on ice prior to filtration.

HPLC was used to separate dUMP from dTMP; we used a 4.6 x 250 mm LiChrosorb RP-18 column, and an isocratic system of 5 mM  $\text{tBu}_4\text{N}^+\text{H}_2\text{PO}_4^-$  (pH 7.0), containing 12.5% methanol. dUMP eluted at 39.5 ml, and dTMP eluted at 53.0 ml.

## Results

**Isolation of a binary dUMP-enzyme complex.** The interaction between the potent TS inhibitor, 10-propargyl-5,8-dideazafolate (CB3717) and the enzyme from *L. casei* (12) was recently reported by this laboratory. Much of that study relied on being able to isolate the ternary complex of CB3717- $^3\text{H}$ dUMP-TS on nitrocellulose filters. When we attempted to repeat this study using the bifunctional enzyme from *L. major*, we

stumbled upon an interesting finding. First, we were able to isolate radioactivity on nitrocellulose after incubating CB3717 and [6-<sup>3</sup>H]dUMP with TS-DHFR from *L. major*; the formation of this ternary complex was time dependent, and the stoichiometry of the complex was equal to that of the FdUMP-CH<sub>2</sub>H<sub>4</sub>folate-enzyme ternary complex.

However, in controls lacking CB3717, a significant amount of [6-<sup>3</sup>H]dUMP was trapped on nitrocellulose filters in the presence of enzyme. The binary complex formation seemed to be both time- and concentration- dependent. In addition, after complex formation was complete and a 500-fold excess of cold dUMP was added to the reaction, we observed a first order rate of dissociation of [6-<sup>3</sup>H]dUMP from the binary complex (Fig 1). The  $t_{1/2}$  of this dissociation was  $50 \pm 5$  min (N=4); the apparent first order rate constant was  $2.3 (\pm 0.3) \times 10^{-4} \text{ sec}^{-1}$ . None of these results had been found with TS from *L. casei*; no radioactivity was isolated when CB3717 was omitted from the reaction mixture (12). We therefore set about to characterize this unique binary complex between dUMP and TS-DHFR from *L. major*.

Initially, we wished to determine if dUMP bound in a specific or nonspecific manner by testing whether dUMP binding showed saturation kinetics. Figure 2 shows the results from incubating TS-DHFR (0.13  $\mu\text{M}$  FdUMP ternary complex sites) with 0.25-17  $\mu\text{M}$  [6-<sup>3</sup>H]dUMP (0.98 Ci/mmol) and monitoring the rate of dUMP association by nitrocellulose binding. For a first approximation to explain the formation of the binary complex, we used the mechanism shown in Scheme I; and assuming that  $k_{-2}$  was significantly less than  $k_2$ , we fitted the data to equation (1).

$$1/v = (K_d/E_t \cdot k_2 \cdot \text{dUMP}) + (1/E_t \cdot k_2) \quad \text{eqn 1}$$

where  $v$  was the initial rate of binding,  $K_d$  was the equilibrium constant for the initial binary complex,  $k_2$  was the rate constant for the formation of the isolable binary complex,

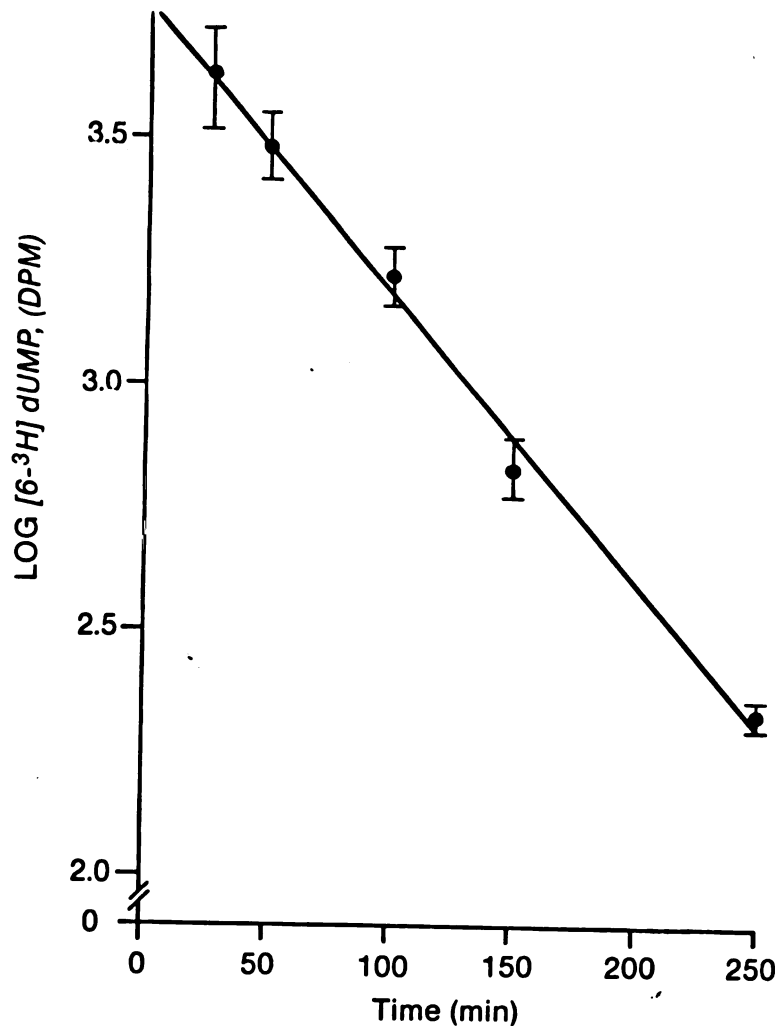
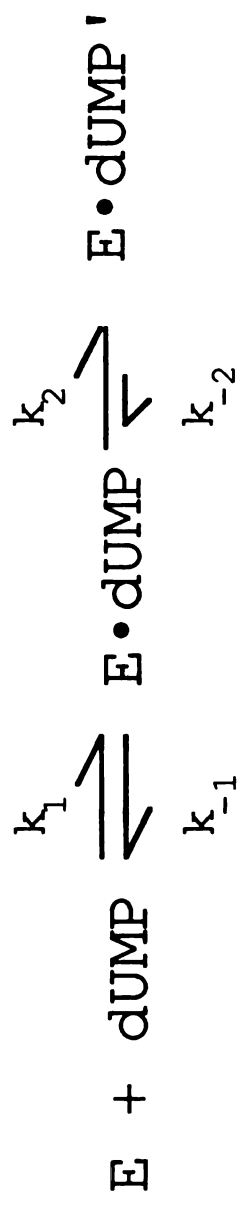


Figure 1. Dissociation of dUMP from the dUMP-enzyme binary complex. TS-DHFR (30 nM, as determined by FdUMP ternary complex sites) was incubated for 3 hr. with 0.2, 0.4, 0.8, and 1.6  $\mu\text{M}$  [6- $^3\text{H}$ ]dUMP (15 Ci/mmol). A 500-fold excess of unlabeled dUMP was then added to each reaction, and 50  $\mu\text{l}$  aliquots were filtered at the indicated time points. Each reaction resulted in the same rate of dissociation, and therefore each time point indicates the average of the four values, with the error bar representing the standard deviation.





Scheme I

and  $E_t$  was the concentration of enzyme sites which bind dUMP. (We made two assumptions which have probably led to some error; we assumed that neither [dUMP] nor [enzyme] changed significantly during the time the initial velocity was measured. The lowest dUMP concentration probably violated the first assumption, and the highest concentration the second assumption.) From the plot of  $1/v$  vs.  $1/dUMP$ , we calculated  $k_2=3.5 \times 10^{-3} \text{ sec}^{-1}$  and  $K_d=0.7 \mu\text{M}$ . In addition, we analyzed the data shown in Figure 2 by assuming the rates of dUMP binding to enzyme reflected a pseudo-first order process, determining the first order rate constant at each concentration of dUMP, and plotting  $1/k_{\text{obs}}$  vs.  $1/dUMP$  according to equation (2).

$$1/k_{\text{obs}} = (K_d/k_2 \cdot dUMP) + 1/k_2 \quad \text{eqn 2}$$

This analysis yielded  $k_2=2.5 \times 10^3 \text{ sec}^{-1}$ , and  $K_d=1.0 \mu\text{M}$ . Although both of these approaches had disadvantages (the second approach assumed that at each concentration of dUMP the first order process went to completion rather than to equilibrium), the similar values for  $k_2$  and  $K_d$  argued that the error which resulted from either approach was small.

Finally, by assuming that  $k_{-1}$ 's contribution to the rate of dissociation was negligible compared to  $k_{-2}$ 's contribution, and multiplying the initial equilibrium constant by the ratio of first order rate constants, we obtained the overall equilibrium constant:  $K_{\text{overall}}=K_d \times k_{-2}/k_2=0.05-0.1 \mu\text{M}$ . We felt that the above results supported the mechanism proposed for the binding of dUMP to the binary complex, with an overall equilibrium constant of about  $0.1 \mu\text{M}$ .

We faced two problems in determining the stoichiometry of binding. First, an excess of enzyme to ligand must be used to determine the efficiency of nitrocellulose filtration. We have not been able to purify a sufficient amount of the bifunctional

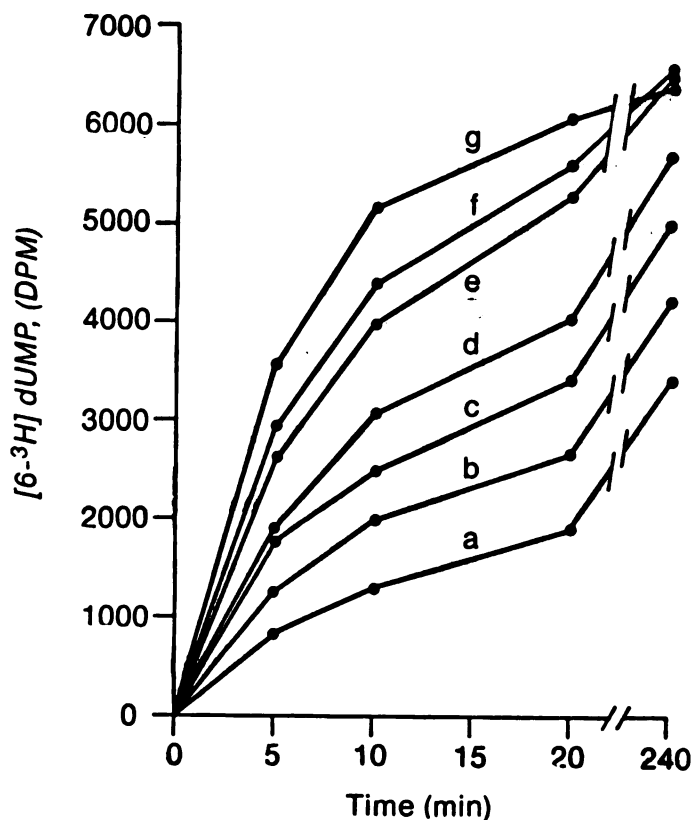


Figure 2. Rates of binary complex formation as a function of dUMP concentration. Reaction solution is described in Materials and Methods; 100 ul were taken at indicated time points. The concentration of  $[6-^3\text{H}]$ dUMP was varied as follows: (a) 0.25  $\mu\text{M}$ , (b) 0.50  $\mu\text{M}$ , (c) 1.0  $\mu\text{M}$ , (d) 2.0  $\mu\text{M}$ , (e) 5.0  $\mu\text{M}$ , (f) 8.2  $\mu\text{M}$ , (g) 17  $\mu\text{M}$ ; the concentration of TS-DHFR was 0.13  $\mu\text{M}$  as determined by FdUMP ternary complex titration. The specific activity of  $[6-^3\text{H}]$ dUMP was diluted to 0.98 Ci/mmol, so that high concentrations of dUMP could be achieved. The final time points indicate values which were true endpoints, i.e., the values were invariant after 120 min of incubation.

TS-DHFR (>2 mg/ml) so that this efficiency could be ascertained. The second disadvantage is the lability of TS activity during purification and storage, which has been well documented (7,8). Because of this, we could not compare the amount of [6-<sup>3</sup>H]dUMP bound to amount of TS (determined by protein). We could only approximate the stoichiometry of binding by assuming that the amount of the ternary complex [6-<sup>3</sup>H]FdUMP-CH<sub>2</sub>H<sub>4</sub>folate-enzyme, as determined by nitrocellulose assay, represented total active TS. Therefore the amount of [6-<sup>3</sup>H]dUMP bound was directly compared to the amount of ternary complex bound. This ratio fluctuated between 0.23 and 0.48 for unknown reasons; however, during any given experiment, the ratio was always a constant value.

We regarded as possible, although unlikely, that the complex isolated on nitrocellulose was actually a ternary complex, resulting from the presence of either residual CB3717 from the culture medium (enzyme was isolated from cells resistant to and growing in CB3717) or a folate analogue remaining from the purification procedure. (TS-DHFR is eluted from methotrexate-Sepharose by H<sub>2</sub>folate; >95% of H<sub>2</sub>folate is removed directly following elution.) We therefore bound purified TS-DHFR to a small DEAE-Sepharose column, washed with 20 times the column volume, eluted with 0.15 M KCl in buffer, and then dialyzed to remove salt (3 X 8 hr changes). Incubating [6-<sup>3</sup>H]dUMP with this enzyme produced the same time- and concentration-dependent formation of the binary complex as was observed previously. In addition, crude extract from wildtype cells was passed through DEAE-Sepahrose and TS-DHFR eluted as previously described (7). Again, incubating this enzyme with [6-<sup>3</sup>H]dUMP resulted in the binary complex. We therefore concluded that we were characterizing a dUMP-enzyme binary complex.

We were also concerned that the binary complex was at least partly due to an artifact of the nitrocellulose binding assay. Therefore, the preformed complex was passed through Sephadex G-25 to separate the enzyme-bound from free [6-<sup>3</sup>H]dUMP (Figure 3).

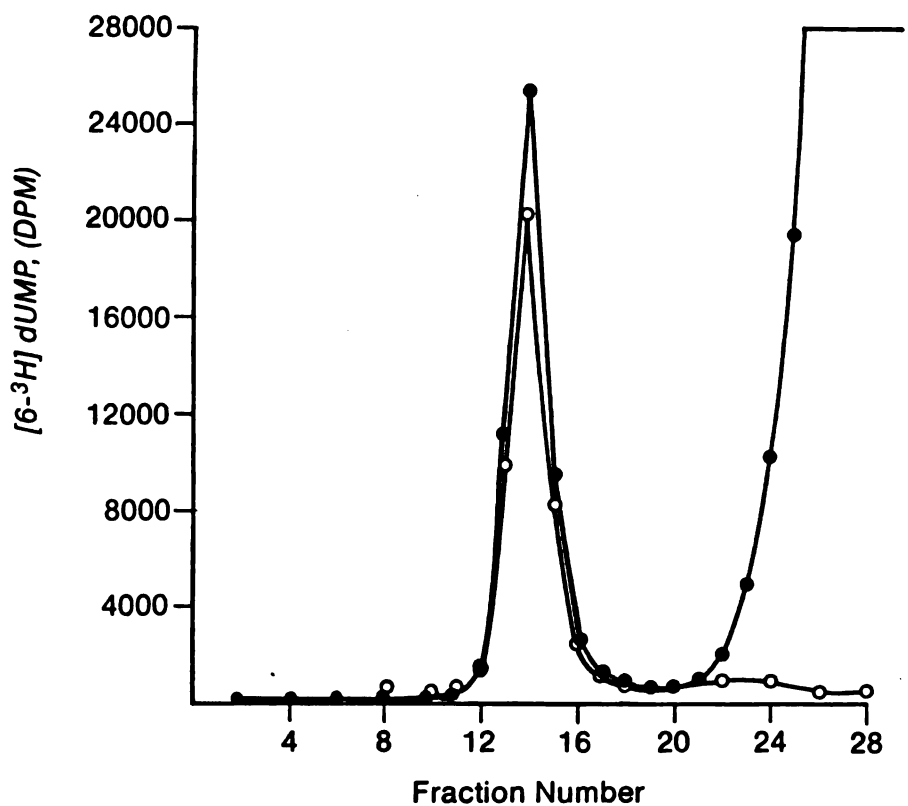


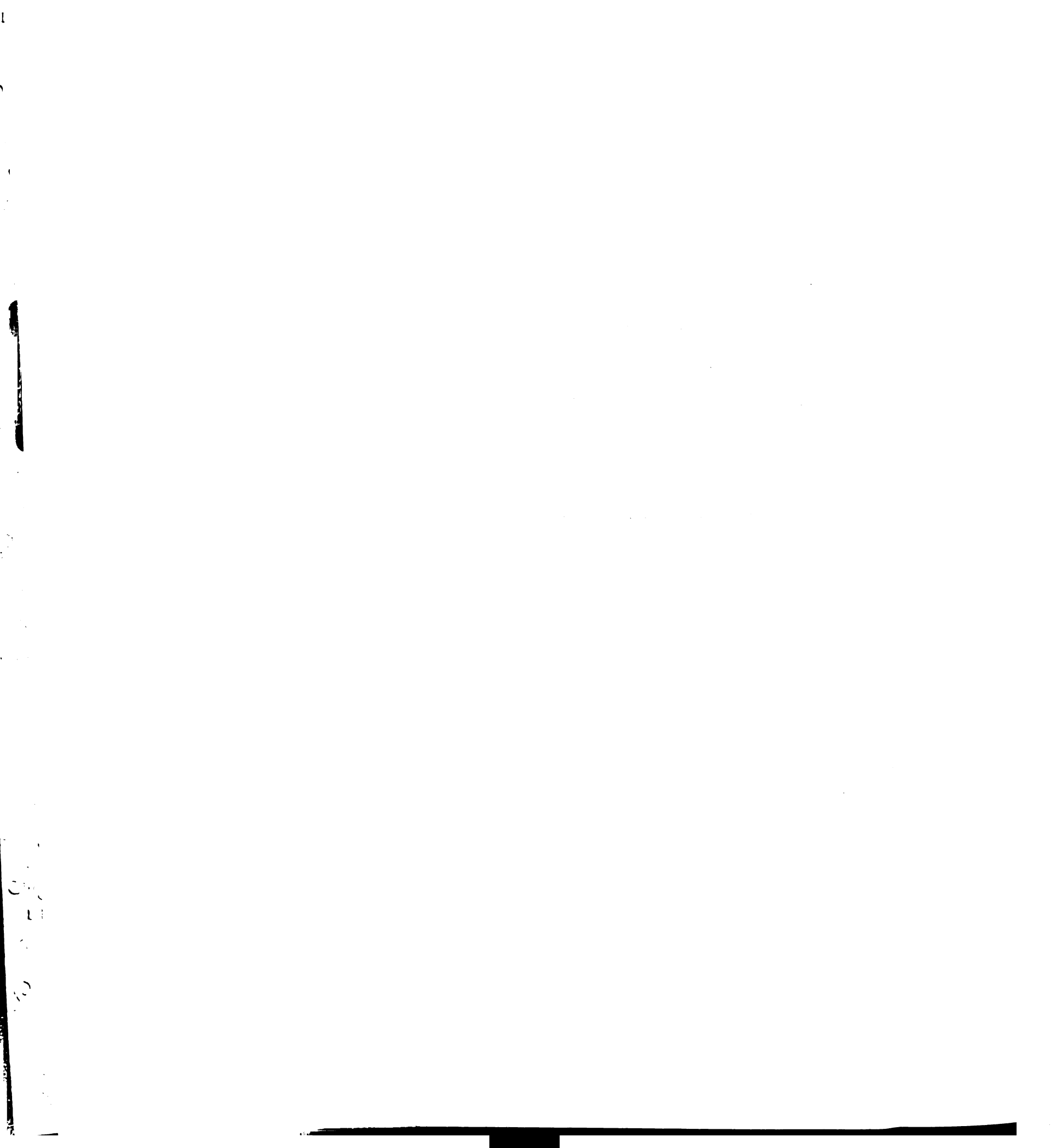
Figure 3. Sephadex G-25 chromatography of the dUMP-enzyme binary complex. TS-DHFR ( $0.15 \mu\text{M}$ , as determined by F<sub>1</sub>dUMP ternary complex sites) was incubated with  $0.75 \mu\text{M}$  [ $6\text{-}^3\text{H}$ ]dUMP ( $15\text{Ci}/\text{mmol}$ ). After four hours,  $0.35 \text{ ml}$  of the reaction was applied to a column of Sephadex G-25. Chromatography and analysis are described in Materials and Methods. The closed circles represent radioactivity that was directly counted from the fractions; open circles indicate values obtained from nitrocellulose filter binding assays. Values have been corrected for the different volumes used in the two assays.

A fraction of the [6-<sup>3</sup>H]dUMP eluted with the macromolecular peak, clearly separate from the free nucleotide, and was shown to be protein-bound by nitrocellulose filter binding. These data confirmed that the isolation of the binary complex was not an artifact of nitrocellulose filter binding. Because the only radioactivity that was applied to nitrocellulose in this experiment was associated with enzyme, this also gave a qualitative picture of the filtration efficiency of nitrocellulose binding of the binary complex. When we compared the total amounts of radioactivity, measured both directly and by filter binding, filtration produced 82% of the direct counts. Based on the rate of dissociation of dUMP from the binary complex, and considering that this rate is probably slower at 4 °C, 6% or less of the bound dUMP would have dissociated prior to filtration. Thus, the above data suggest that ~80% of the binary complex survives nitrocellulose filtration.

**Additional binary complexes.** In addition to the substrate, the substrate analogue FdUMP formed a binary complex with the TS activity in a time- and concentration-dependent fashion. In an experiment similar to the one described in Figure 1, TS-DHFR (30 nM FdUMP ternary complex sites) was incubated with 0.36-1.4 μM [6-<sup>3</sup>H]FdUMP, and the initial rates of binding were measured by nitrocellulose filtration. From plots of 1/v vs. 1/[FdUMP], we calculated  $k_2=8.3 \times 10^{-4} \text{ sec}^{-1}$ , and  $K_d=1.3 \text{ uM}$ . The rate of FdUMP dissociation was determined by adding a 500-fold molar excess of unlabeled FdUMP to the preformed complex, and assaying the mixture over time by filter-binding; the rate of dissociation was first order, and was equal to  $1.2 \times 10^{-4} \text{ sec}^{-1}$ . Because the rates of association and dissociation were different by only seven-fold, we were not as confident in using eqn 1 to analyze the FdUMP data. When FdUMP was used as the chase to measure dUMP dissociation, or when dUMP was used to measure FdUMP dissociation, the same rates were obtained as when the same nucleotide was employed. We therefore assumed that both the substrate and the analogue were binding at the same site(s) on the enzyme.

Curiously, when the cofactor  $\text{CH}_2\text{H}_4\text{folate}$  was used in hopes of turning over the bound  $[6\text{-}^3\text{H}]\text{dUMP}$ , we measured no dissociation of trappable radioactivity. We therefore examined if the product dTMP could bind as a binary complex. When  $[2\text{-}^{14}\text{C}]\text{dTMP}$  ( $1.2\ \mu\text{M}$ ) was incubated with TS ( $0.1\ \mu\text{M}$  FdUMP ternary complex sites) and aliquots were filtered, an increasing amount of radioactivity was isolated on nitrocellulose filters over time. The total amount bound at completion was  $\sim 0.5$  of the amount of FdUMP- $\text{CH}_2\text{H}_4\text{folate}$ -TS sites. When  $\text{CH}_2\text{H}_4\text{folate}$  ( $100\ \mu\text{M}$ ) was included in the dTMP/enzyme reaction mix, the amount of  $[2\text{-}^{14}\text{C}]\text{dTMP}$  that was trapped increased two-fold, so that it equalled the amount of FdUMP ternary complex isolated. In addition, when excess dTMP was used to chase labelled dUMP from its binary complex, the same  $t_{1/2}$  was obtained as when excess dUMP was used. Therefore, in the binary complexes, dUMP, FdUMP, and dTMP all appeared to compete for the same site(s) on the enzyme. We were curious to see if dCMP also bound to TS; possibly these nucleotides were binding to a site outside of the active site. When  $[5\text{-}^3\text{H}]\text{dCMP}$  ( $0.4\ \mu\text{M}$ ) was incubated with TS-DHFR ( $20\ \text{nM}$  FdUMP ternary complex sites), however, no counts were trapped, even after 250 min.

It is noted at this point that a substrate for the DHFR activity of the bifunctional protein, NADPH, chased  $[6\text{-}^3\text{H}]\text{dUMP}$  from its binary complex in a time-dependent fashion. After the dUMP-enzyme complex was allowed to form, a 500-fold excess of NADPH over labeled dUMP was added to the reaction mix and aliquots were taken over time. The rate of dissociation was first order over two half-lives, and was approximately 4 times slower than the rate observed when excess dUMP was used. To examine if the binary complex resided at the DHFR active site(s) of the bifunctional protein, we looked for inhibition of the DHFR activity by the complex. When TS-DHFR was preincubated with  $10\ \mu\text{M}$  dUMP for 60 min, no difference was seen in DHFR activity versus the control of enzyme preincubated in the absence of dUMP. We assumed, therefore, that the effect





of NADPH on the rate of dissociation was not a direct replacement of NADPH for labeled dUMP. Rather, the dissociation of dUMP was a consequence of NADPH binding to the DHFR activity of the bifunctional enzyme. Finally, when an excess of FdUMP and cofactor were added to the preformed dUMP-TS complex, the rate of dissociation increased approximately 3-fold ( $t_{1/2}$  of <20 min vs. 50 min).

**Where does dUMP bind?** Does dUMP bind at the active site(s) of TS when it binds to the enzyme as a binary complex? We approached this question from several directions, and obtained mixed answers. First, we examined the effect of this complex on TS activity. When *L. major* TS-DHFR (90 nM FdUMP ternary complex sites) was incubated with 1  $\mu$ M [6-<sup>3</sup>H]dUMP and aliquots were taken over time to assay directly for both activity and bound radioactivity, TS was not inhibited even though the binary complex had formed. The amount of [6-<sup>3</sup>H]dUMP trapped on nitrocellulose in the presence of TS-DHFR increased in a time-dependent manner from 0 to 2.1 pmol over a 2 hr period; during this same time, there was no inhibition of TS activity versus the control of enzyme incubated with no dUMP. Interestingly, the presence of dUMP actually protected TS against the apparent first order inactivation which occurs when dilute amounts of TS-DHFR are incubated at 25 °C;  $\sim t_{1/2}$  of inactivations were 50 min in the absence of dUMP, and 120 min in the presence of dUMP.

In a separate approach to answer where dUMP binds, the ternary complex of FdUMP-CH<sub>2</sub>H<sub>4</sub>folate-enzyme was used in attempts to block formation of the binary complex, and vice versa. These experiments possessed the inherent assumption that the ternary complex bound at the two active sites of *L. major* TS-DHFR; we have previously demonstrated that two mol of FdUMP bound to one mol of TS-DHFR dimer, in the presence of cofactor (7). In addition, we wished to show that one mol of inhibitor bound per one mol of cofactor. We therefore incubated enzyme (1  $\mu$ M FdUMP ternary complex

sites) with [2-<sup>14</sup>C]FdUMP (10 μM; 4.5 mCi/mmol) and [6-<sup>3</sup>H]CH<sub>2</sub>H<sub>4</sub>folate (100 μM; 26 mCi/mmol) and measured the ratio of FdUMP/cofactor; the ratio for the *L. major* enzyme was  $0.91 \pm 0.10$  (N=3). TS from *L. casei* was used as a control for this experiment; its ratio was  $1.20 \pm 0.08$  (N=3). Thus, having established that the FdUMP-cofactor-TS complex bound in a 2:2:1 stoichiometry, we first attempted to block the formation of the ternary complex by pretreating the enzyme with dUMP. Table I presents data that resulted from measuring separately: 1) the ternary [2-<sup>14</sup>C]FdUMP-cofactor-enzyme complex, 2) the binary [6-<sup>3</sup>H]dUMP complex, and 3) the [2-<sup>14</sup>C]ternary complex with the [6-<sup>3</sup>H]binary complex already formed. (For these experiments, we diluted the specific activity of [6-<sup>3</sup>H]dUMP to 0.32 Ci/mmol; [2-<sup>14</sup>C]FdUMP remained at 52 mCi/mmol.) Although the results did not produce a clear-cut picture, they did demonstrate that the binary complex inhibited the ternary complex from reaching the expectant amount in a time-dependent fashion. The amount of ternary complex formed in the absence of dUMP-enzyme complex was  $8.0 \pm 0.4$  pmol, and this value decreased over time to 5.7 pmol after the enzyme had been incubated with dUMP for 30 min. In addition, when the pmol of dUMP and pmol of FdUMP (in the presence of cofactor) were summed at each time point, the total pmol was a constant number ( $8.2 \pm 0.3$ ).

Similar results were obtained when TS-DHFR was first treated with [2-<sup>14</sup>C]FdUMP (52 mCi/mmol) and CH<sub>2</sub>H<sub>4</sub>folate and then subsequently incubated with [6-<sup>3</sup>H]dUMP (0.32 Ci/mmol) (see Table II for comment). Significantly less binary complex formed over time when the enzyme had been pretreated with inhibitor and cofactor. Again, the total amount of bound ligand at each time point was a constant number ( $9.6 \pm 0.3$ ). The two competition experiments implied that dUMP was binding to the same site(s) to which FdUMP and CH<sub>2</sub>H<sub>4</sub>folate bind: 1) each complex partly, but not completely, inhibited the formation of the other complex, and 2) the sum of the two complexes (calculated in pmol bound) was a constant value.



Table I. Competition between dUMP and FdUMP/CH<sub>2</sub>H<sub>4</sub>folate: dUMP bound first.

TIME (min)	Double Label <sup>c</sup>				
	[2- <sup>14</sup> C] FdUMP/CH <sub>2</sub> H <sub>4</sub> folate <sup>a</sup> (pmole)	[6- <sup>3</sup> H] dUMP <sup>b</sup> (pmole)	[6- <sup>3</sup> H] dUMP (pmole)	[2- <sup>14</sup> C] FdUMP/CH <sub>2</sub> H <sub>4</sub> folate (pmole)	Total (pmole)
0	8.6	0	0	8.2	8.2
10	8.0	2.2	2.0	6.5	8.5
20	8.1	3.2	2.1	6.2	8.3
30	7.5	3.7	2.5	5.7	8.2

<sup>a</sup> TS-DHFR (0.1 μM FdUMP ternary complex sites) incubated in Buffer A. At indicated times, 100 μl aliquots were taken, and 0.4 μM [2-<sup>14</sup>C] FdUMP and 0.1 mM CH<sub>2</sub>H<sub>4</sub>folate were added and incubated for 10 min prior to filtration.

<sup>b</sup> TS-DHFR (0.1 μM sites) incubated in Buffer A with 3 μM [6-<sup>3</sup>H] dUMP (0.32 Ci/mmol). At indicated times, 100 μl aliquots were filtered.

<sup>c</sup> Same reaction mixture as in b. At indicated times, 100 μl aliquots were taken, 0.4 μM [2-<sup>14</sup>C] FdUMP and 0.1 mM CH<sub>2</sub>H<sub>4</sub>folate were added and incubated for 10 min prior to filtration.

Control was minus enzyme (0.31 pmole for [2-<sup>14</sup>C] FdUMP; 0.21 pmole for [6-<sup>3</sup>H] dUMP), and has been subtracted from values.

Table II. Competition between dUMP and FdUMP/CH<sub>2</sub>H<sub>4</sub>folate: FdUMP/CH<sub>2</sub>H<sub>4</sub>folate bound first.

TIME (min)	Double Label <sup>b</sup>			Total (pmole)
	[6- <sup>3</sup> H] dUMP <sup>a</sup> (pmole)	[6- <sup>3</sup> H] dUMP (pmole)	[2- <sup>14</sup> C] FdUMP/CH <sub>2</sub> H <sub>4</sub> folate (pmole)	
0	0	0	9.6	9.6
10	1.6	0.89	8.3	9.2
28	2.6	1.14	8.6	9.7
40	3.0	1.29	8.7	10.0

<sup>a</sup> TS-DHFR (0.1 μM FdUMP ternary complex sites) incubated in Buffer A. After 20 min, 10 μM [6-<sup>3</sup>H] dUMP was added, and 100 μl was filtered at indicated times.

<sup>b</sup> TS-DHFR (0.1 μM FdUMP ternary complex sites) incubated in Buffer A with 0.6 μM [2-<sup>14</sup>C] FdUMP and 0.1 mM CH<sub>2</sub>H<sub>4</sub>folate. After 20 min, 100 μl was filtered, then 10 μM [6-<sup>3</sup>H] dUMP was added, and 100 μl was filtered at indicated times.

Control was minus enzyme (0.31 pmole for [2-<sup>14</sup>C] FdUMP; 0.21 pmole for [6-<sup>3</sup>H] dUMP), and has been subtracted from values.

In a separate experiment, after the initial binary complex was formed (3 hr incubation of 1  $\mu$ M [6-<sup>3</sup>H]dUMP with TS-DHFR (90 nM FdUMP ternary complex sites), the addition of the folate analogue CB3717 (50  $\mu$ M) to the standard reaction mixture increased the amount of [6-<sup>3</sup>H]dUMP bound to enzyme two-fold: 1.9 pmol bound increased to 3.9 pmol bound. This total amount of the dUMP-CB3717-enzyme complex equaled the amount of the FdUMP-CH<sub>2</sub>H<sub>4</sub>folate-enzyme complex which was measured at the same time.

As a final approach to answer where dUMP binds, we posed another question. Is the binary complex catalytically competent; will dUMP turnover? A preformed binary complex was isolated on G-25 Sephadex. Immediately after isolation, CH<sub>2</sub>H<sub>4</sub>folate was added; aliquots were taken over time, boiled for 2 min to denature the enzyme, and samples were then run on HPLC to separate [6-<sup>3</sup>H]dUMP from the enzymatic product [6-<sup>3</sup>H]dTMP. The data (presented in Table III) showed a time-dependent decrease in [6-<sup>3</sup>H]dUMP that was equal to a time-dependent increase in the labelled product; both of these rates were equal to the rate of dissociation of [6-<sup>3</sup>H]dUMP from the binary complex, as determined by adding excess cold dUMP to the isolated complex. Thus, the dUMP-enzyme complex is catalytically incompetent; dUMP must dissociate from the complex before being turned over. The rate of dissociation measured in this experiment was approximately three times slower than previously measured ( $t_{1/2}$  of 128 min vs. 50 min). This difference may be due to the fact that the pH of the buffer used for the G-25 Sephadex chromatography (10 mM KP<sub>i</sub>, pH 7.0), and therefore used in this dissociation experiment, was almost a full unit lower than the pH of the buffer previously used to determine the dissociation constant (50 mM TES, pH 7.8).

**The binary complex protects against limited proteolysis.** We have previously described the limited proteolysis of TS-DHFR by a number of endopeptidases

Table III: Dissociation of [6-<sup>3</sup>H]dUMP from the isolated binary complex<sup>a</sup>.

time (min)	addition of excess dUMP <sup>b</sup>		addition of CH <sub>2</sub> H <sub>4</sub> folate <sup>c</sup>	
	↓dUMP (DPM)	↓dUMP (DPM)	↓dUMP (DPM)	↑dTMP (DPM)
0	26600	53373	2433	
40	19481	36215	20031	
80	15945	28443	25805	
120	12036	21629	33829	
160	10487	<sup>d</sup>	-	
220	7873	-	-	

<sup>a</sup>TS-DHFR (0.2 μM FdUMP ternary complex sites) was incubated in 1 ml of buffer A with 0.8 μM [6-<sup>3</sup>H]dUMP for 4 hr. 0.75 mls of the reaction mix was applied to G-25 Sephadex (Materials and

Methods). The binary complex was isolated (0.6 mls containing 536160 DPMs) as described in the text.

<sup>b</sup>Unlabeled dUMP (90 μM) was added to 0.25 mls of the isolated binary complex, and 40 μl aliquots were filtered at the indicated times.

<sup>c</sup>CH<sub>2</sub>H<sub>4</sub>folate (0.14 mM) was added to 0.33 mls of the above isolated binary complex, and at the indicated times, 0.075 mls of this mix was boiled for 2 min, then put on ice until sample could be applied to HPLC to separate dUMP and dTMP (as described in Materials and Methods).

<sup>d</sup>not determined.

(8). The results that pertain to this study are: 1) TS was rapidly inactivated when incubated with any of the proteases ( $t_{1/2} < 20$  min), and 2) this inactivation occurred at approximately twice the rate of proteolysis, suggesting that proteolysis of one subunit affected the activity of both active sites. In the present study, we treated TS-DHFR with limiting amounts of either the V-8 protease from *Staphylococcus aureus* or trypsin, after first allowing the dUMP-enzyme complex to form. The controlled proteolysis of TS-DHFR possessing the binary complex yielded the same fragments as observed previously (8), but the existence of the binary complex slowed both the rate of TS inactivation and the rate of proteolysis of TS-DHFR (Table IV). The rates of inactivation and proteolysis were approximately equal when limiting amounts of V-8 protease were incubated with TS-DHFR that possessed the binary complex, rather than the two-fold discrepancy observed when dUMP was absent from the enzyme. Thus dUMP appears to both partially protect TS-DHFR against proteolytic digest and also protect the second active site against inactivation if the adjacent subunit has been proteolyzed.

### Discussion

We have presented data here which demonstrate that a binary complex between dUMP and the TS activity of the bifunctional protein TS-DHFR from *L. major* can be isolated by either nitrocellulose filter binding or by gel filtration chromatography. Recent studies have also reported that binary complexes between FdUMP (16), dUMP (29), or dTMP (29) and the *L. casei* TS can be isolated by nitrocellulose filtration, and the authors have suggested that these binary complexes possess covalent character due to its surviving denaturation by either trichloroacetic acid (16,23) or guanidine hydrochloride (16).

We have shown that the formation of the dUMP-enzyme complex is consistent with the mechanism shown in Scheme I, where dUMP first binds to enzyme in a rapid and



Table IV. Limited proteolysis of TS-DHFR, in the presence and absence of the binary complex.

Proteolytic Enzyme	Inactivation of TS (~ $t_{1/2}$ , min)		Proteolysis of TS-DHFR <sup>a</sup> (~ $t_{1/2}$ , min)	
	TS-DHFR	dUMP/TS-DHFR	TS-DHFR	dUMP/TS-DHFR
V-8 protease <sup>b</sup>	8	40	18	44
trypsin <sup>c</sup>	3	32	11	not determined

<sup>a</sup> determined by densitometry scanning of SDS polyacrylamide gels.

<sup>b</sup> Limited digestion of TS-DHFR by V-8 (1% wt/wt). Numbers are averages of two experiments, with the values ranging  $\pm$  10%.

<sup>c</sup> Limited digestion of TS-DHFR by trypsin (1% wt/wt); values are from single experiment.

reversible step prior to a slow step that produces the isolable complex. Thus, the binary complex represents a specific interaction between dUMP and enzyme, and not a nonspecific adsorption of small molecule onto protein. A nucleotide-TS complex was also observed when FdUMP or dTMP was incubated with enzyme, although these interactions were not examined as thoroughly as were the dUMP-TS interactions. We were not able to determine the stoichiometry of binding due to lack of sufficient purified protein (see results); however, we feel that dUMP binds, at most, in a one to one stoichiometry with the bifunctional enzyme for the following reasons: 1) the amount of filterable binary complex was never greater than one half the amount of the FdUMP ternary complex, and 2) the filtration efficiency of the binary complex appeared to be high (~80%) when isolated complex was filtered.

It is conceivable that the binary complexes are artifacts, either due to an extraneous folate present in the TS-DHFR preparation which would participate in a ternary complex with dUMP, or to dUMP binding to inactive TS. (As mentioned above, the TS activity is labile and there is significant loss during storage which results in a significant fraction of TS-DHFR possessing inactive TS.) We have addressed the first possibility both by extensively treating the enzyme to remove folates and by partially purifying TS-DHFR from wildtype, and then assaying these enzymes for the ability to form the binary complex. The second possibility is more difficult to address, but one observation argues against it. Formation of the binary complex protects against inactivation of TS by proteolytic enzymes; thus, the TS-DHFR to which dUMP binds must possess active TS because the binary complex is less susceptible to inactivation.

Where does this binary complex reside? There are two distinct possibilities with very different ramifications. Either dUMP binds at the active site(s) of the *L. major* TS, or it is binding at a specific site elsewhere on the bifunctional protein. Two experiments suggest that the binary complex does not contain dUMP bound to the active site, although neither definitely rule out this possibility: 1) the preformed complex does not inhibit TS

activity, and 2) dUMP must first dissociate from the complex before it is turned over to product. It is possible that a nucleotide binding site exists outside of the active sites of TS and plays a role in regulation. It should be mentioned that no regulatory binding site has ever been observed in the TS protein from other sources. Therefore, if a regulatory site does exist on TS-DHFR, its existence probably is specific to the bifunctional protein. It is conceivable, though unlikely, that dUMP binds to the active site of DHFR. We have dismissed this possibility both because the preformed binary complex does not inhibit DHFR, and because the chemical structure of dUMP does not mimic the structure of either DHFR substrate. (The structure of dCMP is much closer to the structure of dUMP than it is to either DHFR substrate, and a dCMP-TS-DHFR binary complex was not isolated in this study.)

In contrast with the above explanation, the data resulting from competition experiments, in conjunction with what is known about TS from *L. major* and from other sources, support the view that the binary complex resides at the active site(s) of TS. We have shown with data here and previously reported (7) that FdUMP, CH<sub>2</sub>H<sub>4</sub>folate, and the dimeric TS-DHFR from *L. major* form a ternary complex in a stoichiometry of 2:2:1; this is the same stoichiometry that has been observed with TS from other sources (2,10). These data imply that there are two active sites per dimer of TS. The fact that we obtained a constant total amount of bound ligand in the experiments using both [6-<sup>3</sup>H]dUMP and [2-<sup>14</sup>C]FdUMP (in the presence of cofactor) indicates that dUMP in the binary complex binds at the same site(s) as FdUMP occupies in the ternary complex, and therefore suggests that dUMP binds at the active site(s) of TS.

The proposed mechanism for TS catalysis suggests how dUMP might bind at the active site to form an isolable complex. An early event in the catalytic reaction is the attack of a sulfhydryl group of the enzyme at the 6-position of dUMP; this activates the 5-position to react with cofactor (2). This mechanism has been supported by the

observation that FdUMP (in the ternary complex) is covalently attached at the 6-position to the catalytic cysteine of TS (10). Thus, it is possible that dUMP binds at the active site(s) of TS, forms a reversible covalent interaction with the cysteine residue, and, due to a peculiarity of the bifunctional enzyme, exists in an equilibrium that favors attachment to the enzyme.

How do the other data fit into the hypothesis that dUMP binds at the active site(s)? The data that showed dUMP must dissociate from the binary complex before being converted to product can be rationalized. Assuming that dUMP binds to the active site, the binary complex cannot be on the catalytic pathway; the rate of formation of the binary complex ( $3.5 \times 10^{-3} \text{ sec}^{-1}$ ) is several orders of magnitude slower than the catalytic turnover number ( $3 \text{ sec}^{-3}$ ) measured previously (7). Thus, we can hypothesize that the binary complex represents a reversible dead-end complex and must reverse at least to the *Michaelis* complex prior to turnover. The lack of inhibition by the preformed binary complex is not as readily explainable. These data suggest a form of half-the-sites reactivity, where the dUMP-enzyme complex does not inhibit TS activity because only one active site is catalytically active at any given time.

Whereas the lack of inhibition by the binary complex is difficult to explain if the active site is occupied, the data from the competition experiments are inconsistent with dUMP binding at a regulatory site. We and other workers have shown that one mol of TS binds two mol each of FdUMP and  $\text{CH}_2\text{H}_4\text{folate}$  (2,7,10), regardless of the source of the enzyme. We have shown here that the sum of the binary and ternary complexes do not exceed the amount of ternary complex, and that each complex inhibits the binding of the other. Thus, there appears to be no additional sites, other than the two active sites, to which dUMP can bind.

There has been ample evidence for the existence of a binary complex between dUMP and the synthase from *L. casei* (2), and that the complex might possess a

significant degree of covalent character (17,18). Studies (26,27) have also indicated that one mol of dUMP binds to one mol of enzyme; these and additional reports (14,28) suggest that the two active sites are asymmetric with regards to ligand binding. Consistent with all of these studies is the evidence that both the catalytic mechanism of TS (13) and the binding of nucleotide and cofactor to TS (14) are ordered, with the nucleotide binding first. Thus, the existence of the binary complex between dUMP and the TS from *L. major* is not surprising; what is unusual is the ability to isolate this complex. Obviously, something is different in the *L. major* enzyme to allow for this behavior: either a second, regulatory site exists, or a unique event occurs in the bifunctional protein after dUMP binds in the *Michaelis* complex that allows the binary complex to be isolated. Either possibility is intriguing. A regulatory site would be the first such site described for a TS enzyme. Alternatively, if the binary complex does reside at the active site(s), many questions concerning TS could be addressed: 1) Does dUMP form a reversible covalent attachment with the catalytic cysteine prior to cofactor binding; 2) Does dUMP bind to one active site in the absence of cofactor; 3) If dUMP binds to one site, is this due to an inherent inaccessibility of the second site, as has been proposed for the *L. casei* synthase (14,25); and, most intriguing, 4) Arising from the fact that the binary complex does not inhibit TS activity, does a form of half-the-sites reactivity exist in TS from *L. major*, in which only one of the two active sites is catalytically active at any given time.

### References

1. Abbreviations: TS, thymidylate synthase; DHFR, dihydrofolate reductase; dUMP, deoxyuridylate; FdUMP, 5-fluorodeoxyuridylate; dTMP, deoxythymidylate; CH<sub>2</sub>H<sub>4</sub>folate, 5,10-methylenetetrahydrofolate; H<sub>2</sub>folate, 7,8-dihydrofolate; CB3717,10-propargyl-5,8-dideazafolate.
2. Santi, D.V. and Danenberg, P.V. (1984) in Folates and Pteridines (Blakley, R.L.,

- and Benkovic, S.J., Eds.) Vol. 1, pp. 1038-1069, Macmillan, New York.
3. Santi, D.V. (1980) J. Med. Chem. **23**, 103.
  4. Danenberg, P.V. (1977) Biochem. Biophys. Acta **473**, 73.
  5. Ferone, R., and Roland, S. (1980) Proc. Natl. Acad. Sci. USA **77**, 5802-5806.
  6. Garrett, C.E., Coderre, J.A., Meek, T.D., Garvey, E.P., Claman, D.M., Beverley, S.M., and Santi, D.V. (1984) Mol. Biochem. Parasitol. **11**, 257-265.
  7. Meek, T.D., Garvey, E.P., and Santi, D.V. (1985) Biochem. **24**, 678-686.
  8. Garvey, E.P., and Santi, D.V. (1985) Proc. Natl. Sci. USA **82**, 7188-7192.
  9. Grumont, R. Washtien, W.L., Caput, D., and Santi, D.V. (1986) manuscript submitted.
  10. Maley, F., Belfort, M., and Maley, G. (1984) Adv. Enzyme Regul. **22**, 413-430.
  11. Locksin, K.D., and Danenberg, P.V. (1979) J. Biol. Chem. **254**, 12285-12288.
  12. Pogolotti, A.L., Danenberg, P.V., and Santi, D.V. (1986) J. Med. Chem., manuscript in press.
  13. Daron, H.H., and Aull, J.L. (1978) J. Biol. Chem. **253**, 940-945.
  14. Danenberg, P.V., and Danenberg, K.D. (1978) Biochem. **17**, 4018-4024.
  15. Moore, M.A., Ahmed, F., and Dunlap, R.B. (1984) Biochem. Biophys. Res. Comm. **124**, 37-43.
  16. Ahmed, F., Moore, M.A., and Dunlap, R.B. (1985) Anal. Biochem. **145**, 151-159.
  17. Lockshin, A., Mondal, K., and Danenberg, P.V. (1984) J. Biol. Chem. **259**, 11346-11352.
  18. Lewis, C.A., Ellis, P.D., and Dunlap, R.B. (1981) Biochem. **20** 2275-2285.
  19. Wataya, Y., and Santi, D.V. (1977) Methods Enzymol. **46**, 307-312.
  20. Bruice, T.W. (1980) Ph.D. dissertation.
  21. Garvey, E.P., Coderre, J.C., Santi, D.V. (1985) Mol. Biochem. Parasitol. **17**, 79-91.

22. Santi, D.V., McHenry, C.S., and Periard, E.R. (1974) Biochem. **13**, 467-470.
23. Wahba, A.J., Friedkin, M. (1961) J. Biol. Chem. **236**, PC11.
24. Hillcoat, B., Nixon, P., and Blakley, R.L. (1967) Methods Enzymol. **21**, 178-189.
25. Washtien, W.L., and Santi, D.V. (1979) Cancer Res. **39**, 3307-3403.
26. Galivan, J.H., Maley, G.F., and Maley, F. (1976) Biochem. **15**, 356-362.
27. Leary, R.P., Beaudette, N., Kisliuk, R.L., and Gaumont, Y. (1977) Arch. Biochem. Biophys. **179**, 272-278.
28. Danenberg, K.D., and Danenberg, P.V. (1979) J. Biol. Chem. **254**, 4345-4348.
29. Moore, M.A., and Dunlap, R.B. (1985) Federation Proceedings **44**, 1442, Abstract #6032.

## **Appendix 1**

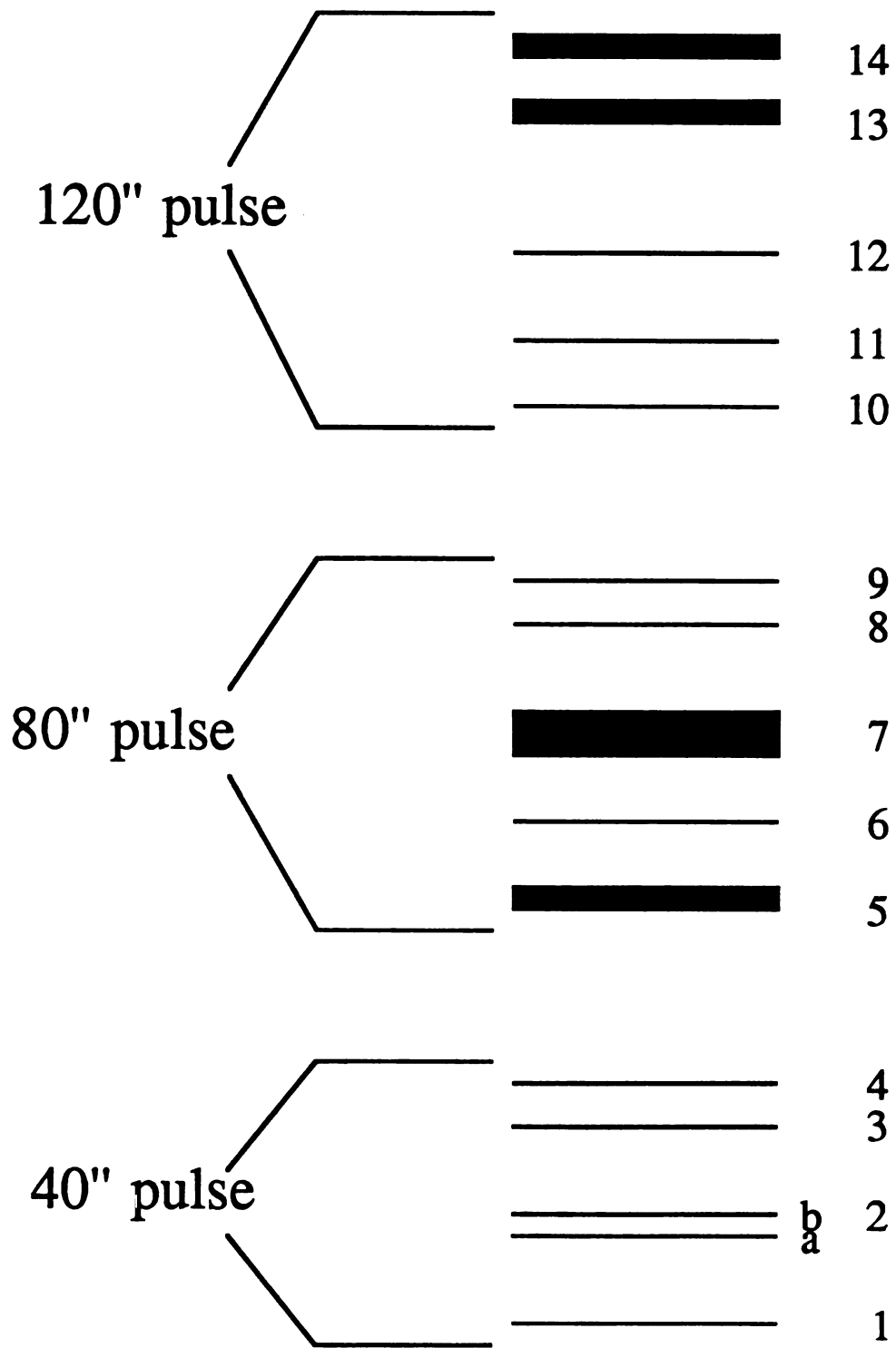
### **Empirically Determined Parameters for Orthogonal-Field-Alternation Gel Electrophoresis**



Chapter 3 describes results which were obtained by orthogonal-field-alternation gel electrophoresis (OFAGE). The fundamental premise of this technique is that linear DNAs (eg. chromosomes) will respond to a change in the field of a current as a function of their size. The larger the DNA, the slower it will respond to the change in field, therefore the slower it will migrate through the gel. At short pulse times, small chromosomes will respond quickly to a change in field, relative to large chromosomes. Thus, short pulse times will resolve small DNAs, and will not resolve large DNAs. Conversely, long pulse times allow large chromosomes to respond to the change in field; they resolve larger DNAs, and are actually too long to greatly affect smaller DNAs.

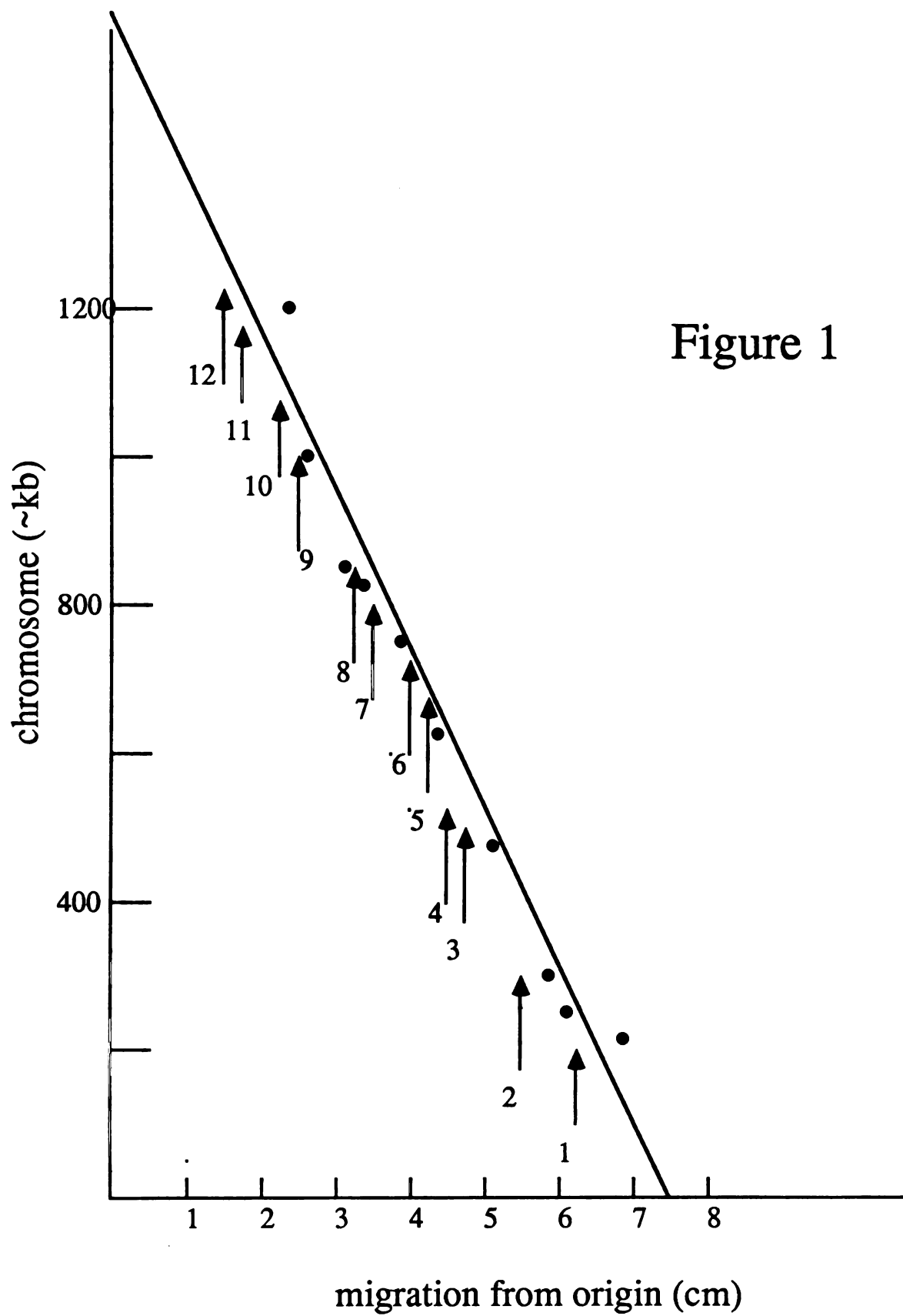
The determination of how exact pulse times affect which chromosomes from a specific species is achieved empirically. This is in part fine art, consistent preparation of materials, and good fortune. The affect of different pulse times on the chromosomes from *L. major* is presented in Scheme I. If a gel was run at a 40-s pulse time for ~24 hr, the first four chromosomes were fully resolved, and chromosome 2 was actually resolved into two components. At this 40-s pulse time, the remainder of the DNAs migrated almost as a single band. If a gel was run at a 120-s pulse time, as were most of the gels shown in Chapter 3, then the largest chromosomes were resolved as indicated, and the first nine chromosomes were barely resolved into six bands. At a 80-s pulse time, a truly intermediate resolution was achieved: ~10 of the 14 bands were clearly resolved. (Under all conditions, no resolution of band 7 was ever realized.) We have found with the system used here that the optimum overall resolution of leishmanial chromosomes were achieved when the gel was run for a few hours at a short pulse time (~4-5 hr at ~45 s), followed by many hours at a longer pulse time (~20 hr at ~100 s).

Figure 1 shows the relation between size of DNA and migration in a gel that was run for 9 hr at a 40 sec pulse time, 11 hr at a 80 sec pulse time, and 2 hr at a 120 sec pulse time, with a change of buffer between the 40 and 80 sec pulse times. The points represent the migrations of ten chromosomes (out of 15 possible chromosomes) from yeast, and the



Scheme I

Figure 1



line is an approximate fit through these points. The size of these chromosomes were taken from Mortimer and Schild (1985; see ref. 9 in chapter 3). It appears that the relation between size and migration is a linear one. The arrows represent the migrations of the 12 leishmanial chromosomes that were resolved on the same gel.

Many other factors, besides the pulse times, are crucial in the resolution of DNAs. A few of these are stressed. (1) A complete change of buffer after ~12 hr of electrophoresis; a loss in resolution was observed even when the buffer was partly changed. (2) Temperature; all of these gels were run at 14 °C. Poor resolution resulted when the circulating pumps were inadvertently turned down, which caused a temperature gradient inside the electrophoretic box. (3) Current; all gels were run with the current beginning at ~160 mAmps and increasing to ~210 mAmps over the course of 12 hours. When current began at ~200 mAmps, the increase in current was greater, and the current actually became limiting (>300 mAmps). (4) Consistency of buffer preparation; even with utmost care in buffer preparation, new buffer sometimes resulted in slightly different effects. A new batch of Tris (from Sigma) seemed to give slightly different results. (5) Percentage of agarose in gel; all gels were 1.5%. A 1.2% gel did not give as good a resolution as a 1.5% gel. (6) Electrophoresis of a gel containing two large DNA blocks consistently gave better overall results than a gel containing many small DNA blocks. Finally, even though smaller and larger size gels were never run (all gels were 12.5 x 12.5 cm in size), parameters and results would probably be greatly affected by the different angles the two fields would make across the gel. Therefore, if a smaller or larger gel is cast and run, the parameters listed above most likely will have to be changed.

Finally, the specifics of preparing the DNA agarose blocks that were used in these experiments are listed. Two parameters are needed to calculate the necessary amount of cells to harvest: 1) ~2 µg DNA/small gel slot has been used throughout this project, and 2) ~0.3 µg DNA/10<sup>6</sup> cells is obtained from *L. major*.. If 10 mls of cells which are at ~3 x

$10^7$  cells/ml are harvested, there will be  $\sim 90 \mu\text{g}$  of DNA. These cells are washed with PBS, respun, and taken up in 2.4 mls PBS. 2.4 mls of 1.2% low-melt agarose (in PBS) is then added to give a final concentration of  $\sim 18 \mu\text{g}$  DNA/ml in 0.6% low-melt agarose (in PBS). This is aliquoted into the casting molds. Each mold holds  $\sim 0.6$  mls; therefore, 4.8 mls is enough mix to cast 8 x 0.6 ml-DNA blocks. The eight DNA blocks are cast, put into the frig to quicken the hardening of agarose. These blocks are then treated as described in Figure 1 of Chapter 3. Under the conditions stated, the DNA blocks have shown no signs of degradation when stored up to three months, in 0.2 M EDTA, pH 8.0, at  $4^\circ\text{C}$ .

## **Appendix Two**

### **Cross-Reactivity of the Antibody for Thymidylate Synthase-Dihydrofolate Reductase to Other TSs and DHFRs.**

The polyclonal antibody (Ab) for the bifunctional protein TS-DHFR was isolated from rabbit, as described in Chapter 5. We analyzed this Ab for cross-reactivity to a number of TSs and DHFRs, and also examined whether the bifunctional protein cross-reacts to Ab's for TS from T2 bacteriophage or for DHFR from *E. coli*. We used the Elisa Well Assay, as described below, to examine cross-reactivity.

50 ng (in 50 ul PBS) of pure TS-DHFR/well is placed in microtiter plate; this is allowed to bind to plastic overnight. Solutions are removed, and wells are washed by filling with 5% calf serum (2 quick washes; 3x10' washes). Plate is slapped on a paper towel to remove all solution. 50 ul of Ab (straight or diluted in 5% calf serum)/well is added; and incubated at room temperature for at least 2 hr. Rinse with 5% calf serum as described above, except that a wash with 0.02% NP-40 in 5% calf serum is added. 50 ul/well of goat anti-rabbit Ab-horse radish peroxidase conjugate (from Cappel: need to dilute 1/2500 with 5% calf serum) is added; and incubated at room temperature for at least 1 hr. Rinse as described above (including NP-40 wash). Rinse three times with PBS. Add 100 ul of Elisa Assay substrate/well [Elisa Assay substrate = 1 mg/ml 2,2'-azido-di-(3-ethylbenzylthiozoline sulfonic acid) (ABTS), 0.01% H<sub>2</sub>O<sub>2</sub> (freshly made) in 0.1 M sodium acetate, 0.05 M sodium phosphate (mono sodium salt)]. To quantitate binding, 50 ul/well is taken, diluted to 1 ml with 0.1 M sodium acetate, 0.05 M sodium phosphate buffer, and absorbance is read at 405 nm. Dilutions were corrected for, and Abs. vs. dilution of Ab were plotted. Titer is the ~value of dilution of Ab which gives half-maximal binding. Several controls have been used. If antigen is left out of the wells (i.e., no TS-DHFR), the amount of background is the same as when anti-serum is substituted with pre-bleed serum (serum from the pre-immune bunny). With the assays used here, this background resulted in a titer of ~1/5-1/10. Because these backgrounds were the same, we normally used a control of minus antigen. If serum (either pre-bleed or anti-serum) was omitted, no binding was seen at all.

The results from these studies are presented in Table I, and can be summarized succinctly. The TS-DHFR Ab cross-reacts to all TSs used, with the degree of reactivity decreasing from *L. casei* to *E. coli* to T2 phage. The TS-DHFR Ab does not cross-react to either DHFR from *L. casei* or from *E. coli*; nor does the *E. coli* DHFR Ab cross-react to the bifunctional protein from *L. major*. These data correspond well with the degrees of homology found recently when the TS-DHFR nucleotide sequence was determined and the predicted amino acid sequence was compared with the known primary structures of various TSs and DHFRs. TSs from human, *E. coli*, and T4 phage show 59%, 49%, and 39% identity when compared with the *L. major* TS domain of the bifunctional protein. DHFRs from these three sources do not show a significant amount of homology when either compared with each other or with the *L. major* enzyme (the protozoan DHFR seems to best align with the enzyme from human). Appropriately, when homology or identity does occur between DHFRs, it is between residues which are known to reside inside the protein (based upon crystallographic knowledge of DHFR from bacteria and chicken). Therefore, it is not surprising that DHFR Ab's do not display cross-reactivity.

The cross-reactivity of the Ab for the *L. major* TS-DHFR to the bifunctional protein from other *Leishmania* species and from *Crithidia fasciculata* was examined by Western blot analysis (experimental procedure is referenced in Chapter 5). Although the technique did not give a quantitative analysis of cross-reactivity, it clearly showed that the bifunctional TS-DHFR from *L. donovani*, *L. mexicana*, *L. braziliensis*, and *C. fasciculata* each reacted to the Ab for TS-DHFR from *L. major*.

The procedure used for Western Blot analysis is as follows. The unfixed polyacrylamide gel is placed with nitrocellulose paper, under buffer, between Whatman filter papers, in an orientation such that protein will travel from the gel onto the nitrocellulose by travelling toward the anode (red). Two Whatman papers should be placed behind the nitrocellulose. This sandwich is placed into the cassette provided with the electroelution kit, and the cassette is then placed into box. The transfer buffer is 192



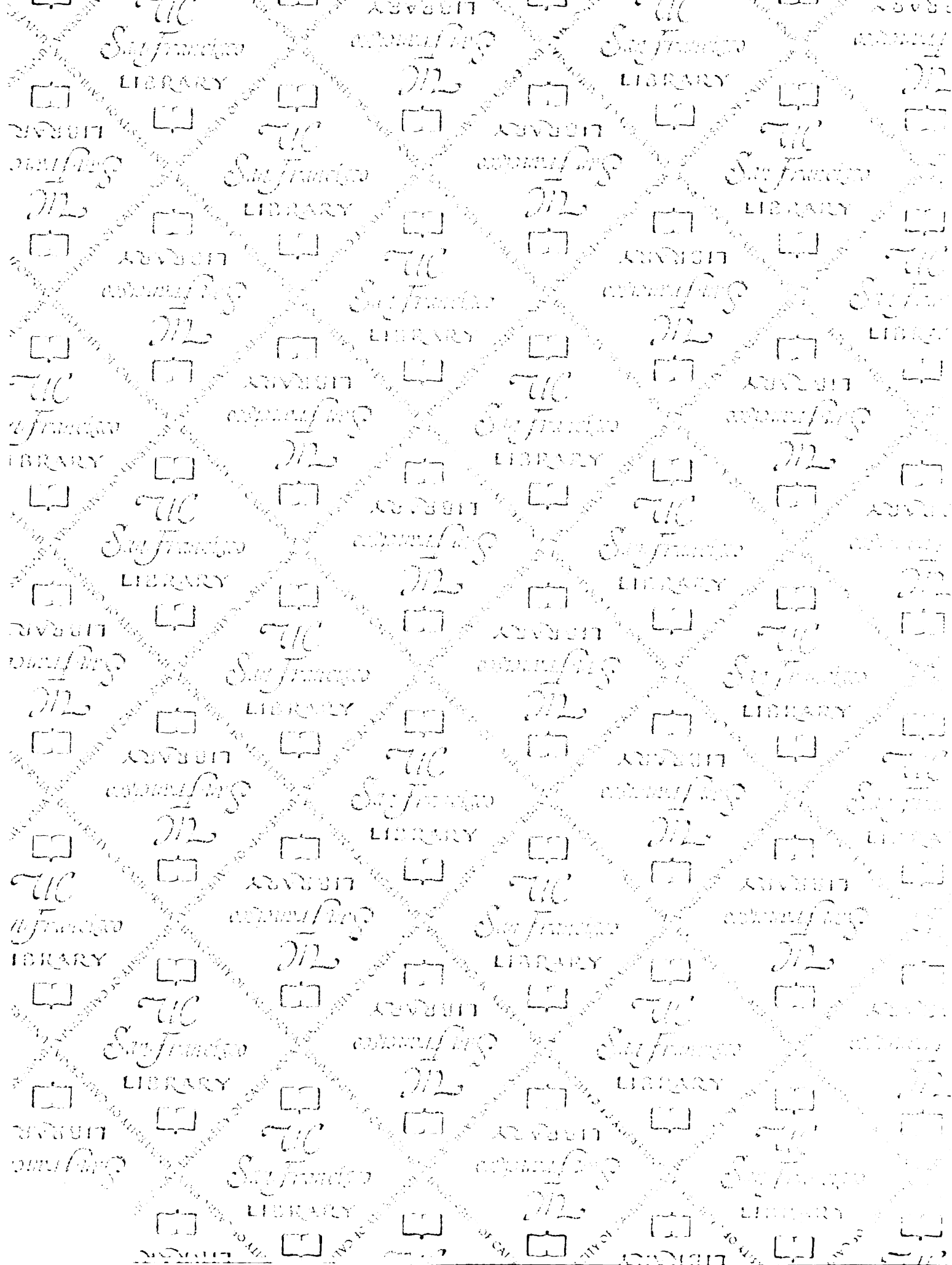
mM glycine, 25 mM tris base, 20% MeOH. The electroelution box (from Hoeffler) requires ~4 L of buffer, and the loading of the gel under buffer requires ~2 L of buffer. Electroelution is performed for ~45-50 min, beginning the elution at ~0.7 Amps. The current will increase over the course of the elution to ~1.2 Amps. (Of course, this is high, lethal current; therefore care should be taken.) The nitrocellulose is then put into a baggie, and ~10 mls of 20 mg/ml BSA is added. This is incubated on a shaker for at least 2 hr. The BSA is drained, and ~10 mls of 20 mg/ml BSA in {150 mM NaCl, 10 mM NaH<sub>2</sub>PO<sub>4</sub> (pH 7.4), 0.1% triton X-100, and 0.02% SDS (=Low Salt Buffer)} containing a 1/100 dilution of the Ab for TS-DHFR (100 µl Ab in 10 ml solution) is added to the bag. This is incubated for at least 4 hr on a shaker. The nitrocellulose is removed from the bag and washed 3 x 10 min with the Low Salt Buffer ; then 3 x 10 min with same buffer, except that NaCl is at 500 mM (=High Salt Buffer). Next, a goat anti-rabbit Ab-alkaline phosphatase conjugate (from Boehringer Mannheim) is diluted 1/3000 with 20 mg/ml BSA in Low Salt Buffer, and 10 mls of this solution is incubated for at least 3 hr with the nitrocellulose in a bag on a shaker. The antibody conjugate solution is removed and the nitrocellulose is washed exactly as above, with a final additional wash (10 min) of 1 M glycine, pH 9.6 (titrated with NaOH). Finally, the alkaline phosphatase is assayed by incubating the nitrocellulose in a bag containing 10 mls of 50 mM glycine, pH 9.6, 4 mM MgAcetate, 0.1 mg/ml NBT (p-nitroblue tetrazolium), 0.05 mg/ml 5-bromo-4-chloro-3-indolyl phosphate. This reaction requires at least 30 min to develop enough color to locate bands; some Western blots have taken ~1 hr to develop. The nitrocellulose is taken out of bag when reaction seems complete, and washed quickly in 1M glycine. The nitrocellulose is stored away from light.

Table I. Cross-reactivity of Ab for TS-DHFR<sup>a</sup>

PROTEIN	ANTIBODY			
	<i>L. major</i> TS-DHFR	<i>E. coli</i> TS	T2 phage TS	<i>E. coli</i> DHFR
<i>L. major</i>				
TS-DHFR	1/625	1/50	1/10	0
<i>L. casei</i>				
TS	1/100	_b	-	-
<i>E. coli</i>				
DHFR	0	-	-	-
<i>L. casei</i>				
DHFR	0	-	-	1/3000

<sup>a</sup>Values indicate the ~titer of the reactivity, as determined by the Elisa Well Assay.

<sup>b</sup>Lines indicate that the reactivity was not examined.



**FOR REFERENCE**

**NOT TO BE TAKEN FROM THE ROOM**



CAT. NO. 23 012





